

# **A new cell line-based coculture model of the human air-blood barrier to evaluate the interaction with aerosolized drug carriers**

Dissertation

zur Erlangung des Grades des

Doktors der Naturwissenschaften

der Naturwissenschaftlich-Technischen Fakultät III

Chemie, Pharmazie, Bio- und Werkstoffwissenschaften

der Universität des Saarlandes

von

Stephanie Kletting

Saarbrücken

2016

Tag des Kolloquiums:	22.09.2016
Dekan:	Prof. Dr.-Ing. Dirk Bähre
Berichterstatter:	Prof. Dr. Claus-Michael Lehr Jun.-Prof. Dr. Thorsten Lehr
Vorsitz:	Prof. Dr. Guido Kickelbick
Akad. Mitarbeiter:	Dr. Britta Diesel

Die vorliegende Arbeit entstand im Zeitraum von

Oktober 2012 bis Dezember 2015

unter Anregung und Anleitung von Herrn Prof. Dr. Claus-Michael Lehr

am Lehrstuhl für Biopharmazie und Pharmazeutische Technologie

an der Universität des Saarlandes

und am

Helmholtz-Institut für Pharmazeutische Forschung Saarland.

***Für meine Eltern***

***und***

***meinen Bruder***

*Inmitten der Schwierigkeiten liegt die Möglichkeit.*

Albert Einstein

This thesis was conducted as part of the project  
“Collaboration on the Optimization of Macromolecular Pharmaceutical Access to  
Cellular Targets (COMPACT)”,  
financially supported by the Innovative Medicines Initiative (IMI) Joint  
Undertaking under grant agreement n°115363.

---

## Table of contents

Table of contents.....	7
Short summary.....	10
Kurzzusammenfassung.....	11
1. Introduction.....	12
1.1 Respiratory tract: its functions and clearance mechanisms .....	12
1.2 Pulmonary drug delivery and nanoparticles .....	15
1.3 <i>In vivo</i> models of the lung .....	17
1.4 <i>In vitro</i> models of the lung .....	18
2. Aim of the work.....	23
3. Characterization of the newly established human alveolar epithelial lentivirus immortalized cell line (hAELVi).....	25
3.1 Introduction .....	26
3.2 Materials and Methods.....	28
3.2.1 Cell culture .....	28
3.2.2 Transepithelial electrical resistance (TEER) .....	28
3.2.3 Confocal laser scanning microscopy (CLSM) .....	29
3.2.4 Histology .....	30
3.2.5 Transport studies .....	31
3.2.6 Statistical analysis.....	32
3.3 Results and Discussion.....	33
3.3.1 hAELVi cells exhibit tight barriers when cultivated under liquid covered conditions (LCC) and at air liquid interface (ALI) .....	33
3.3.2 hAELVi cells exhibit tight barriers when cultivated in higher passages ..	37
3.3.3 Morphological analysis of monocultures under liquid covered conditions (LCC) and at air liquid interface (ALI) via histological cross-sections .....	38
3.3.4 hAELVi monocultures represent promising models to study drug absorption and transport.....	39
3.4 Conclusion .....	42
4. Set-up and characterization of a new 3D <i>in vitro</i> model mimicking the human air-blood barrier in a healthy state.....	43
4.1 Introduction .....	44
4.2 Materials and Methods.....	47

---

4.2.1 Cell culture .....	47
4.2.1.1 Monocultures .....	47
4.2.1.2 Cocultures .....	47
4.2.1.3 Macrophage-conditioned medium .....	49
4.2.2 Transepithelial electrical resistance (TEER) .....	49
4.2.3 Morphological and ultrastructural analysis of mono- and cocultures.....	49
4.2.3.1 Confocal laser scanning microscopy (CLSM) .....	49
4.2.3.2 Scanning electron microscopy (SEM).....	51
4.2.3.3 Transmission electron microscopy (TEM).....	51
4.2.4 Transport studies .....	52
4.2.5 Statistical analysis.....	53
4.3 Results and Discussion .....	54
4.3.1 Differentiation of THP-1 into macrophage-like cells .....	54
4.3.2 Coculture: epithelial barrier properties .....	55
4.3.2.1 Influence of SAGM and RPMI media on TEER values .....	57
4.3.3 Coculture: morphological characterization .....	59
4.3.4 Coculture: ultrastructural characterization.....	64
4.3.5 Transport studies .....	67
4.3.6 Long-term cocultivation.....	68
4.4 Conclusion .....	71
5. Application of the established alveolar 3D coculture model for nanoparticle deposition.....	73
5.1 Introduction .....	74
5.2 Materials and Methods.....	77
5.2.1 Nanoparticle preparation and characterization .....	77
5.2.1.1 Poly (D, L)-lactide-co-glycolide nanoparticles-/chitosan nanoparticles (PLGA NPs) .....	77
5.2.1.2 Silver nanoparticles (Ag NPs).....	77
5.2.1.3 Starch nanoparticles (starch NPs).....	78
5.2.2 Cell culture .....	79
5.2.3 Transepithelial electrical resistance .....	79
5.2.4 Cell viability determination via MTT assay .....	79
5.2.5 Cellular interaction studies.....	80
5.2.6 Statistical analysis.....	80



---

5.3 Results and Discussion.....	81
5.3.1 Nanoparticle characterization .....	81
5.3.2 Proof-of-concept I: PLGA-CS nanoparticles .....	82
5.3.3 Proof-of-concept II: Silver nanoparticles (Ag NPs).....	84
5.3.4 Application and evaluation of newly developed starch nanoparticles ....	87
5.4 Conclusion .....	95
6. Summary and outlook .....	97
List of abbreviations .....	100
References .....	104
Scientific output .....	123
Curriculum vitae .....	127
Acknowledgements / Danksagung .....	129

---

## Short summary

Besides reducing animal testing, *in vitro* models allow for the pre-screening of new drug candidates in terms of safety and efficacy before they enter clinical trials. To date, models mimicking the deep lung show limitations such as cellular origin or lack of appropriate barrier properties. Therefore, the focus of this work was on the establishment of a robust and reproducible cell line-based coculture model that reflects the two major barrier structures present in the alveolar region, namely intercellular junctions and macrophages.

This model was characterized regarding its morphology and barrier properties, with permeability assays showing its applicability for evaluating drug transport and absorption. Long-term cocultivation implied its suitability to assess the lung in diseased state mainly regarding chronic diseases.

The application of small amounts of Ag nanoparticles resulted in high cytotoxicity in a monoculture of macrophage-like cells, whereas the coculture showed only low toxicity. Newly developed starch nanoparticles intended for pulmonary drug delivery of proteins were nebulized onto the coculture and were evaluated with respect to their impact on the epithelial barrier, cell viability and cellular interactions.

In summary, as a more physiologically-relevant representation of the deep lung, the new established coculture can be applied as a useful tool to evaluate new formulations intended for pulmonary delivery and further contribute to their optimization.

---

## Kurzzusammenfassung

Neben der Reduzierung von Tierversuchen, erlauben *in vitro* Modelle die Voruntersuchung neuer Formulierungen hinsichtlich Sicherheit und Effektivität, bevor diese in klinischen Studien eingesetzt werden. Bisher verwendete Modelle zur Nachbildung der tiefen Lunge zeigen Limitationen bzgl. Zellursprung, Barriereeigenschaften oder Reproduzierbarkeit.

Daher wurde im Rahmen dieser Arbeit ein auf humanen Zelllinien basierendes Kokulturmodell entwickelt, welches neben dichten Zell-Zell-Verbindungen eine zweite Barrierestruktur, in Form von Immunzellen, aufweist.

Das Modell wurde hinsichtlich Morphologie und Barriereeigenschaften charakterisiert. Weitere Studien zeigten dessen Eignung für die Evaluierung von Wirkstofftransport. Langzeitkokultivierung impliziert den Einsatz für zukünftige krankheitsrelevante Fragestellungen. Während die Applikation schon geringer Mengen an Silber-Nanopartikeln bei makrophagen-ähnlichen Zellen in einer hohen Zytotoxizität resultierte, zeigte die Kokultur nahezu keine Toxizität. Des Weiteren wurden neuartige, für die pulmonale Applikation von Proteinen entwickelte, Stärke-Nanopartikel vernebelt und deren Effekt auf die Zellbarriere, -viabilitäten sowie das zelluläre Interaktionsverhalten untersucht.

Zusammenfassend lässt sich sagen, dass das hier entwickelte Kokulturmodell, zwei für die tiefe Lunge charakteristischen Barrierestrukturen beinhaltend, als nützliches Werkzeug zur Evaluierung neuer Formulierungen und deren Optimierung eingesetzt werden kann.

# 1. Introduction

## 1.1 Respiratory tract: its functions and clearance mechanisms

Oxygen ( $O_2$ ) forms the basis of almost all life, and is involved in many processes in the body. To exert an effect,  $O_2$  must first reach the bloodstream, from which it is further transported to the cells and tissues. The so-called respiratory tract, composed of the conducting airways and the alveolar region, is responsible for this transfer of  $O_2$ . In general, after entering the body through the nose or mouth, inhaled air passes through the branching structures of the lung - starting with the trachea, followed by bronchi and bronchioles - and finally reaches the alveoli, where gas exchange of  $O_2$  (from the alveoli to the blood) and  $CO_2$  (from the blood to the alveoli) takes place. With regard to physiological functions, cellular morphology and amount of cells, the epithelium changes along the respiratory tract (Figure 1.1). The lung also possesses several drug transporters [1-3] including peptide transporters [4], P-glycoprotein (P-gp), breast cancer resistance protein (BCRP), multidrug resistance-related proteins (MRPs) [5, 6] and organic cation transporters (OCTs) [7-9] that have an effect on drug absorption [10].

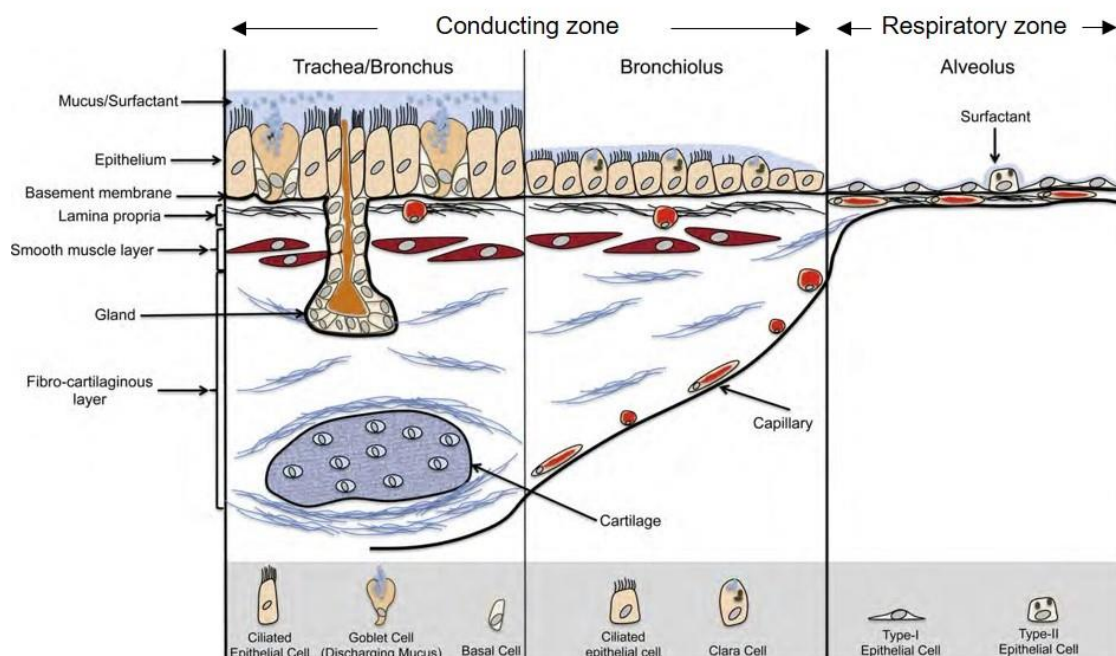


**Figure 1.1. Epithelial changes along the respiratory tract.** *The lung comprises many different cell types, that differ in function and morphology. Whereas the conductive epithelium is lined by 7 different cell types, the air-blood barrier within the respiratory zone is formed by two kinds of cells that are involved in gas exchange. Adapted and modified with permission from [11], modified from [12].*

### Conducting zone

The conducting airways begin at the nasal epithelium, followed by the trachea, which branches into the bronchi and further into the terminal bronchioles, while becoming progressively smaller in diameter [13]. Besides directing airflow, the conducting airways also filter, warm and humidify the inhaled air [14].

The airway epithelium is composed of different cell types, which vary in function and morphology [14-16]. These include goblet cells, basal cells, ciliated cells, brush cells, serous cells, Clara cells and neuroendocrine cells [1, 17]. Together, they form a pseudostratified layer in which the apical membranes are joined by tight junctions (TJs). These cell-cell connections divide cellular membranes into functional distinct domains, and are further responsible for membrane barrier properties [18-20].

The main cell population in the tracheal epithelium are ciliated cells, which constitute approximately 50% of the total cell population [21, 22]. Almost the entire epithelial surface is covered by mucus-producing goblet and so-called Club cells, originally known as Clara cells [1, 23, 24]. Besides secreting glycoproteins, Club cells are capable of self-renewal and are known to be involved in the repair of the bronchioles [25-27]. Further, recent publications describe their involvement in the differentiation of alveolar epithelial type II (ATII) cells after severe lung injury [27].

The entire airway epithelium is covered with lining fluid, the so-called mucus [28]. This mobile non-cellular barrier is located at the tips of the cilia, and is one of the most important defense mechanisms in the human lung. Inhaled particles and organisms are captured by the mucus which is transported by ciliary beating to the esophagus [29, 30], where it is either eliminated by expectoration or can be swallowed and further transferred to the digestive tract [16]. To guarantee the optimal level of clearance the mucus blanket is composed of two phases, differing in their physical properties. Whereas the upper layer of mucus, most proximal to the airspace, has a high viscosity, the region of mucus in close contact with the epithelium is a thin and watery layer with a low viscosity. A layer consisting of phospholipids lowers the surface tension between these two mucus regions [13, 31]. Besides glycoproteins (mucins, 2%), proteins (1%), inorganic

salts (1%) and lipids (1%), mucus is composed mainly of water (95%) and is primarily secreted from the serous cells of submucosal glands and goblet cells [32]. Its thickness depends on the location in the airways as well as on the presence of pathological conditions [28]. This can vary between 10 and 30  $\mu\text{m}$  in the trachea and 2 and 5  $\mu\text{m}$  in the bronchioles [33]; in diseases such as cystic fibrosis (CF) the layer is thicker [34].

### Respiratory zone

Due to its extensive surface area ( $\sim 140 \text{ m}^2$ ) and also its thinness of 0.1-0.5  $\mu\text{m}$ , the alveolar epithelium, also known as the “air-blood barrier”, permits rapid gas exchange by passive diffusion [16, 35, 36], while protecting the body from external threats e.g. inhaled toxins, particles and microorganisms. Around 99% of the epithelium is made up of two cell types: alveolar type I (ATI) and ATII cells [37]. These cells are in contact with the underlying capillary bed, consisting of micro vessels formed of endothelial cells, with a surface area of  $130 \text{ m}^2$  [13, 16].

ATI cells cover  $\sim 96\%$  of the alveolar surface and display a flattened shape, with a diameter of approximately 50-100  $\mu\text{m}$  and an average thickness of just 0.26  $\mu\text{m}$ . Considering this rather short diffusion path, ATI cells are known to be responsible for gas exchange and drug transport. Morphologically, they exhibit a large cytoplasmic volume and only a few cellular organelles [16, 35, 37].

In contrast, the smaller ATII cells exhibit a diameter of  $\sim 10 \mu\text{m}$  and an average thickness of 5-10  $\mu\text{m}$ . Cuboidal in shape, they cover about 3% of the alveolar surface [37]. Moreover, ATII cells are involved in the renewal of injured ATI cells as a result of proliferation and subsequent transformation to the squamous cell type [13, 35, 38]. Contributing to the regulation of immune defense, ATII cells express molecules of the class II major histocompatibility complex (MHC) that are important for presentation of antigens and further activation of T cells as well as intracellular adhesion molecules such as ICAM-I [13, 39-41].

Besides these functions, ATII cells are characterized by the capability to synthesize and secrete surfactant, a lining fluid that covers the alveolar epithelium similar to the way in which mucus covers the airways and comprises a

mixture of phospholipids (90%) and proteins (10%). Four surfactant-associated proteins (SPs) are present in particular: SP-A, -B, -C and -D [28, 42-47]. Whereas the hydrophilic surfactant proteins SP-A and SP-D are participating in the pulmonary immune defense mechanisms by preventing the adhesion of inhaled particles or microorganisms to the alveolar epithelium [48], SP-B and SP-C are involved in reducing the alveolar surface tension at the air-epithelium interface, thus preventing the alveoli from collapsing during exhalation [46, 49-52]. Further, they facilitate the formation as well as the stabilization of the surfactant film [28], a thin layer with an average thickness of 0.05-0.08  $\mu\text{m}$  [33, 53].

As the mucociliary escalator does not reach the alveoli, macrophages provide an alternative means of protection by patrolling the alveolar surface [13]. Arising from monocytes in the bone marrow, these phagocytic cells reach the alveoli *via* the capillaries [16]. They play an important role in defense against inhaled bacteria and particles by ingesting such foreign matter. Macrophages can be cleared from the alveoli to the bronchioles by the lining fluid, and are further eliminated along the mucociliary pathway [13, 16, 24, 54].

## **1.2 Pulmonary drug delivery and nanoparticles**

To date, oral application is the most preferred way to deliver active pharmaceutical ingredients (APIs) to their site of action [13]. Besides its advantages including high patient compliance, low production costs of oral dosage forms [55] and a large absorption surface [56], some drawbacks have always to be considered which may influence the successful action of the used drug. These include extremes of pH, especially occurring in the stomach, as well as extensive enzymatic activity; the mucus layer lining the entire epithelium may also impact on drug absorption and so action, as may the presence of food [57, 58]. Another common systemic route of administration is *via* the skin, a natural barrier against particle penetration [59] that is not easy to overcome; as such, it is therefore often associated with means of administration which are invasive in nature.

The lung represents an important alternative route for drug delivery, due to the possibility to administer drugs in a non-invasive way to a large epithelial surface [60], a relatively low enzymatic activity compared to the gastrointestinal tract (GI) [61, 62], high vascularization [1], and avoidance of the first pass effect [13, 63]. Besides the local treatment (“air-to-lung”) of respiratory diseases such as asthma, chronic obstructive pulmonary disease (COPD) and cystic fibrosis (CF) [1, 64-66], the pulmonary route also permits systemic availability of the drug (“lung-to-blood”) due to absorption *via* the thin alveolar epithelium. This allows for treatment of diseases such as diabetes [67] or thrombosis [68, 69]. Thus, the application of therapeutics *via* the lung constitutes a promising means to administer drugs with poor oral absorption or which show instability in the gastrointestinal tract, including small molecules and in particular macromolecules *e.g.* proteins and peptides [13, 33, 70].

To facilitate and further enhance drug delivery, pharmaceutical companies make use of nanotechnology which allows for encapsulation of APIs or diagnostic agents in nanosized carriers such as nanoparticles (NPs), and is therefore also referred to as nanomedicine [71-73]. Such NPs can protect the drug from external influences during its application and can enhance drug permeation through cellular membranes [74]. Further, due to their size and surface characteristics NPs are able to evade pulmonary clearance mechanisms, to permit cell-specific targeting, and importantly, to reduce drug side effects [63].

In general, NPs are defined as particles with sizes between 1 and 100 nm and a resulting high surface-to-volume ratio [72, 75, 76]. They can be divided into natural NPs, occurring as a consequence of dusts, forest fires or volcanic activity [77], and engineered NPs [78] that can be found in different application areas including electronics, biomedicine, pharmaceuticals, remediation, construction, cosmetics and in food packaging [78-82]. Nevertheless, despite their wide usage, there is still a huge concern regarding safety of NPs due to the rapid increase in nanotechnology worldwide and an increased exposure of humans to uncharacterized particles [77]. Airborne NPs smaller than 100 nm seem to have unrestricted access to most areas of the lung - their small size facilitates their uptake into cells as well as transcytosis across epithelial and endothelial cells into the blood and lymphatic circulation, from where they have the potential ability



to reach sensitive target sites such as bone marrow, lymph nodes, spleen, and heart [77, 83, 84]. The exposure to airborne particles is known to contribute to many chronic pulmonary diseases, while exposure to high particle concentrations has been associated with increased pulmonary and cardiovascular mortality [77, 83].

Therefore, in the context of pulmonary drug delivery, it is of utmost importance that not only the API but also all excipients as well as the final formulation are evaluated with regard to their potential toxicological risks. Therefore, both *in vivo* and (more commonly) *in vitro* models have been established and utilized for decades to determine the safety and efficacy of future drug candidates and their parent materials [85].

### **1.3 *In vivo* models of the lung**

Potential drug candidates can be defined by applying *in vitro* bioassays that evaluate properties such as their impact on cell viability or bacterial growth behavior. However, *in vivo* toxicity and efficacy of inhaled drugs cannot be determined using these assays [86]. Thus, animal experiments can better provide an indication of the therapy outcome and further improve the understanding of pharmacokinetics and dynamics of a potential formulation [85, 87]. However, in addition to substantial differences in lung anatomy, several critical points including fluctuating clearance, issues related to long-term therapy or drug binding to serum proteins may vary between species, meaning that even the relevance of animal models may sometimes be questionable [88]. They are probably still the best choice to determine clearance, systemic side effects and pharmacokinetic parameters in spite of such points however [85].

Until today, most *in vivo* drug screens have been performed in rodents including mice, rats, guinea pigs or rabbits. Long developmental periods and high maintenance costs hinder a high-throughput screening approach however. Therefore, *Caenorhabditis elegans* with its microscopic size, short life cycle, genetic tractability, and low-cost laboratory maintenance is an attractive model organism for infection and life-span studies [89-94].

Animal models for chronic infections or diseases such as asthma, COPD and CF are also well-established and have made great progress in terms of genetic modifications, but they still do not fully reflect the morphology of the lung in diseased states and therefore continue to need some improvement [95, 96]. The failure rate of translating data from animals to humans also still remains high, in spite of the considerable advances that have been made in *in vivo* models; this fact forms part of an ongoing discussion on the utilization of animal models [97].

#### **1.4 *In vitro* models of the lung**

Cell- and tissue-based models serve as important alternatives to animal testing for predicting safety and efficacy of new drug candidates and formulations, as well as for the evaluation of inhaled chemicals or particulate matter [98, 99]. While these models cannot mimic the whole organism, the deliberate reduction of biological complexity that they provide can in fact be an advantage, permitting the study of particular scientific questions under well-controlled conditions, *e.g.* understanding of transport mechanisms across epithelial barriers [13]. *In vitro* models can help to focus on diverse levels of cellular organization and therefore they may allow for studying processes in more depth than is possible with *in vivo* models. But it has always to be kept in mind, that these models have their limitations as the employed cells are sometimes not strictly physiologically-relevant with respect to their origin or not suitable for mimicking the deep lung due to an absence of barrier properties. Further, artifacts may occur in such models, causing misleading results [85].

In the case of pulmonary delivery, it is essential that epithelial cell models form a tight barrier against solutes or particles, similar to the *in vivo* situation. *In vitro*, this parameter can be monitored by measuring the so-called transepithelial electrical resistance (TEER) [13] and by determining the apparent permeability coefficient ( $P_{app}$ ) of paracellular markers [85]. In general, functional epithelia exhibit high TEER values in combination with low permeability levels [24, 100, 101]. To further evaluate particle safety and impact on respiratory epithelia, assays measuring cytotoxicity (*i.e.* 3-(4,5-dimethylthiazol-2-yl)-2,5-diphenyltetrazolium bromide (MTT) assay [102]), changes in gene expression,

production of reactive oxygen species (ROS) or the secretion of pro-cytokines with inflammatory responses are utilized [85]. Several *in vitro* models including mono- and advanced cocultures mimicking the upper airways or the deep lung to evaluate safety and uptake of nanoparticles [103] have already been described in literature.

### Single cell-based cultures

To mimic the upper airways, a number of cell lines have been extensively used. Calu-3 cells, derived from a submucosal adenocarcinoma [24, 104], are probably the most commonly used cell line to evaluate pulmonary drug delivery [24, 105-107]. Whereas cells cultivated at air liquid interface (ALI) conditions are able to differentiate and build a mucus layer similar to the physiological situation, cultures grown under liquid covered conditions (LCC) exhibit an altered differentiation and permeability to substances [101, 108]. Besides Calu-3 cells, 16HBE14o- cells (of human bronchial epithelial origin) have been used in studies addressing drug absorption and interaction with the epithelium [109-113]. Although exhibiting a tight barrier and expressing important transporters such as P-gp and the lung resistance-related protein (LRP) [114], these cells lack cilia and mucus production when cultivated at ALI [109]. Another cell line of bronchial origin, NCI-H441, exhibits biochemical and morphological characteristics of both ATII cells and Club cells [1, 23], forms a polarized monolayer with functional tight junctions, and expresses drug transporters such as P-gp and OCTs [9, 85, 115]. These features make NCI-H441 cells very well-suited for evaluating drug and carrier transport. Besides cell lines, primary cells have also been used in pulmonary drug delivery. For example, commercially available primary normal human bronchial epithelial (NHBE) cells show barrier properties and express important drug transporters, such as P-gp [116]. Besides evaluating drug transport, this model can also be utilized to evaluate anti-inflammatory drugs or carriers, due to the fact that air pollutants can induce inflammatory responses [117].

In contrast to the upper airways, only a few models are available mimicking the deep lung. The A549 cell line, derived from an alveolar epithelial cell

adenocarcinoma [118] is the most commonly used cell line for mimicking the alveolar region, even though it lacks epithelial barrier function [100, 119]. A549 cells have been intensively used in studies addressing drug transport [100, 111, 120-122], and particle interactions [123-126].

Due to their capacity to express functional tight junctions, resulting in high TEER, primary ATI-like cells are the best model to mimic the human air-blood barrier. Therefore, filter-grown human alveolar epithelial cells (hAEpC) in primary culture were established to evaluate transport of drugs or carriers [100, 127, 128]. However, their use is limited due to the restricted access to primary tissue, short cell life-span and inter-individual differences, which leads to low reproducibility. This fact excludes them from use in high-throughput screening of new formulations. In this respect, a new human transduced ATI cell line (TT1) was obtained by immortalization of primary ATII cells, to study inflammatory responses and NP uptake [129, 130]. However, these cells also lack expression of tight junctions, and as such models of the deep lung that maintain cell differentiation and barrier properties are still needed.

### Advanced cell culture models

Modeling the lung with its complex structure is quite challenging, since these models must incorporate alveolar epithelial cells, fibroblasts, endothelial cells, immune cells and potentially also other cell types. Therefore, advanced *in vitro* models based on cocultures cultivated on permeable filters or on a chip have been established, aiming to mimic basic interactions between various respiratory cell populations [14, 85].

More information on coculture models can be found in literature [1, 13, 14, 16, 85]. As an example, Rothen-Rutishauser and colleagues established a triple cell culture model composed of epithelial cells (A549), monocyte derived macrophages, and dendritic cells, which, when cultivated at ALI showed greater efficacy in predicting *in vivo* toxicity compared to monocultures [126]. Immune cells most certainly play a crucial role in forming an additional barrier in such models and also *in vivo*, due to particle-phagocytosis

and inflammatory responses [85]. The transport of polyelectrolyte microcapsules within the above described triple coculture model was recently shown by Kuhn *et al.* [131]. Further, to study the potential toxic effect of particles in the lung, Klein *et al.* established a tetra-culture comprising four different human cell lines, including epithelial cells (A549), macrophages (THP-1), mast cells (HMC-1) and endothelial cells (EA.hy 926) [132]. A coculture model mimicking the alveolar-capillary barrier evaluating the damage caused by silica NPs in the deep lung has also been introduced, by Kasper *et al.* They showed that the developed coculture comprising the epithelial cell line NCI-H441 and ISO-HAS-1 as endothelial cells was less sensitive regarding toxic effects compared to conventional monocultures, but conversely much more sensitive in terms of mimicking inflammatory responses [133]. Moreover, a suitable coculture model to evaluate adsorption, uptake and trafficking of nanosized carriers under different physiological conditions was established by Hermanns *et al.*, involving NCI-H441 in coculture with either primary isolated human pulmonary microvascular endothelial cells (HPMECs) or endothelial cells (ISO-HAS-1). Within these cocultures, epithelial cells acted differently when compared to epithelial monocultures with respect to barrier properties and inflammatory responses [134].

Although these coculture models showed several advantages compared to monocultures, they still lack the expression of functional tight intercellular connections whose alteration is known to be involved in pathogenesis, as noted for example in asthma and chronic bronchitis [135, 136].

Recently, an autologous coculture composed of primary ATI-like cells and alveolar macrophages was established by Hittinger *et al.* to evaluate the safety of airborne particles [137]. The advantage of this model is the use of primary cells, which form functional tight junctions and exhibit a similar physiology to what is observed *in vivo* [100, 128]. Moreover, primary alveolar macrophages obtained from the same donor allow a better *in vivo-in vitro* correlation. Nevertheless, their use is limited due to restricted access to primary tissue, short life-spans of primary cells and inter-individual differences.

Currently, so-called organs-on-a-chip, micro-engineered biomimetic systems containing microfluidic channels lined by living human cells, have been developed to meet the high-throughput needs for drugs and particle toxicity tests [138, 139]. The application of mechanical stress to lung-on-a-chip models has shown higher toxic and inflammatory responses as well as particle uptake compared to conventional, comparable static monocultures [138]. Although their standardization is still challenging, these models serve as promising alternatives to animal models in the case of pharmaceutical, chemical and environmental applications [85].

---

## 2. Aim of the work

Until now, several *in vitro* models mimicking the lung have been used to evaluate the impact of inhaled components including NPs, chemicals, microorganisms and toxins. Nevertheless, there is still a need for models of the deep lung that maintain cell differentiation and barrier properties. In this regard, an autologous coculture model comprising primary alveolar epithelial cells and alveolar macrophages was recently established. While primary cells show similarities to *in vivo* physiology, the isolation of primary cells is time consuming and expensive. Moreover, their short life-span and variability between donors results in low reproducibility of primary cell-based models, further restricting their use for high-throughput screening of new formulations.

To increase the reproducibility and further facilitate high-throughput screening of new drug candidates, a more robust cell line-based coculture model mimicking the human air-blood barrier in healthy state was investigated within this work. For this purpose, the new established ATI-like cell line, hAELVi, was combined with previously differentiated macrophage-like cells (THP-1 cell line). Whereas hAELVi cells represent a diffusional barrier within the system by exhibiting functional tight junctions, the macrophages should represent an immunological barrier in particular for larger molecules and NPs similar to the *in vivo* situation.

The first part of this thesis includes the characterization of the hAELVi cell line cultivated under LCC and at ALI with respect to its barrier properties and suitability for assessing drug transport.

The second and main part of this thesis includes the set-up and subsequent characterization of the hAELVi-/THP-1 coculture models with regard to examination of cellular morphology by confocal laser scanning microscopy (CLSM), scanning electron microscopy (SEM) as well as transmission electron microscopy (TEM), determination of barrier properties by measurement of TEER, and assessment of its suitability to evaluate drug transport.

This work is part of the COMPACT project, a European association of academic and industrial partners which is funded by the Innovative Medicines Initiative (IMI) and the European Federation of Pharmaceutical Industries and Associations (efpia). The consortium comprises several work packages (WPs) that are focusing on the identification and characterization of transport pathways (WP3) across biological barriers involving oral (WP4), brain (WP5), lung (WP6) and skin (WP7) delivery and cell membranes. Further, construction and characterization of formulations for non-invasive delivery of peptide- and protein (WP1) as well as nucleic acid-based (WP2) drugs are investigated in COMPACT.

With this regard, the last part of this thesis includes the application of different kinds of NPs. Well-characterized Poly (D, L)-lactide-co-glycolide-(PLGA) / chitosan (CS) that are known to be non-toxic and have already been used as drug delivery system (DDS) for pulmonary delivery as well as commercially available silver (Ag) NPs were applied to the newly established coculture model to assess its ability to evaluate NP safety. In this respect the impact of NPs on cell viability, barrier properties and inflammatory responses was determined. In terms of pharmaceutical relevance, a newly developed DDS, namely starch NPs intended for pulmonary delivery of proteins and peptides (PhD thesis, Sarah Barthold) prepared within COMPACT, was nebulized onto hAELVi-/THP-1 monocultures as well as the coculture cultivated at ALI. The system was further evaluated regarding cell viability (MTT assay), barrier properties (TEER) and cellular interactions. Additionally, starch NPs loaded with a model cargo (Immunoglobulin G1; IgG1) were applied in a similar set-up and were evaluated in the same way.

In summary, the overall aim of this thesis was to successfully establish a cell line-based coculture model of the human air-blood barrier in the healthy state. This model should serve as a tool to evaluate interactions of aerosolized drug carriers with the epithelium (by allowing for determination of *e.g.* cytotoxicity and cellular interactions-uptake) and further contribute to the improvement of new drug formulations.



---

### **3. Characterization of the newly established human alveolar epithelial lentivirus immortalized cell line (hAELVi)**

The author of this thesis made the following contributions to this chapter:

Performed all cell culture experiments, measured TEER, interpreted the experimental data, cultivated, fixed and stained the cells for confocal analysis, histological cross-sections and wrote the chapter. Confocal images were made by Dr. Cristiane de Souza Carvalho-Wodarz. Further sample preparation, cutting, staining and imaging of histological cross sections were performed by Marijas Jurisic at Saarland University.

### **3.1 Introduction**

According to the 3R principle (replace, reduce, refine) [140], new *in vitro* models that contribute to a reduction in the use of animal models for evaluating safety of inhaled components including chemicals, (nano) materials and drugs are of utmost significance. So far, the most commonly used cell line that mimics the alveolar region and is further applied in assays that aim to evaluate toxicity of inhaled materials is A549, which is adenocarcinomic in origin [118]. As already mentioned in the first chapter, A549 cells are deficient in the expression of functional tight intercellular connections. In contrast, to mimic the upper airways, cell lines such as Calu-3, 16HBE14o- or NCI-H441 [23, 101, 108, 109, 112, 113] are commonly used. Although these are not suitable for mimicking the deep lung, models consisting of such cells have been successfully applied to assess safety and uptake of NPs intended for inhalation.

Isolated cells in primary culture are the so-called “gold standard” to mimic the human air-blood barrier [141]. These cells allow for a better representation of the situation that can be found *in vivo* [142], as they reflect physiological phenotypes and form functional tight junctions [6, 100, 128]. Nevertheless, their use is restricted due to limited access to primary material, short cell survival time periods, and the potential for high variability in data obtained from such cultures (as a result of inter-donor differences). The latter leads to low reproducibility which limits the use of primary cell-based models in high-throughput screening of new drug candidates. To combat these problems, an ATI cell line (TT1) has been obtained by immortalization of primary ATII cells. This cell line reflects the physiological phenotype of ATI cells, and has been used in studies for evaluating inflammatory responses and NP uptake [129]. Nevertheless, these cells are not able to express functional tight junctions [130]. Thus, by applying a novel immortalization regime comprising a defined set of immortalizing genes, an ATI-like cell line, namely human alveolar epithelial lentivirus immortalized (hAELVi) cells that display functional intercellular connections could be generated. Detailed information regarding the different steps and selection criteria that finally led to the obtained cell line, as well as first initial characterization studies including TEER measurements, SEM and CLSM images

for morphology, as well as polymerase chain reaction (PCR) -analysis of ATI-specific markers can be found in the thesis "*Immortalization of primary human alveolar epithelial cells: A new in vitro model of the air-blood barrier forming functional tight junctions*" by Anna Kühn [143]. The following chapter describes the characterization of this prospective model for drug delivery with regard to the formation of tight intercellular junctions and drug transport.

The two obtained clones (hAELVi.A and hAELVi.B) of this new cell line were cultivated under LCC as well as at ALI, and were further evaluated and compared regarding barrier properties by means of TEER measurements, and staining of the tight junction proteins *zonula occludens* (ZO-1) and *occludin* (OCLN). Moreover, their suitability for predicting drug absorption was evaluated *via* transport studies, using sodium fluorescein (NaFlu), a hydrophilic molecule typically employed to assess paracellular transport.

## **3.2 Materials and Methods**

### **3.2.1 Cell culture**

hAELVi.A or hAELVi.B cells were cultivated onto fibronectin (1% (v/v); FN; Corning, USA) / collagen (1% (v/v); COL; Sigma; Germany)-coated Transwell® membranes (Corning, USA) with a pore size of 0.4 µm and growth areas of 0.33 cm<sup>2</sup> (Corning: 3470; for TEER measurement) and 1.12 cm<sup>2</sup> (Corning: 3460; for TEER, CLSM, and transport studies). Cells were seeded at 1x10<sup>5</sup> cells/cm<sup>2</sup> in small airway growth medium (SAGM; Lonza) containing 1% fetal bovine serum (FBS; Lifetechnologies, Germany) and 1% penicillin/streptomycin (P/S; 10.000 U/mL, Gibco Lifetechnologies, USA) under LCC, *i.e.* 200 µL apical / 800 µL basolateral (0.33 cm<sup>2</sup> Transwell® membranes) and 500 µL apical / 1.5 mL basolateral (1.12 cm<sup>2</sup> Transwell® membranes). To set up ALI cultures, the cells were seeded under LCC; after two days in culture the medium was then completely aspirated, and the cells were further fed from the basolateral compartment only, *i.e.* 200 µL for Transwells® with a growth area of 0.33 cm<sup>2</sup> and 500 µL for bigger Transwells® with 1.12 cm<sup>2</sup> cultivation space. The cells were cultivated at 37 °C, 5% CO<sub>2</sub> and 95% humidity and the medium was changed every second day. To characterize and compare hAELVi cells under both conditions, measurements of the TEER were performed over a period of 7 or 14 days. Afterwards, the cells were fixed and stained for immunohistochemistry, or transport studies were conducted. To determine the ability of hAELVi cells to grow in higher passages and further to exhibit TEER, the cells were routinely cultivated in a six-well plate in a ratio of 1:3 and seeded as previously described every 2-4 weeks to determine the TEER.

### **3.2.2 Transepithelial electrical resistance (TEER)**

The TEER is a parameter that describes the integrity of a cell layer [13]. To determine this factor, hAELVi cells were seeded as previously described in section 3.2.1 and TEER determined as described previously [108, 127, 144, 145]. Briefly, to avoid fluctuation in TEER due to temperature

influences, the cells were placed on a heating plate (37 °C) and resistance measurements were conducted using a chopstick electrode and an epithelial voltohmmeter (EVOM) both from World Precision Instruments, Sarasota, USA. To further determine the TEER in samples exposed to ALI, medium was refilled into Transwell® compartments to LCC levels, *i.e.* 500 µL (apical) and 1.5 mL (basolateral). After 1 h of equilibration TEER measurements were conducted. Afterwards, the medium was aspirated and the cells were fed and re-cultivated at ALI. The TEER was calculated by subtracting the resistance value of black inserts containing only medium (39 Ω for 0.33cm<sup>2</sup> / 110 Ω for 1.12 cm<sup>2</sup>) from all samples, with further multiplication by the cultivation area of the inserts.

#### 3.2.3 Confocal laser scanning microscopy (CLSM)

To visualize the formation of tight junctions, 1x10<sup>5</sup> hAELVi cells/cm<sup>2</sup> were seeded on FN/COL-coated Transwell® filters with a pore size of 0.4 µm and a growth area of 1.12 cm<sup>2</sup>. The samples were further cultured under LCC and at ALI as previously described in section 3.2.1, and were fixed with 3% methanol free paraformaldehyde (PFA; stock 16%; 15710-S, Electron Microscopy Sciences, USA) in phosphate buffered saline (PBS) for 30 min after 7 and 14 days in culture. Afterwards, the samples were treated and stained as previously described [146] with minor modifications. Briefly, the samples were quenched with 50 mM NH<sub>4</sub>Cl/PBS for 10 min and subsequently blocked and permeabilized by using a mixture of 0.5% bovine serum albumin (BSA) / 0.025% Saponin in PBS for 30 min. All steps including fixation, blocking and permeabilizing were performed at room temperature (RT) and from the apical side. Primary antibodies against the tight junction proteins OCLN (mouse anti-occludin, Catalog No 33-1500, Invitrogen) and ZO-1 (rabbit anti-ZO-1, Catalog No 61-7300, Invitrogen) were diluted 1:200 in 0.5% BSA / 0.025% Saponin in PBS and incubated with cells overnight at 4 °C. The secondary antibodies for OCLN (polyclonal Alexa-Fluor 488 conjugated rabbit anti-mouse, Catalog No. A11059, Invitrogen) and ZO-1 (polyclonal Alexa-Fluor 633, conjugated goat anti-rabbit, Catalog No. A21070, Invitrogen) were diluted 1:400 in PBS and incubated with

cells for 1 h at 37 °C. Afterwards, the samples were washed twice with PBS and counterstained with 4',6-diamidino-2-phenylindole (DAPI) diluted 1:50000 (nuclei, Stock 1 mg/mL; LifeTechnologies™, Darmstadt, Germany) in PBS. Transwell® membranes were removed from insert holders with a scalpel, put on an objective slide and mounted in DAKO medium (Product No. S302380-2, DAKO, USA), before they were analyzed by CLSM (Zeiss LSM710, Zeiss, Germany). Microscopy images of fixed samples were acquired at 1024 × 1024 resolution, using a 63x water immersion objective and z-stacks of around 6 µm. Confocal images were analyzed using Zen 2012 software (Carl Zeiss Microscopy GmbH) and Fiji Software (Fiji is a distribution of ImageJ available at <http://fiji.sc>).

#### 3.2.4 Histology

To characterize the hAELVi cells regarding morphology, histological cross-sections were prepared. For that, hAELVi cells were cultivated under LCC and at ALI as previously described in 3.2.1 and fixed on days 7 and 14 with 3% methanol free PFA for 30 min at RT. Afterwards, the samples were dehydrated with gradual ethanol concentrations (35-50-70-95-100-100% for 10 min each, diluted in H<sub>2</sub>O), followed by the removal of alcohol by using Histo-clear II (Histological Clearing Agent; National diagnostics, USA) for 2x 10 min. Subsequently, the samples were embedded in paraffin (Histowax® Embedding Medium; Leica Microsystems, Germany) for 2x 1 h and stored overnight at 4 °C before they were cut in 4 µm slices using a Microtome-Reichert Jung 2040 Autocut (Boston Laboratory Equipment, USA). In a next step, the slices were stained with hematoxylin/eosin, mounted with Roti®-Histokitt (Carl Roth GmbH + Co. KG, Germany) and analyzed with a Zeiss light microscope (Zeiss Imager M1m, Zeiss, Germany), using a 100x objective.

### 3.2.5 Transport studies

To evaluate the suitability of this model for analyzing drug absorption, the transport of the paracellular marker NaFlu alone and in combination with ethylenediaminetetraacetic acid (EDTA), a modulator of tight junctions, was determined. For this purpose, hAELVi.A monolayers were cultured under LCC and at ALI to further determine the  $P_{app}$  - a parameter that describes the ability of a compound to overcome the epithelial barrier and in doing so may give a hint as to its potential bioavailability *in vivo* [13].

Briefly,  $1 \times 10^5$  cells/cm<sup>2</sup> were seeded on FN/COL-coated Transwell® filters with a pore size of 0.4 µm and a growth area of 1.12 cm<sup>2</sup>. Two days after seeding, the seeded Transwell® filters were divided into two groups, one for culturing under LCC and the other at ALI. TEER measurements were conducted every two days to monitor the cell growth, until the transport studies were performed on days 7 and 14 for LCC and ALI cultures, respectively. Transport experiments were then conducted according to previous protocols [100, 114] with minor modifications. Briefly, before starting the experiment, the cells were washed twice with pre-warmed Krebs-Ringer Buffer (KRB; 142.03 mM NaCl, 2.95 mM KCl, 1.49 mM K<sub>2</sub>HPO<sub>4</sub>·3H<sub>2</sub>O, 10.07 mM HEPES, 4.00 mM D-Glucose, 1.18 mM MgCl<sub>2</sub>·6H<sub>2</sub>O, 4.22 mM CaCl<sub>2</sub>·2H<sub>2</sub>O; pH 7.4) and were further incubated with KRB for 45 min. TEER was measured before and after the experiment to check barrier integrity. To start the transport study, KRB was aspirated and 520 µL NaFlu (10 µg/mL in KRB) ± 16 mM EDTA were added to the apical (donor) compartment, and 1.7 mL KRB was put into the basolateral compartment (acceptor). Samples were directly taken from the donor (20 µL) just at the start and the end of the experiment as well as from the acceptor compartment (200 µL) and were subsequently transferred into a 96-well plate. During the transport study, the plates were placed on a MTS orbital shaker (150 rpm; IKA, Germany) in the incubator at 37 °C. Samples from the basolateral compartment were taken and replaced with 200 µL of fresh KRB every 30 min for 3 h. The samples were then measured using a Tecan® plate reader (Tecan Deutschland GmbH, Germany) at wavelengths of 488 nm (em) and 530 nm (ex).

### 3.2.6 Statistical analysis

Data represent of 2-3 experiments and are shown as mean  $\pm$  standard error of the mean (SEM\*). Two-way ANOVA with Bonferroni's post hoc test was performed using GraphPad Prism 5 software (GraphPad).



### **3.3 Results and Discussion**

#### **3.3.1 hAELVi cells exhibit tight barriers when cultivated under liquid covered conditions (LCC) and at air liquid interface (ALI)**

Epithelial barriers play a crucial role in animal survival, by protecting these organisms from external threats such as pathogens or toxins. As they are permeable to ions, gases, nutrients and macromolecules, epithelial barriers also contribute to the regulation of hydric balance and overall homeostasis [37, 147, 148]. Besides adherent junctions, gap junctions and desmosomes, TJs are an essential component of the epithelial barrier [148]. TJs were first identified *via* electron microscopy in 1963 by Farquar and Palar [149] and are composed of various transmembrane proteins such as claudins, OCLN, tricellulin, and junctional adhesion molecules (JAMs); cytoplasmic linker or adaptor proteins which connect them to the actin cytoskeleton including ZO-1, -2, -3, cingulin, and MAPP1; and signaling molecules such as Protein kinase C [150-154]. TJs are able to change their permeability and functional properties in response to stimuli, regulating and permitting the transit of ions, water or molecules while restricting the passage of large molecules [155-158]. Further, they divide cell membranes into functionally distinct apical and basolateral domains, that lead to cell polarity and result in cell barrier properties [16, 18-20, 159, 160]. Measurement of TEER can be partly used to characterize these properties with regard to the cell layer integrity [13]. Usually, *in vitro*, functional epithelial barriers exhibit high TEER values, ranging from ~400-600  $\Omega\cdot\text{cm}^2$  in the case of the intestine [161], 1000-1500  $\Omega\cdot\text{cm}^2$  for the bronchial epithelium [24, 101], and in the order of >1000  $\Omega\cdot\text{cm}^2$  for the alveolar epithelium [85, 100].

To evaluate the ability to form a barrier comparable to that of primary cells, which more closely represent the *in vivo* situation, the new established hAELVi cell line was seeded onto previously-coated permeable filter membranes, and TEER was determined every second day for 7 and 14 days (Figure 3.1). After 7 days, cells cultivated at ALI showed higher TEER, up to 332  $\Omega\cdot\text{cm}^2$ , compared to samples under LCC where values of ~135  $\Omega\cdot\text{cm}^2$  could be observed. On day 12 cells in both culture conditions reached TEER values up to 770  $\Omega\cdot\text{cm}^2$ , and even higher

resistance values of up to 3100  $\Omega \cdot \text{cm}^2$  (ALI) and 2400  $\Omega \cdot \text{cm}^2$  (LCC) were noted after 14 days in culture.

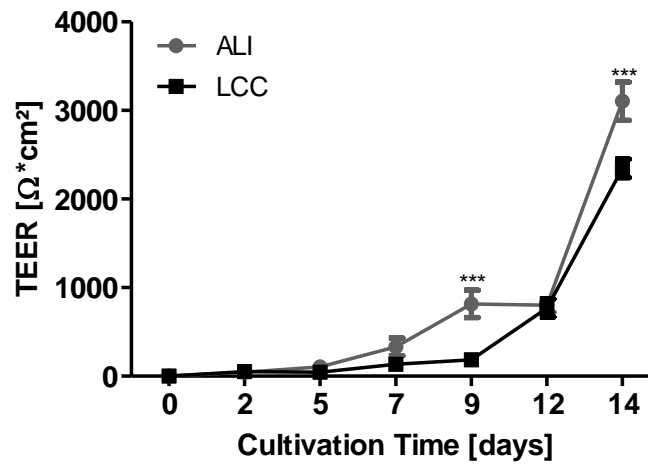


**Figure 3.1. Barrier properties of hAELVi cells.** hAELVi cells were cultured under LCC and at ALI. TEER was measured every second day for a period of 7 and 14 days. Data shown are mean  $\pm$  SEM\* ( $n=12$ ) from three independent experiments; \* $P<0.05$ ; \*\* $P<0.01$ ; \*\*\* $P<0.001$  vs. LCC.

Comparable values were observed in human alveolar epithelial cells in primary culture (hAEPc) that developed a maximum TEER of 2000  $\Omega \cdot \text{cm}^2$  after approx. 6-8 days in culture. Whereas hAEPc exhibit short life-spans of around 15 days resulting in decrease of TEER after this time [100, 127], hAELVi cells maintained high TEER values for up to 25 days [162].

To further confirm the formation of TJs, the expression of two characteristic proteins associated with the TJs, namely OCLN (Figure 3.2 A, C, E, G; green) and ZO-1 (Figure 3.2 B, D, F, H; red) were analyzed and further visualized via CLSM.

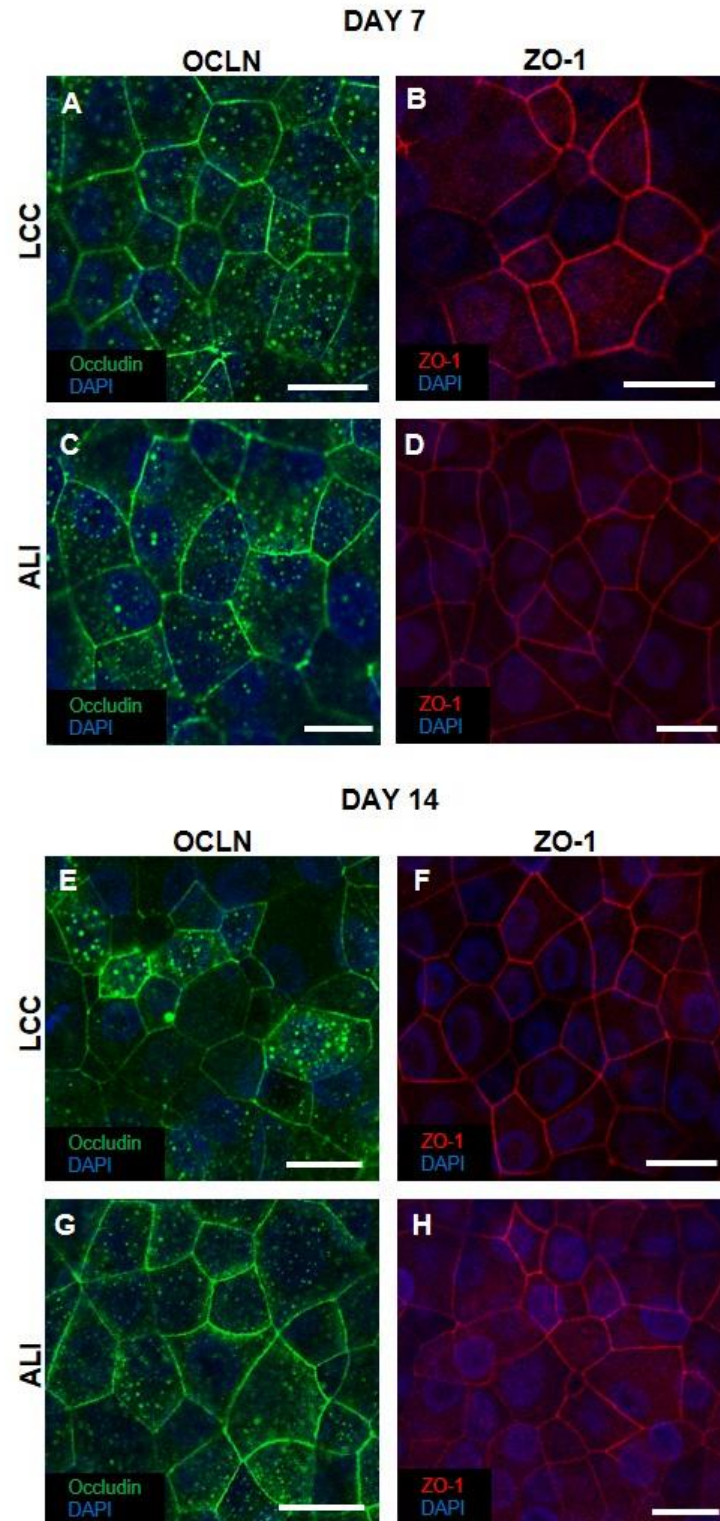


**Figure 3.2. Visualization of tight junction proteins occludin (OCLN) and zonula occludens-1 (ZO-1) in hAELVi monolayers.** Z-stack images from confocal laser scanning microscopy of hAELVi cells cultured under LCC (A, B, E, F) and at ALI (C, D, G, H) for 7 (A-D) and 14 days (E-H). tight junctions (occludin, green; ZO-1, red). Nuclei are counterstained with DAPI (blue). Scale bar: 20  $\mu$ m.

Samples cultured under LCC for either 7 or 14 days expressed both OCLN (Figure 3.2 A, E) and ZO-1 (Figure 3.2 B, F), that appears as a thin continuous line between the adjacent cells, indicating a densely packed monolayer with clearly labeled TJ complexes. Comparable to samples grown under LCC, no difference in the expression of OCLN (Figure 3.2 C, G) and ZO-1 (Figure 3.2 D, H) could be observed in cells when cultivated at ALI for 7 and 14 days. Whereas TEER measurements showed differences with regard to cultivation times and magnitude of values, no differences could be observed in CLSM images of TJ-associated proteins. This can be possibly explained by the longer period of time which TJs require to mature to functional TJs, which ultimately results in increasing TEER values.

OCLN, with a molecular weight of ~65 kDa, was the first protein found to be a major component of the TJ in 1993 [163]. It was later proposed to be involved in signaling pathways and TJ assembly [164]. Van Itallie and colleagues further investigated its role in cell-cell adhesion in several OCLN-deficient fibroblast cell lines that, however, do possess well-developed ZO-1-containing adherent junctions. They could show that exogenous OCLN co-localized with ZO-1 at points of cell-cell contact and further conferred cell-cell adhesion in these cells [165]. Further, *in vitro* and *in vivo* binding assays have shown, that ZO-1 interacts with OCLN as well as with F-actin, suggesting that ZO-1 acts as a linker between OCLN and the actin cytoskeleton [166].

As the TJs are crucial for maintaining cell polarity and junctional integrity, and therefore are forming a barrier between compartments, it is not surprising that a range of diseases are associated with the disruption of the TJs. In most cancer tissues, cells lose their polarity and contact inhibition, which further leads to migration of undifferentiated cells. Alterations in TJ integrity are also known to be involved in inflammatory diseases including inflammatory bowel disease [167, 168], multiple sclerosis [169], and diabetes [170], and may be important for the course of infections in the lung, such as asthma and CF [136, 171].

### 3.3.2 hAELVi cells exhibit tight barriers when cultivated in higher passages

To further characterize the hAELVi cells with regard to their growth behavior and their ability to exhibit a tight epithelial barrier at higher passage numbers, both hAELVi clones (hAELVi.A and hAELVi. B) were cultivated in six-well plates and seeded as previously described every 2-4 weeks to determine the TEER.

Differences were observed both in the magnitude of TEER values and in the time at which the cells started to build functional TJs. The hAELVi.A clone reached higher TEER in a shorter period of time compared to the hAELVi.B clone (Figure 3.3), indicating a faster differentiation of hAELVi.A cells. This behavior could also be observed in lower passage numbers [162]. This shift in exhibiting a tight epithelial barrier can be clearly observed at passage 69, where hAELVi.A cells displayed TEER values of  $\sim 2900 \Omega \cdot \text{cm}^2$  compared to significant lower values of  $\sim 390 \Omega \cdot \text{cm}^2$  in samples of hAELVi.B cells. This trend can clearly be observed at passage 75, where hAELVi.B showed significant lower TEER values of  $\sim 400 \Omega \cdot \text{cm}^2$  compared to hAELVi.A that already showed  $\sim 3000 \Omega \cdot \text{cm}^2$  after 17 days in culture. However, after 21 days in culture (p75) hAELVi.B cells also exhibited high values of around  $2500 \Omega \cdot \text{cm}^2$  (p75\*).

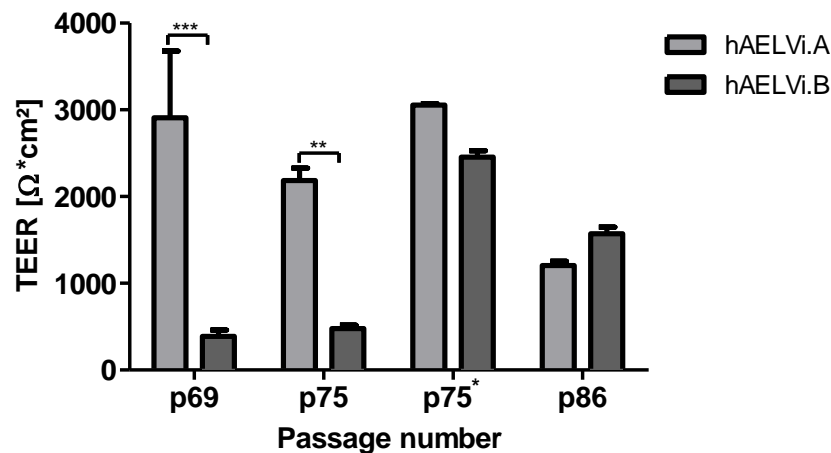


**Figure 3.3. Barrier properties of hAELVi monolayers in higher passages.** Both hAELVi clones were cultivated under LCC and TEER was measured for 17 days (p69 and p75), 21 days (p75\*) and 15 days (p86). Data shown are mean  $\pm$  SEM\* (n=4); \*\*P<0.01; \*\*\*P<0.001.

These results show that the hAELVi cells can be cultivated in higher passages and maintain their barrier function up to passage number 86, at which both clones exhibit higher TEER ( $>1000 \Omega \cdot \text{cm}^2$ ) after 15 days. To evaluate if a change in the expression of TJ proteins or an alteration in the karyotype can be responsible for such a shift, further TEER measurements in combination with analysis of TJ proteins *via* visualization or PCR as well as karyotyping should be performed in following passages.

3.3.3 Morphological analysis of monocultures under liquid covered conditions (LCC) and at air liquid interface (ALI) via histological cross-sections

Besides the characterization *via* TEM and SEM [162], histological cross-sections were conducted to characterize the hAELVi cells with regard to their morphology. Therefore, the cells were grown for 7 and 14 days before they were fixed and processed for histology examinations.

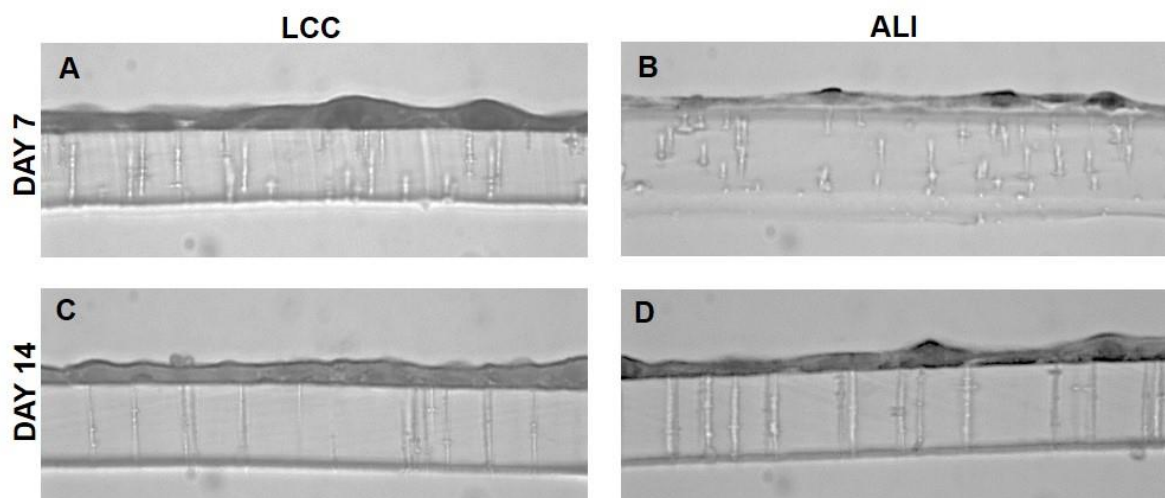


**Figure 3.4. Morphology of hAELVi cells.** *hAELVi cells cultivated under LCC (A, C) and at ALI (B, D) for 7 (A, B) and 14 days (C, D) are shown on top of Transwell® filter membranes, with membrane pore cross-sections.*

Samples cultivated under LCC for 7 days (Figure 3.4 A) showed a thicker monolayer compared to those cultivated at ALI (Figure 3.4 B). One explanation for this can be the set-up of ALI conditions, in which the cells are only fed from the basolateral compartment; hence, the cells become flattened to extend their

surface for getting nutrients. However, after 14 days in culture no difference could be observed in the histology of LCC and ALI cultured samples (Figure 3.4 C, D). This can possibly be explained by the process of sample preparation, which influences the appearance of the cells. In contrast, analyses using a normal light microscope showed differences in the appearance of the cells cultivated under LCC or at ALI. Whereas cells grown at ALI showed a homogenous monolayer, samples under LCC seemed to be heterogeneous (data not shown).

#### 3.3.4 hAELVi monocultures represent promising models to study drug absorption and transport

Further, the suitability of hAELVi cells to predict drug absorption kinetics was evaluated in cultures grown under LCC and at ALI, for 7 (Figure 3.5 A) or 14 days (Figure 3.5 B), by measuring the permeability of NaFlu through cell monolayers. This hydrophilic molecule is typically used as a marker to assess paracellular transport, alone or in combination with EDTA, the latter of which is known to modulate TJs. As TJs are attributed a so-called “fence-function” by mechanically restricting diffusion of lipids and proteins *via* the paracellular route, high TEER is always accompanied with low paracellular transport [148, 154, 157, 160].

This effect could be observed at day 7 and even more prominently at day 14, when the cells displayed TEER values of 600  $\Omega\cdot\text{cm}^2$  (LCC) and more than 1000  $\Omega\cdot\text{cm}^2$  (ALI). In the presence of EDTA, the TEER dropped to almost zero and the  $P_{\text{app}}$  value of NaFlu reached a maximum level, indicating complete opening of the TJs, resulting in elevated transport of NaFlu to the basolateral compartment.

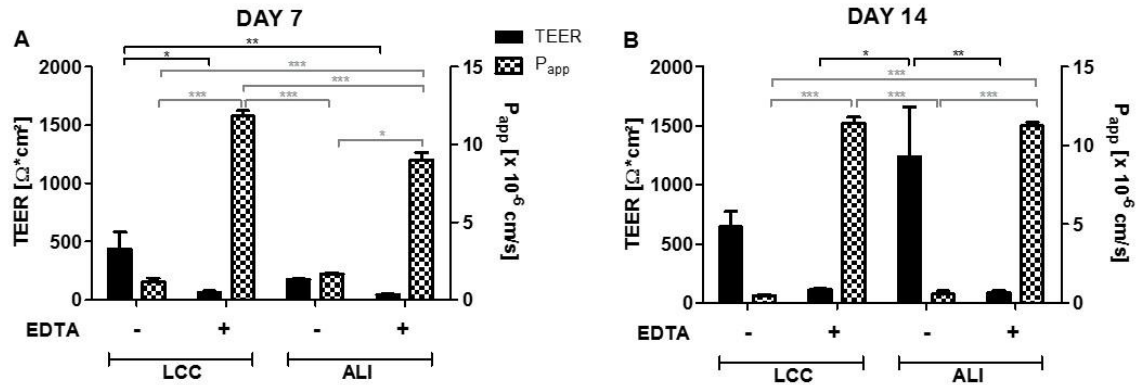


**Figure 3.5. Permeability studies in hAELVi monolayers.** Transport of NaFlu across hAELVi monolayers after 7 (A) and 14 days (B), cultivated under LCC and at ALI. Both graphs show the relation of TEER and  $P_{app}$ . Data shown are mean  $\pm$  SEM ( $n=6$ ); \* $P<0.05$ ; \*\* $P<0.01$ ; \*\*\* $P<0.001$ .

The process of removing/adding calcium ( $\text{Ca}^{2+}$ ) to cells to study TJ assembly has been used for years as it is crucial for the maintenance of cell-cell junctions [172]. Transient removal of  $\text{Ca}^{2+}$  with the aid of chelators from the culture media results in disruption of the TJs, separating the cells from each other; thus, the OCLN band around each cell is retained. This results in a decrease in the TEER and dramatic increase in the transepithelial permeability to tracers [148, 173-176].

So far, A549 cells, an adenocarcinoma-derived cell line representing a rather ATII-like phenotype, including important type II cell features such as lamellar bodies [177, 178], is a common model of the lung epithelium and has further been used in drug transport studies [122], despite the fact that A549 cells are not able to form a functional barrier. The previously established immortalized human ATI-like cell line TT1 also lacks the capacity to form a diffusional barrier to hydrophilic molecules. Nevertheless, in addition to A549 cells [100, 111, 126], TT1 has also been utilized to evaluate NP uptake and inflammatory responses [129, 130].

With respect to the tight alveolar epithelium, these cell lines are of limited value for predicting drug transport and absorption. In contrast, lung cell lines such as Calu-3 [101, 105, 106] or 16HBE14o- [110, 112-114] may be used to assess pulmonary drug delivery. However, these cell lines are of bronchial origin and differ in morphology compared to alveolar epithelial cells as they feature cilia and mucus. Regardless of their shortcomings, extensive work has been performed



using these cells - either grown in monoculture or in cocultures together with other cell lines or primary cells - to determine drug transport, to investigate cellular mechanisms or to determine interactions with particles. For example, A549 cells were cocultured with primary HPMEC cells to study the mechanisms of injury in the peripheral lung [179], or with human blood monocyte-derived macrophages and dendritic cells to evaluate the interaction with particles [126]. Considering the lack of a tight barrier, the relevance and results of such studies with regard to predicting transport across the alveolar epithelium have to be reviewed critically.

In contrast, transport studies with NaFlu showed that the hAELVi cells maintain their barrier properties and represent a promising tool to evaluate drug transport and absorption. The fact that the TJs within this model can be modulated with EDTA, in combination with the increasing knowledge of TJs and how they can be “opened” and “closed”, creates the possibility for this model to help develop new therapies for diseases where compromised TJ function is present [148].

Moreover, to enable a better comparison to primary cells and other cell lines, the occurrence of transporters that are located in the lung such as active transporters of peptides, e.g. PEPT-2, efflux systems including MRPs, P-gp and BCRP or organic cation transporters [3-6, 8, 9, 180, 181] should be examined in hAELVi cells in further experiments.

### **3.4 Conclusion**

The newly established hAELVi cell line forms monolayers with high functional and morphological resemblance to those of ATI cells, as well as tight intercellular junctions, when grown on permeable filters (Transwells®). The two obtained clones exhibited high TEER values when cultivated under LCC and at ALI, but differed in the time point at which the cells started to build functional tight junctions. hAELVi.A reached higher TEER earlier than hAELVi.B, indicating a faster differentiation. They were also able to be cultivated in higher passages and to maintain their barrier functions up to passage number 86.

CLSM images confirmed the expression of the TJ proteins OCLN and ZO-1 when hAELVi cells were cultivated under LCC and at ALI, the latter of which permits the deposition and further evaluation of aerosolized particles *via* nebulization, or dry powder formulations *via* the Pharmaceutical Aerosol Deposition Device on Cell Cultures (PADD OCC) [182].

hAELVi cells exhibit a tight barrier result in a formidable diffusion barrier for molecules that are transported *via* the paracellular route. This was confirmed by the transport of the hydrophilic molecule NaFlu, making them a promising model of the alveolar air-blood barrier for drug transport and metabolism studies.

As TJs are crucial for maintaining cell polarity as well as junctional integrity and are therefore associated with disease development, hAELVi cells can contribute in increasing the knowledge of TJ participation in various states of disease. They may further help in the development and testing of new therapies for diseases in which compromised TJ barriers are present.

To sum up, from the obtained results it can be concluded that the hAELVi cells have great potential to form the basis of meaningful *in vitro* cell models, so presenting an alternative to animal testing both in the context of pulmonary drug delivery as well as inhalation toxicology.

---

#### **4. Set-up and characterization of a new 3D *in vitro* model mimicking the human air-blood barrier in a healthy state**

The author of this thesis made the following contributions to this chapter:

Performed all cell culture experiments, measured TEER, fixed, stained, prepared samples for imaging, took confocal images and wrote the manuscript. Dr. Xabier Murgia made the profile and 3D images of the coculture. Dr. Cristiane de Souza Carvalho-Wodarz made the 3D images of the long-term coculture, Dr. Chiara De Rossi obtained the profile images of the long-term coculture and scanning electron microscope images, and transmission electron microscope images from mono-and cocultures were prepared by Dr. Urska Repnik at the University of Oslo, Norway.

## **4.1 Introduction**

*In vitro* models represent an important alternative to animal models with regard to the assessment of safety and efficacy of newly developed formulations. There are well-established *in vitro* models mimicking different organs such as the skin [183-185], intestine [144, 161, 186] or the lung [100, 126, 187, 188] utilized for several applications. As previously mentioned in the first chapter, A549 cells in monocultures [119, 189, 190], or in combination with other cell lines [189, 191-194] or primary cells [113, 126, 195] are the most commonly used model for mimicking the deep lung so far. But again, these cells are not able to form functional tight junctions. In contrast, isolated cells in primary culture reflect physiological phenotypes and form functional TJs [6, 100, 128]; but, due to limited access to primary material, short life-spans of primary cells and inter-individual differences between cell donors, they are also not suitable for high-throughput screening of new drug candidates.

For the deep lung, besides the ATI and ATII cells that form the respiratory epithelium, alveolar macrophages also play an important role in the air-blood barrier. As part of the immune system they patrol the epithelial surface and phagocytose inhaled particles, allergens, and microorganisms that are able to overcome the mucociliary barrier, and therefore are responsible for the clearance within the alveolar region [13, 16, 24, 37].

With respect to drug delivery, there is no cell line-based coculture mimicking the deep lung which displays functional TJs and also contains macrophages - two important components for studying the interaction with aerosolized drug carriers or inhaled compounds.

Therefore, this chapter describes the establishment of a new coculture consisting of the recently described hAELVi cell line, which when grown on permeable filters (Transwells®) forms monolayers with high functional and morphological resemblance to ATI cells, as well as tight intercellular junctions. To model the alveolar macrophages, the human cell line THP-1 was utilized. This commercially available cell line is derived from a human acute monocytic leukemia [196]. After treatment with phorbol-12-myristate-13-acetate (PMA), these cells can be

differentiated into macrophage-like cells that further mimic native monocyte-derived macrophages in several respects [197-200]. Numerous studies have shown that the treatment with PMA leads to the expression of macrophage-characteristic cell-surface markers such as CD11b, CD14 and toll-like receptor (TLR) 2 [198, 200-202]. Besides other immortalized human monocyte or macrophage cell lines such as HL 60, U937, ML-2 or Mono Mac 6 cells, differentiated THP-1 cells behave more like native monocyte-derived macrophages and are therefore the most commonly used cell line applied to study monocyte/macrophage differentiation and function [197, 202-206].

Technically, THP-1 cells have some advantages over human primary monocytes or macrophages. Firstly, they possess a homogenous genetic background that minimizes the degree of variability in the cell phenotype [202, 206-208]. Further, the genetic modification of THP-1 cells is relatively easy compared to primary cells [205]. In contrast to primary cells, THP-1 cells can be stored indefinitely in liquid nitrogen. Moreover, a lack of availability, and inter-individual differences due to donor variability or contamination with other blood components - drawbacks of primary cells - are not associated with cell lines such as THP-1 [202]. Another advantage of using THP-1 cells is that they can be further activated into M1 and M2 cells [202, 206]. Whereas M1 cells inhibit cell proliferation resulting in tissue damage, M2 cells promote cell proliferation and are involved in tissue repair [209]. It should always be kept in mind that cell lines mainly have a malignant background that may serve as a risk of experimental bias, as the cultivation outside their natural environment possibly results in diverging sensitivity and responses [210]. But *in vitro* coculturing may serve as an alternative to relativize these drawbacks [205].

As THP-1 cells are well-characterized and commonly used in *in vitro* models for evaluating drug delivery [211-215], inflammation [210, 216-218] and infection [219-223], they were selected for use in the current coculture model and were seeded on pre-formed hAELVi monolayers.

The coculture system was further characterized regarding barrier properties by measuring TEER, and morphological as well as ultrastructural analysis was performed with CLSM, SEM and TEM. Further, long-term cocultivation was

#### 4. Set-up and characterization of a new 3D coculture mimicking the air-blood barrier

conducted to determine the suitability of the model to study chronic lung diseases (e.g. cancer or infectious diseases). Additionally, transport studies using NaFlu, a hydrophilic marker transported *via* the paracellular route, were performed to evaluate the potential of the model to act as a tool to predict drug transport and absorption.

## **4.2 Materials and Methods**

### **4.2.1 Cell culture**

#### *4.2.1.1 Monocultures*

Epithelial cells. hAELVi cells were seeded onto permeable filters with a pore size of 0.4  $\mu\text{m}$  and growth areas of 0.33  $\text{cm}^2$  or 1.12  $\text{cm}^2$ ; the samples were cultured as previously described in section 3.2.1.

Macrophages. THP-1 cells (No. ACC-16), a monocyte-derived cell line [196], was obtained from the Deutsche Sammlung von Mikroorganismen und Zellkulturen (DSMZ; Braunschweig, Germany). The cells were grown in T75 culture flasks using Roswell Park Memorial Institute (RPMI) 1640 medium (Gibco<sup>®</sup> by Lifetechnologies<sup>™</sup>, Paisley, UK) supplemented with 10% FBS. Before using them in experiments, the suspension cells were differentiated by adding 7.5 ng/mL PMA (Sigma, Germany) to cell culture medium [198] and further incubated for 48 h [161]. Afterwards,  $9.4 \times 10^4$  cells were seeded on Transwell<sup>®</sup> filters with a pore size of 0.4  $\mu\text{m}$  and a growth area of 1.12  $\text{cm}^2$  under LCC (500 mL apical / 1.5 mL basolateral) in RPMI medium containing 10% (v/v) FBS and 1% (v/v) P/S. After allowing the cells to adhere for 4 h they were divided into two groups: one group was kept cultivated under LCC, the other was set on ALL, *i.e.* the cells were further fed from the basolateral compartment only with 500  $\mu\text{L}$  of RPMI.

Monocultures of hAELVi and THP-1 cells cultivated alongside the coculture were used as internal controls.

#### *4.2.1.2 Cocultures*

Epithelial cells were pre-grown for 14 days before the cocultures were set up. After differentiation for 48 h with 7.5 ng/mL PMA, THP-1 cells were seeded on top of the epithelial layer in a ratio of 3:1 (hAELVi cells:THP-1) [224]. To set up the coculture under LCC, 500  $\mu\text{L}$  RPMI medium containing THP-1 cell

#### 4. Set-up and characterization of a new 3D coculture mimicking the air-blood barrier

suspension was added to the apical compartment and 1.5 mL SAGM was added to the basolateral compartment. For cocultures cultivated at ALI, 6  $\mu$ L RPMI containing THP-1 cells was carefully pipetted into the middle of the apical compartment and 500  $\mu$ L SAGM was added to the basolateral area. The cocultures were cultivated for 24 h before the experiments were conducted.

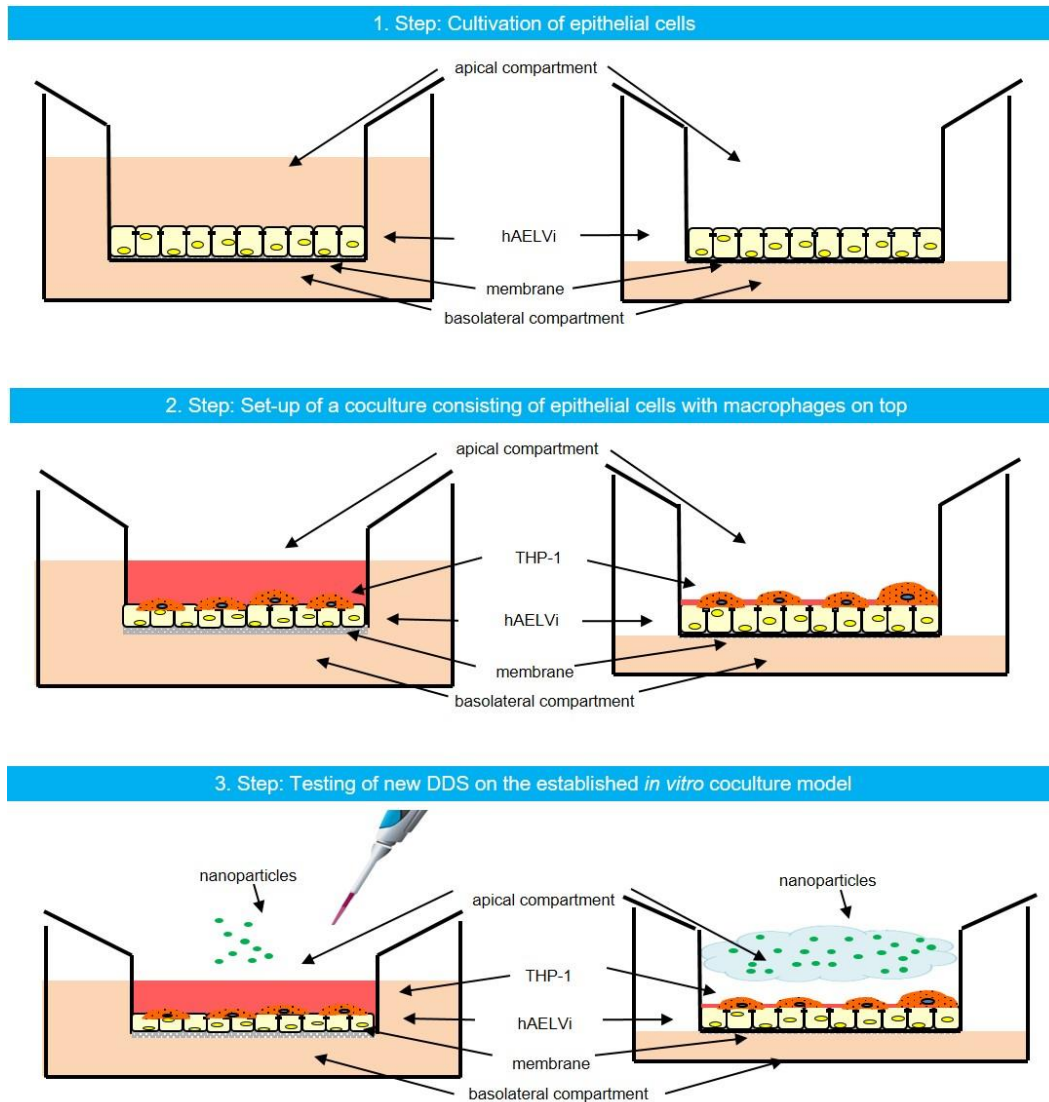


**Figure 4.1. Experimental design of the coculture set-up.** After seeding and subsequent cultivation of epithelial cells under liquid-covered conditions (left images) and at air-liquid interface (right images), previously differentiated macrophage-like cells are seeded on top. Further, new drug delivery systems (DDS, namely, nanoparticles) are added by pipetting or via nebulization onto the coculture and subsequently evaluated regarding cytotoxicity, their impact on barrier functions and cellular interaction.



#### 4. Set-up and characterization of a new 3D coculture mimicking the air-blood barrier

To evaluate the capability of the system to be used for studying chronic diseases or infections, the coculture was set up as previously described. In addition to a 24 h / 1 day coculture, the model was further cocultivated for 3 and 7 days. To monitor the cell viabilities and the integrity of the epithelial barrier, CLSM analysis and TEER measurements were conducted.

The main experiments were performed at ALI and were further compared to samples cultivated under LCC.

##### *4.2.1.3 Macrophage-conditioned medium*

To evaluate the impact of macrophages on the epithelial barrier, hAELVi monocultures were incubated with conditioned media in the apical compartment, whereas SAGM was added in the basolateral compartment. The conditioned media was either obtained from THP-1 monocultures or from previously set up cocultures. hAELVi monocultures incubated with RPMI in the apical compartment and SAGM in the basolateral compartment as well as hAELVi-THP-1 cocultures were used as controls. TEER measurements were conducted to monitor the effect of those conditioned media.

##### 4.2.2 Transepithelial electrical resistance (TEER)

TEER was evaluated as previously described in section 3.2.2.

##### 4.2.3 Morphological and ultrastructural analysis of mono- and cocultures

###### *4.2.3.1 Confocal laser scanning microscopy (CLSM)*

To analyze the coculture with CLSM, previously differentiated THP-1 cells were pre-stained before set up of the coculture. For that, a live cell dye was used: 7-hydroxy-9H-(1,3-dichloro-9,9-dimethylacridin-2-one)-succinimidyl ester (DDAO-SE, CellTrace™ Far Red; Molecular Probes, USA), following the

manufacturer's protocol. Briefly, the lyophilized tracer was solubilized with 20  $\mu$ L dimethyl sulfoxide (DMSO) to obtain a stock solution with a concentration of 1 mM DDAO-SE. To pre-label the cells, 7 mL pre-warmed PBS containing 5  $\mu$ M DDAO-SE was added to the cells and further incubated for 15 min at 37 °C. After aspirating the staining solution, the differentiated THP-1 cells were incubated with 12 mL medium for a further 30 min before seeding onto the epithelial cells.

Immunohistochemical staining for the TJ protein OCLN was performed as previously described [146, 162] with minor modifications. Briefly, after 24 h in coculture the system was fixed with 3% methanol free PFA (stock 16%; 15710-S, Electron Microscopy Sciences, USA) in PBS from basolateral side overnight at 4 °C. The monocultures of hAELVi were treated in a similar way. The following steps including quenching, blocking, permeabilizing and staining were then performed from the apical compartment of cocultures and monocultures, similar to the procedure described in chapter 3. In brief, the samples were quenched with 150  $\mu$ L of 50 mM  $\text{NH}_4\text{Cl}$  in PBS for 10 min, followed by a blocking and permeabilizing step using a mixture of 0.5% BSA / 0.025% Saponin in PBS for 30 min at RT. The primary antibody against OCLN (mouse anti-occludin, Catalog No 33-1500, Invitrogen) was diluted 1:200 in 0.5% BSA / 0.025% Saponin/PBS-solution; 150  $\mu$ L was then added apically followed by an incubation at 4 °C overnight. The secondary antibody (polyclonal Alexa-Fluor 488 conjugated rabbit anti-mouse, Catalog No. A11059, Invitrogen) was diluted 1:400 in PBS and incubated for 1 h at RT. The samples were washed with PBS and counterstained with DAPI (1:50000). Transwell® membranes were then cut out of the filter insert structure, mounted in DAKO mounting medium (Product No. 85 S302380-2, DAKO, USA) and analyzed by CLSM (Zeiss LSM710, Zeiss, Germany). Lasers at 405 nm (DAPI), 488 nm (OCLN) and 633 nm (DDAO-SE) were applied for detection. Microscopic images were acquired at 1024  $\times$  1024 resolution, using 63x water immersion objective. Confocal images were analyzed using Zen 2012 software (Carl Zeiss Microscopy GmbH) and Fiji Software (Fiji is a distribution of ImageJ available at <http://fiji.sc>).

To visualize long-term cocultures, hAELVi cells were cultivated as mentioned earlier. THP-1 cells were pre-labeled with DDAO-SE as previously described

before setting up the coculture. 3D and profile images of the cocultures cultivated 3 and 7 days were obtained by CLSM (Leica TCS SP 8; Leica, Mannheim, Germany), using the same laser and magnification settings. Analysis was performed using LAS X software (Leica Application Suite X; Leica, Mannheim, Germany).

##### *4.2.3.2 Scanning electron microscopy (SEM)*

Mono- and cocultures were set up as described above in section 4.2.1, and fixed after 24 h by adding 3% PFA to the basolateral compartment with a 4 °C overnight incubation. The next day, the samples were dehydrated by treatment with graduated ethanol concentrations (30, 50, 60, 70, 80, 90, 96, 100 and a further 100% solution, for 10 min each) followed by incubation with hexamethyldisilazane (HMDS) for 10 min. After aspiration of HMDS, the samples were dried under a fume hood. Then, the Transwell® membranes were cut out of the filter insert structure with a scalpel, put on a carbon disc and further sputtered with gold before examination by SEM. Images were taken with a Zeiss SEM EVO® HD15 (Zeiss, Germany) under high pressure conditions with a secondary electron detector and using 10 kV acceleration voltage.

##### *4.2.3.3 Transmission electron microscopy (TEM)*

Mono- and cocultures were cultivated as described earlier in sections 4.2.1.1 and 4.2.1.2. Fixation was performed after 15 days (hAELVi monocultures) or 24 h (THP-1 monocultures, cocultures) using a 1% final concentration of glutaraldehyde (GA). This was achieved either by adding 1 or 2% GA to well compartments. 1% or 2% solutions of GA were prepared by dilution of 50% GA stock solution with 200 mM 2-[4-(2-hydroxyethyl) piperazin-1-yl] ethanesulfonic acid (HEPES) buffer, pH 7.4. Thus, samples cultured at ALI were fixed by adding 1% GA to the apical (1 mL) and the basolateral (1.5 mL) compartment. Samples cultivated under LCC were fixed by adding 500 µL 2% GA to the apical and

1.5 mL of 1% GA to the basolateral compartment. All samples were incubated with GA overnight at 4 °C. For further sample preparation and imaging, Transwell® membrane inserts were transferred to 50 mL falcon tubes filled with 200 mM HEPES buffer and subsequently shipped to Dr. Urska Repnik and Prof. Dr. Gareth Griffiths at the University of Oslo, Norway. The samples were further processed as described by Susewind *et al.* [161] with minor modifications. Briefly, for epon embedding the samples were post-fixed with a 2% OsO<sub>4</sub> (EMA, PA, USA) solution containing 1.5% potassium ferricyanide for 1 h on ice, and stained *en bloc* with 1.5% aqueous uranyl acetate (EMS, PA, USA) for 30 min. Cells were then dehydrated at RT using a graded ethanol series (70, 80, 90, 96, (4x)100% for 10 min each), and progressively infiltrated with epoxy resin (50, 75 and 100%) (Sigma-Aldrich; St. Louis/MO, USA). Transwell® membranes with cells were flat embedded and blocks were polymerized overnight at 70 °C. Ultrathin sections of 70-80 nm, perpendicular to the filter plane, were cut with a Leica ultra-microtome Ultracut EM UCT (Leica Microsystems, Austria) using an ultra-diamond knife (Diatome, Switzerland) and examined with a JEM-1400 transmission electron microscope (JEOL, USA). The images were taken with a TemCam-F216 camera (Tvips, Germany).

#### 4.2.4 Transport studies

Transport experiments were performed as previously described in chapter 3 with minor modifications. Briefly, monocultures of hAELVi cells and cocultures were set up and cultivated under LCC and at ALI as described earlier. The transport of NaFlu alone and in combination with 16 mM EDTA was performed. After 24 h of coculture, the samples were washed once with pre-warmed KRB. To avoid losing macrophages during the washing step, the supernatant of the coculture was collected and centrifuged. Afterwards, the pellet was resuspended in 500 µL KRB and added to the apical compartment. Both mono- and cocultures were further incubated with KRB for 45 min. After TEER measurements to ensure the initial integrity of the monolayer, the medium was aspirated and treated as described before. The centrifuged pellet was resuspended in 520 µL NaFlu

#### 4. Set-up and characterization of a new 3D coculture mimicking the air-blood barrier

(10 µg/mL in KRB) ± 16 mM EDTA, which was then added to the apical compartment (donor). A 1.7 mL volume of KRB was added to the basolateral compartment (acceptor). The following steps including taking samples, measurements and analysis were performed as previously described in section 3.2.3.

#### 4.2.5 Statistical analysis

Data represent 1-3 independent experiments and are shown as mean ± standard error of mean (SEM<sup>\*</sup>). Two-way ANOVA with Bonferroni's post hoc test was performed using GraphPad Prism 5 software (GraphPad).

### **4.3 Results and Discussion**

#### **4.3.1 Differentiation of THP-1 into macrophage-like cells**

THP-1 cells are round monocytic cells that normally grow in suspension [196], (Figure 4.2 A). Before their use in the coculture model, they were differentiated into macrophage-like cells by treatment with PMA [197-200].

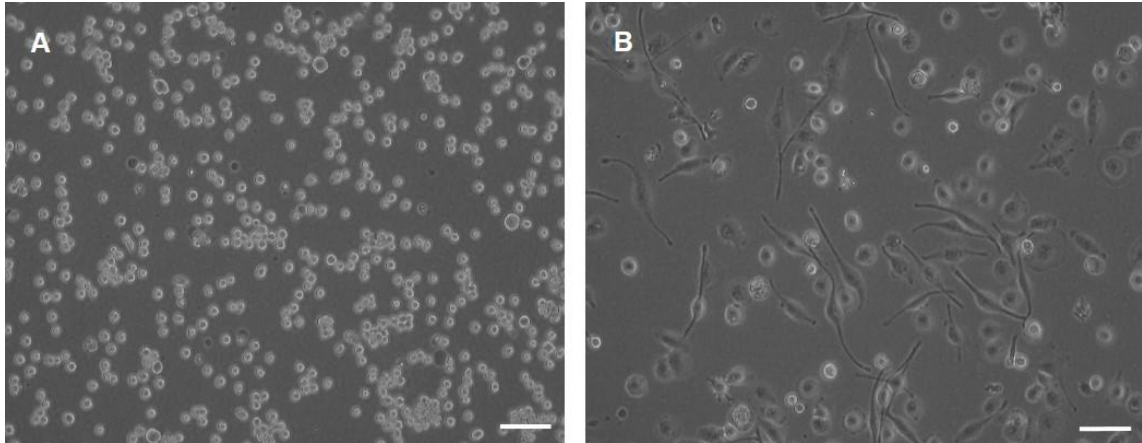


**Figure 4.2. Differentiation of THP-1.** A: THP-1 monocytes, normally growing as suspension cells. B: THP-1 macrophage-like cells after differentiation with PMA. Such cells become adherent, exhibit cellular extension and lose their ability to proliferate. Scale bar: 5  $\mu\text{m}$ .

The differentiation is also accompanied by an alteration in morphology: cells become flat and amoeboid in shape [197, 203]. Further, it results in loss of proliferation due to cell cycle arrest in the  $G_1$ -phase *via* complex mechanisms associated with the modulation of the expression of several cell cycle regulators [199]. Further, cells become adherent to cell culture plastic [197], (Figure 4.2 B).

### 4.3.2 Coculture: epithelial barrier properties

The coculture of hAELVi cells and THP-1 macrophages was set up at ALI and under LCC. Both conditions were assessed simultaneously in order to better compare the differences between these culture conditions. For this purpose, hAELVi cells were seeded on prior FN/COL-coated polyester membranes with a pore size of 0.4  $\mu\text{m}$  under LCC for two days. Afterwards, some samples were exposed to ALI, while others were kept under LCC. After 14 days in culture, previously differentiated THP-1 cells were added on top of the epithelial cells. TEER values were determined after 1 day in coculture.

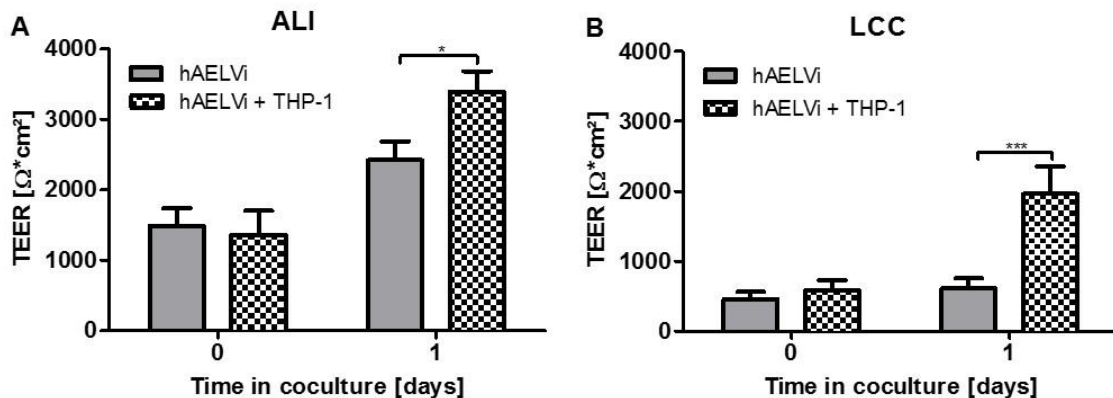


**Figure 4.3. Barrier properties of hAELVi/THP-1 cocultures.** TEER-measurements of hAELVi cell monolayers pre-grown for 14 days, immediately before (0 day) and 1 day after coculture with THP-1 cells, either at ALI (A) or under LCC (B). Data shown represent mean  $\pm$  SEM\* (n=9) from three independent experiments; \*P<0.05; \*\*\*P<0.001.

The results showed that hAELVi cells maintained higher TEER in coculture as compared to the monocultures (Figure 4.3 A, B). This effect was more distinct in samples grown under LCC. Indeed, an increase in the TEER has been observed in the coculture of 16HBE14o- and human umbilical vein endothelial cells (HUVEC) as introduced by Chowdhury *et al.* [225]. They suggested that endothelial-derived factors contributed to the increased TEER. To address the possibility that also THP-1 cells secrete factors that influence the epithelial barrier, hAELVi monocultures were incubated with supernatants from THP-1 monocultures (SN<sub>A</sub>) or from cocultures (SN<sub>B</sub>) obtained after 24 h in coculture. These results were compared to the coculture under LCC (hAELVi + THP-1), in which hAELVi cells were fed from the apical side with RPMI medium and with

SAGM from the basolateral. Epithelial cells grown with the same medium composition but without macrophages (hAELVi monoculture) were used in order to exclude the effect of macrophages themselves on the barrier property (Figure 4.4).

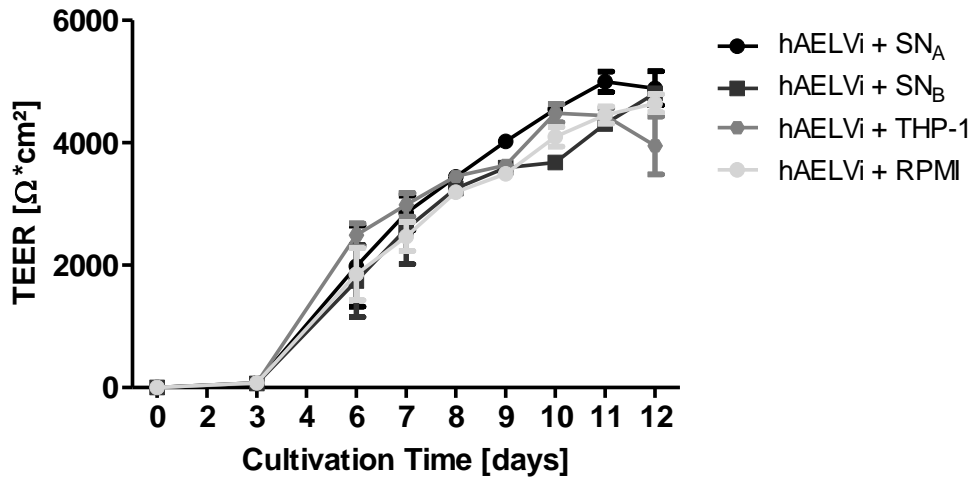


**Figure 4.4. Impact of macrophages on barrier properties of hAELVi cells.** *TEER* measurements of hAELVi cells in coculture with THP-1 cells, hAELVi cells incubated with pure RPMI and supernatants of THP-1 (“hAELVi + SN<sub>A</sub>”) and from previously set up cocultures (“hAELVi + SN<sub>B</sub>”). Data shown represent mean ± SEM\* (n=3) of two independent experiments.

The results showed no difference in the TEER when hAELVi cells were incubated with supernatant samples compared to the coculture, which suggests that there are no factors secreted from THP-1 cells either alone or when in contact with hAELVi cells that could interfere with the epithelial barrier integrity. Moreover, cell-cell interaction between macrophages and epithelial cells also did not influence the TEER, since hAELVi monocultures cultivated with the same medium composition as used for the coculture (*i.e.* RPMI in the apical compartment and SAGM in the basolateral) showed as high TEER as the coculture. Taken together, these results suggest that the higher TEER observed in the cocultures is due to the fact that hAELVi cells are in contact with different media (RPMI and SAGM).



#### 4.3.2.1 Influence of SAGM and RPMI media on TEER values

SAGM is a complex medium containing several growth factors such as bovine pituitary extract, hydrocortisone, human epidermal growth factor, epinephrine, transferrin, insulin, retinoic acid, triiodothyronine, BSA-fatty acid free, antibiotics such as gentamicin/amphotericin-B and 1% (v/v) P/S, as well as 1% (v/v) FBS. By comparison, RPMI 1640 medium lacks these ingredients and includes only 10% of serum. hAELVi cells in coculture cultivated under LCC are supplied with 500  $\mu$ L RPMI in the apical and 1.5 mL SAGM in the basolateral compartment. Therefore, of the complete media in contact with hAELVi cells, approximately 25% is constituted by RPMI, with the remaining 75% represented by SAGM. To address the effect of different proportions of media on the TEER values, hAELVi monocultures were incubated with the following SAGM:RPMI proportions (%): 100:0, 20:80, 30:70, 40:60, 60:40 and 0:100.

The results showed that hAELVi cells do not form any barrier when cultivated in pure RPMI, which is expected due to the lack of growth factors normally supplied by the SAGM. hAELVi cells cultivated with SAGM alone showed a maximum TEER of  $\sim 1000 \Omega \cdot \text{cm}^2$  after 9 days, whereas for all media combinations the TEER reached values in a range of  $\sim 2500\text{-}3700 \Omega \cdot \text{cm}^2$  (Figure 4.5). Unexpectedly, hAELVi cells formed a barrier also with a minimum amount of SAGM (e.g. 20%; Figure 4.5). This indicates a synergistic effect of both media that requires only a small amount of RPMI to result in an enormous increase in TEER. To get a detailed insight into the mechanism by which RPMI possibly influences the formation of TJs, protein expression and finally the associated barrier properties of hAELVi cells should be evaluated in future studies. Nevertheless, it can be concluded that the barrier properties of hAELVi cells are not affected when in contact with the culture medium of THP-1 cells. This medium can be therefore used in the coculture set-up.

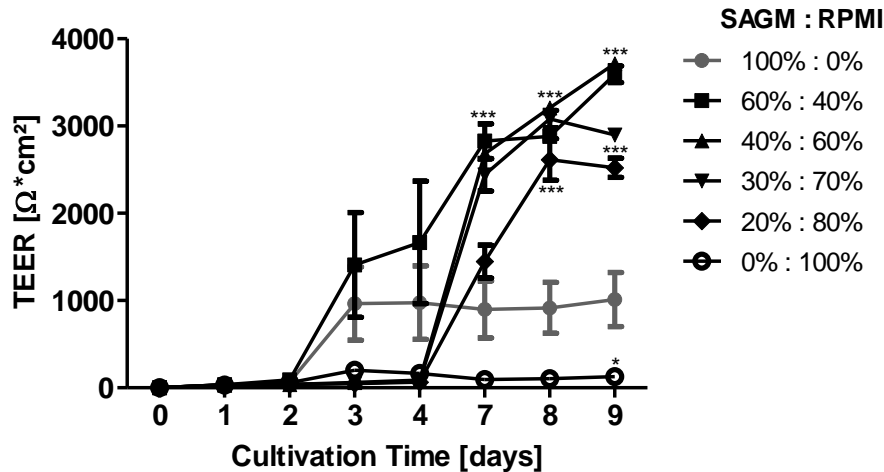


**Figure 4.5. Impact of different medium compositions on hAELVi cells, cultured under LCC.** TEER measurements of hAELVi monocultures incubated with mixed media (SAGM:RPMI) in different ratios. Data shown represent mean  $\pm$  SEM\* (n=6) from two independent experiments; \* $P < 0.05$ ; \*\* $P < 0.01$ ; \*\*\* $P < 0.001$  vs. 100%:0%.

As previously mentioned, hAELVi and THP-1 cells are usually cultivated in SAGM and RPMI media, with 1% or 10% (v/v) FBS, respectively. This difference can account for the higher TEER even when hAELVi cells are supplied with 20% of SAGM, as shown above (Figure 4.5). Therefore, hAELVi monocultures grown on permeable filters were cultivated with pure SAGM or RPMI containing 1 or 10% of FBS. Additionally, RPMI containing 1 or 10% FBS was applied in the apical compartment, whereas SAGM with 1% serum was added in the basolateral compartment. These variants were compared with the classical medium of hAELVi cultivation (SAGM + 1% FBS; Figure 4.6).

The results showed that hAELVi cells do not form any barrier when cultivated in RPMI regardless of the serum concentration (RPMI 1% or 10% FBS). However, hAELVi cells incubated with SAGM supplemented with 10% FBS showed higher TEER after 12 days (up to  $\sim 4000 \Omega \cdot \text{cm}^2$ ) compared to TEER values observed in samples incubated with the same medium containing 1% of FBS ( $\sim 1700 \Omega \cdot \text{cm}^2$ ). Indeed, such TEER was similar to that observed in the coculture with classical coculture set-up (RPMI + 10% FBS together with SAGM + 1% FBS), which indicate that serum concentration contribute to higher TEER values in hAELVi cells. This was even more evident when RPMI containing 10% of FBS and SAGM with 1% serum were incubated on the hAELVi cells (Figure 4.6).

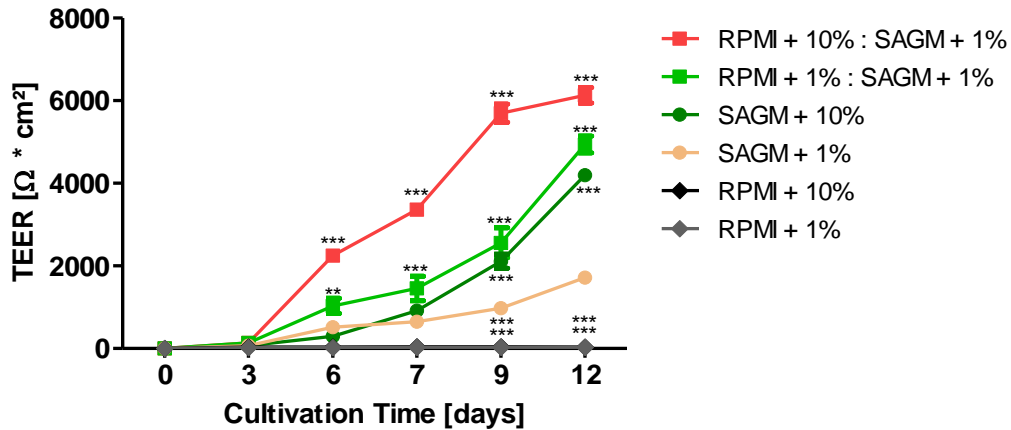


**Figure 4.6. Influence of pure and mixed media containing different amounts of serum on hAELVi cells, grown under LCC. TEER measurements of hAELVi monocultures. Data shown represent mean  $\pm$  SEM\* ( $n=6$ ) from two independent experiments; \*\*\* $P<0.001$  vs. SAGM + 1%. % indicates the concentration of FBS in the media.**

Taken together, these results show that the higher TEER observed in the cocultures is mainly due to the higher serum concentration in RPMI medium. Nevertheless, as already discussed, a synergistic effect of RPMI in combination with SAGM contributes to the increased TEER. Moreover, these results could validate the use of hAELVi cells with medium comprising a lower proportion of SAGM, which would reduce the cost of maintaining these cells.

#### 4.3.3 Coculture: morphological characterization

CLSM images confirmed the findings of developed TEER in cocultures as preserved TJs could be observed when grown at ALI and under LCC (Figure 4.3 A, B). In contrast to cocultures set up at ALI, where macrophages were located on top of the epithelial cells (Figure 4.7 A), only few THP-1 cells could be found on hAELVi monolayers under LCC (Figure 4.7 B).

#### 4. Set-up and characterization of a new 3D coculture mimicking the air-blood barrier

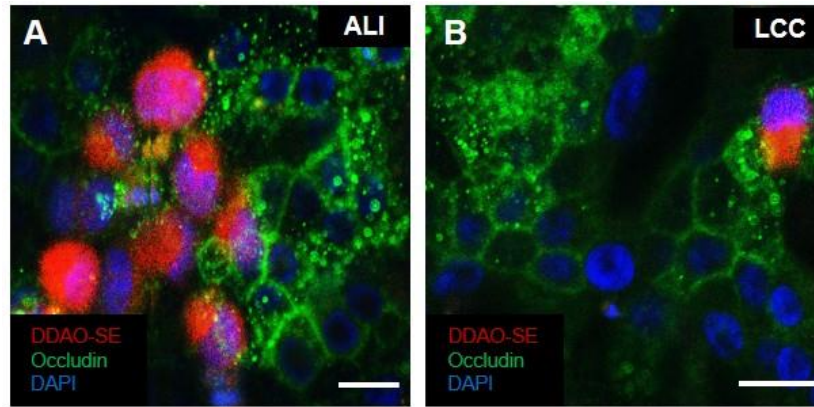


**Figure 4.7. Morphology of hAELVi-/THP-1 cocultures.** Confocal laser scanning microscopic (CLSM) images of hAELVi-/THP-1 cocultures, cultivated at ALI (A) and under LCC (B). THP-1 cells (DDAO-SE; red), tight junctions (occludin; green). Nuclei are counterstained with DAPI (blue). Scale bar: 20  $\mu\text{m}$ .

Z-stacks (Figure 4.8 A, B, D, and E) as well as cross-section views of the cocultures (Figure 4.8 C, F) reinforce the observation from Figure 4.7, in which fewer macrophages are observed in cultures under LCC.

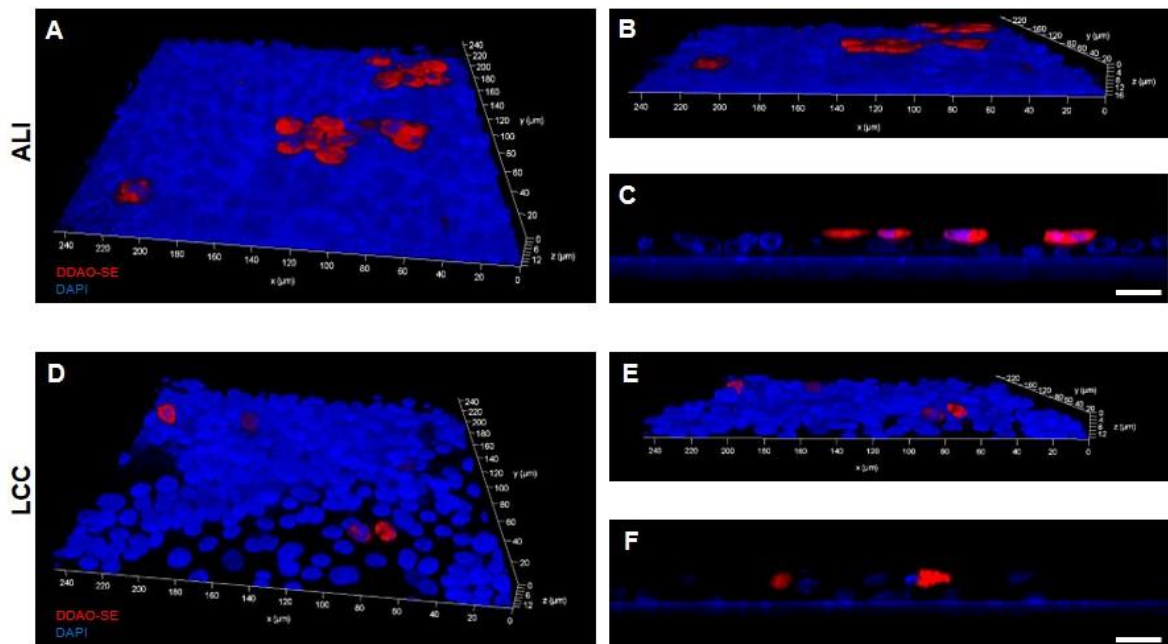


**Figure 4.8. Morphology of hAELVi-/THP-1 cocultures.** 3D images (A, B, D, E) and cross-sections (C, F) of hAELVi-/THP-1 cocultures, grown at ALI (A-C) and under LCC (D-F) for 1 day. THP-1 cells (DDAO-SE; red). Nuclei are counterstained with DAPI (blue). Scale bar: 40  $\mu\text{m}$ .

The intrinsic limitation of the coculture set-up under LCC may still lead to a reduction of macrophages to a significant extent, *e.g.* during the change of cell culture medium. This suggests a rather weak interaction between macrophages and epithelial cells when cultivated under LCC, as samples grown at ALI showed more THP-1 cells when analyzed with CLSM although the samples were processed in the same way. In any case, the use of cocultures at ALI is recommended as this is the physiological condition in the alveoli.

However, when comparing ALI and LCC, SEM images showed similar amounts of macrophages homogeneously distributed on top of epithelial cells (Figure 4.9 A, B). This contradiction in observations by CLSM and SEM is most likely due to the sample preparation rather than the culture condition itself. Whereas for CLSM analysis the fixation procedure was conducted from the apical side, labeling and washing steps were conducted from the basolateral side. In contrast, all steps in the preparation for SEM imaging was done from basolateral side, which might reduce the loss of macrophages.

Epithelial cells cultivated under LCC, display additional structures on their surfaces (Figure 4.9 D). As all samples were handled as “cocultures”, in which the loss of macrophages should be minimized during sample preparation, the medium was carefully aspirated from the apical compartment, further washing steps were left out and all steps during preparation were performed from the basolateral side. As these structures could not be observed on cells grown at ALI, it seems to be more likely that these are residues from the medium applied in the apical compartment during cultivation. Additionally, cells exposed to ALI appeared more homogeneous in size (Figure 4.9 C).

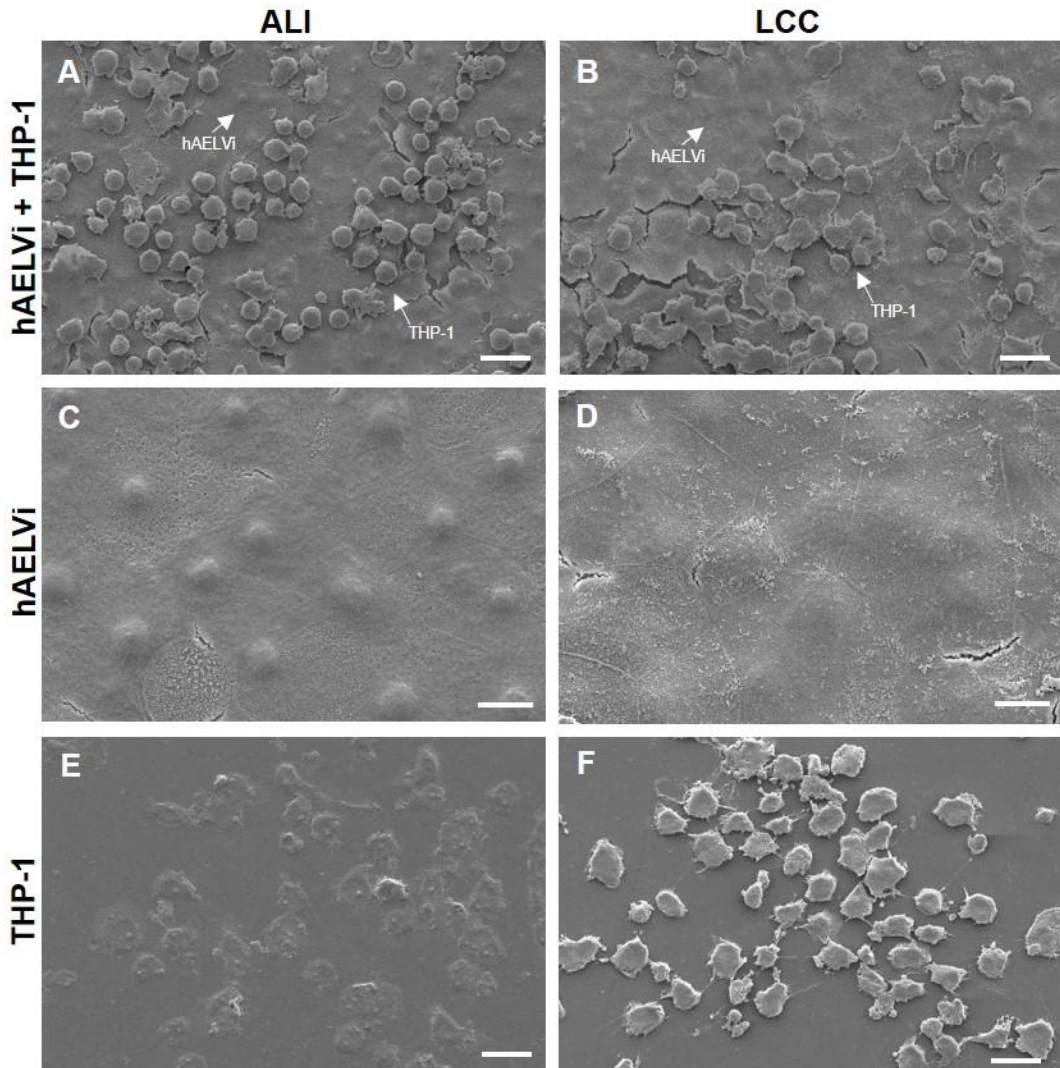


**Figure 4.9. SEM images of hAELVi and THP-1 monocultures as well as cocultures.** *A, B: Cocultures of hAELVi and THP-1 grown at ALI (A) and under LCC (B). Scale bar: 30  $\mu$ m. C, D: hAELVi cells in monoculture, cultivated at ALI (C) and under LCC (D) for 15 days. Scale bar: 10  $\mu$ m. E, F: THP-1 monocultures grown for 1 day, either at ALI (E) or under LCC (F). Scale bar: 30  $\mu$ m.*

Furthermore, THP-1 cells grown at ALI seem to be more attached to the membrane and appear flattened in shape (Figure 4.9 E). One explanation could be that the cells extend their surface to increase their capacity of nutrient uptake. Under LCC displayed different phenotypes ranging from rounded to amoeboid with cellular extensions (Figure 4.9 F). But under both culture conditions, they display cellular extensions, with which they get in contact with each other.

To further visualize differentiated THP-1 cells with CLSM, cells were pre-labeled with a red dye before seeding into chamber slides either under LCC or at ALI for 24 h. CLSM images showed that THP-1 cells grown at ALI (Figure 4.10 A) are bigger in size compared to those cultivated under LCC (Figure 4.10 B).

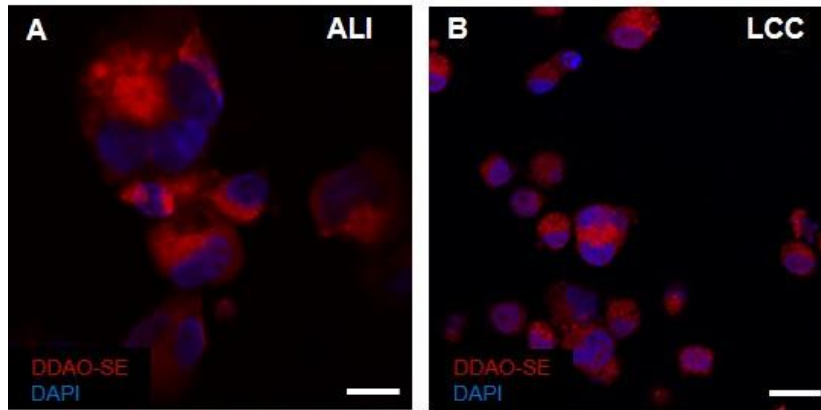


**Figure 4.10. Morphology of THP-1 monocultures.** CLSM images of differentiated THP-1 cells grown at ALI (A) and under LCC (B). THP-1 cells (DDAO-SE, red); nuclei were further counterstained with DAPI (blue). Scale bar: 20  $\mu$ m.

This may be explained by the fact that THP-1 cultivated under LCC are in contact with medium from two compartments, resulting in more serum supply. In contrast, cells grown at ALI just get their nutrients from the basolateral compartment, resulting in cell enlargement in order to extend their surface and increase their nutrient ingestion. These findings were also supported by data of Kreft *et al.* who observed that Calu-3 cells cultivated under LCC were significantly smaller than those grown at ALI in the first week of culturing [226].

For hAELVi cells in monoculture the results obtained here regarding morphological characterization by CLSM or SEM agree with those previously described in chapter 3.

#### 4.3.4 Coculture: ultrastructural characterization

To further characterize the coculture, ultrastructural analysis was conducted in collaboration with the University of Oslo. TEM images of coculture samples that were set up at ALI showed several macrophages located on top of the epithelium (Figure 4.11 A), interacting to some extent with epithelial cells (Figure 4.11 B). While hAELVi cells interact with pseudopodia and express TJs (Figure 4.11 C), confirming the results obtained by immunostaining of the TJs (see section 4.3.5), THP-1 cells communicate *via* pseudopodia (Pp; Figure 4.11 G) that are not located on the whole surface of the cell, but more on the lateral and underside, indicating a sampling of the epithelial area. As the macrophage-like cells seem to be in a “resting” state, the application of particles may lead to activation in terms of motility and display of pseudopodia which are known to be involved in phagocytosis [227-229].

Interestingly, when in coculture, THP-1 cells are covered with an extracellular matrix layer and hAELVi cells are covered with a glycocalyx-like structure, a protective layer that has been shown to shield the human airway epithelial cells from virus-mediated gene transfer [230]. As this could not be observed in THP-1 monocultures, it can be speculated that either hAELVi cells secrete factors that modify the surface of macrophage-like cells or sediment on top of these cells. To get more detailed information about the crosstalk between both cell types, appropriate experiments should be included in future studies, for example to test the effect of conditioned medium.

Ultrastructural analysis of hAELVi monocultures was already carried out in the course of the characterization of the recently established hAELVi cell line [162]. Nevertheless, to run a complete set-up, hAELVi cells were also grown under LCC and at ALI in parallel to THP-1 monocultures and combined cell systems. As the epithelial monocultures showed no additional information however, they are not shown in this thesis.



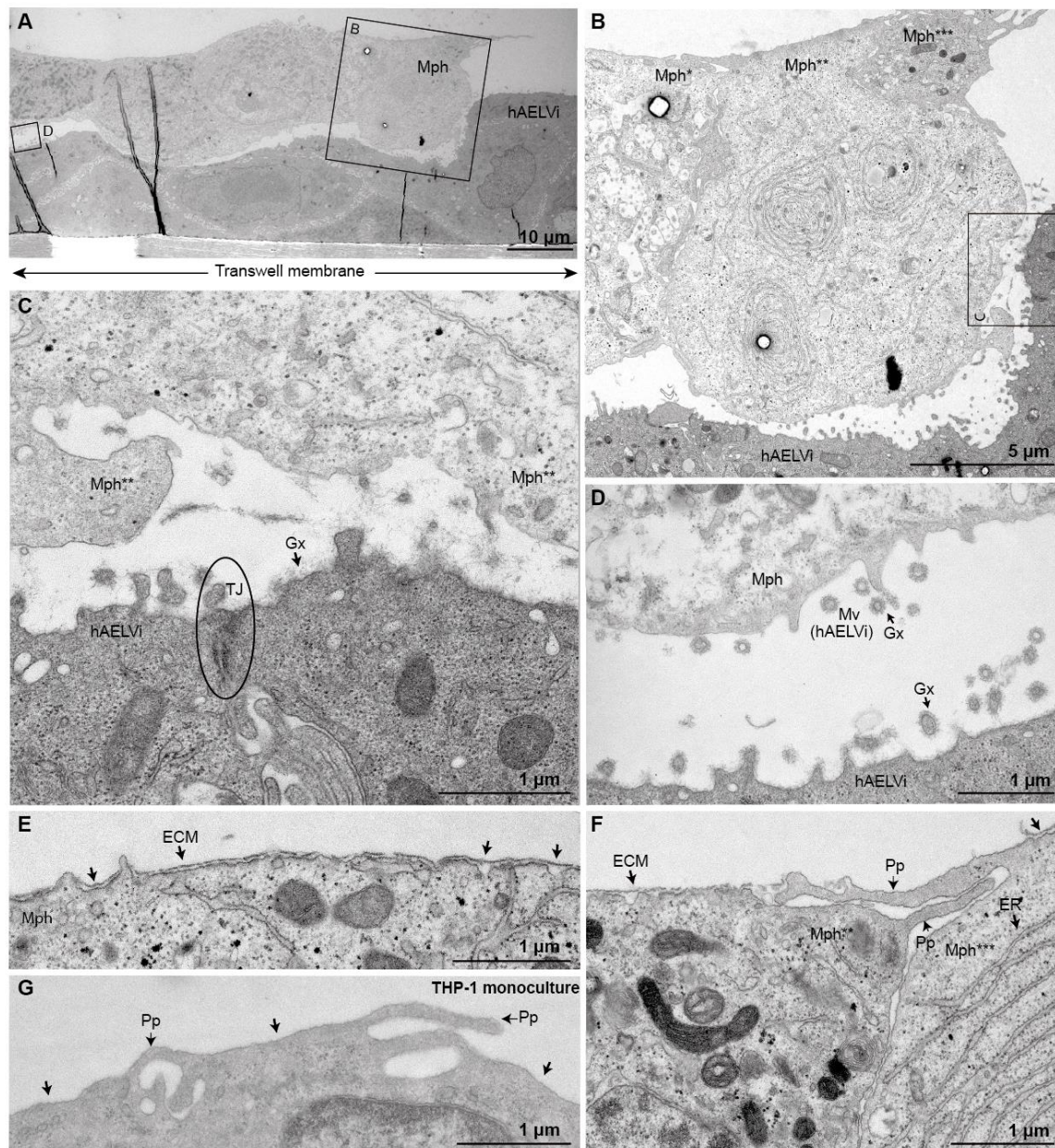


**Figure 4.11. Ultrastructural analysis of hAELVi-THP-1 cocultures.** Transmission electron microscopic (TEM) images of hAELVi cells after 24 h in coculture with THP-1 cells. A: Overview of several macrophage-like cells on top of epithelial cells. B: Slight interaction of a THP-1 cell with hAELVi cells (magnification of A). C: Cleft between both cell types; hAELVi cells display tight junctions (TJ), microvilli (Mv) and glycocalyx (Gx) on top (magnification of B). D: Cross-sections of the space between hAELVi cells and THP-1. E, F: Surfaces of a THP-1 cell, either exposed to the air (E) showing Gx, or under LCC (F). G: Communication of two THP-1 cells via pseudopodia (Pp), expressing ER cisternae.

#### 4. Set-up and characterization of a new 3D coculture mimicking the air-blood barrier

TEM images of THP-1 monocultures showed several differences between both culture conditions, although the cells display cellular extensions, so-called pseudopodia, on their surfaces when grown under LCC (Figure 4.12 A) as well as at ALI (Figure 4.12 C). Besides involvement in moving processes, pseudopodia are mainly responsible for engulfing foreign particles or cell debris [231-236]. When cultured under LCC, THP-1 cells display a prominent Golgi apparatus (GA\*), phagocytic vacuoles in the cytoplasm and endoplasmic reticulum (ER) cisternae (Figure 4.12 B), confirming the findings of differentiated THP-1 already described in literature [197, 203].

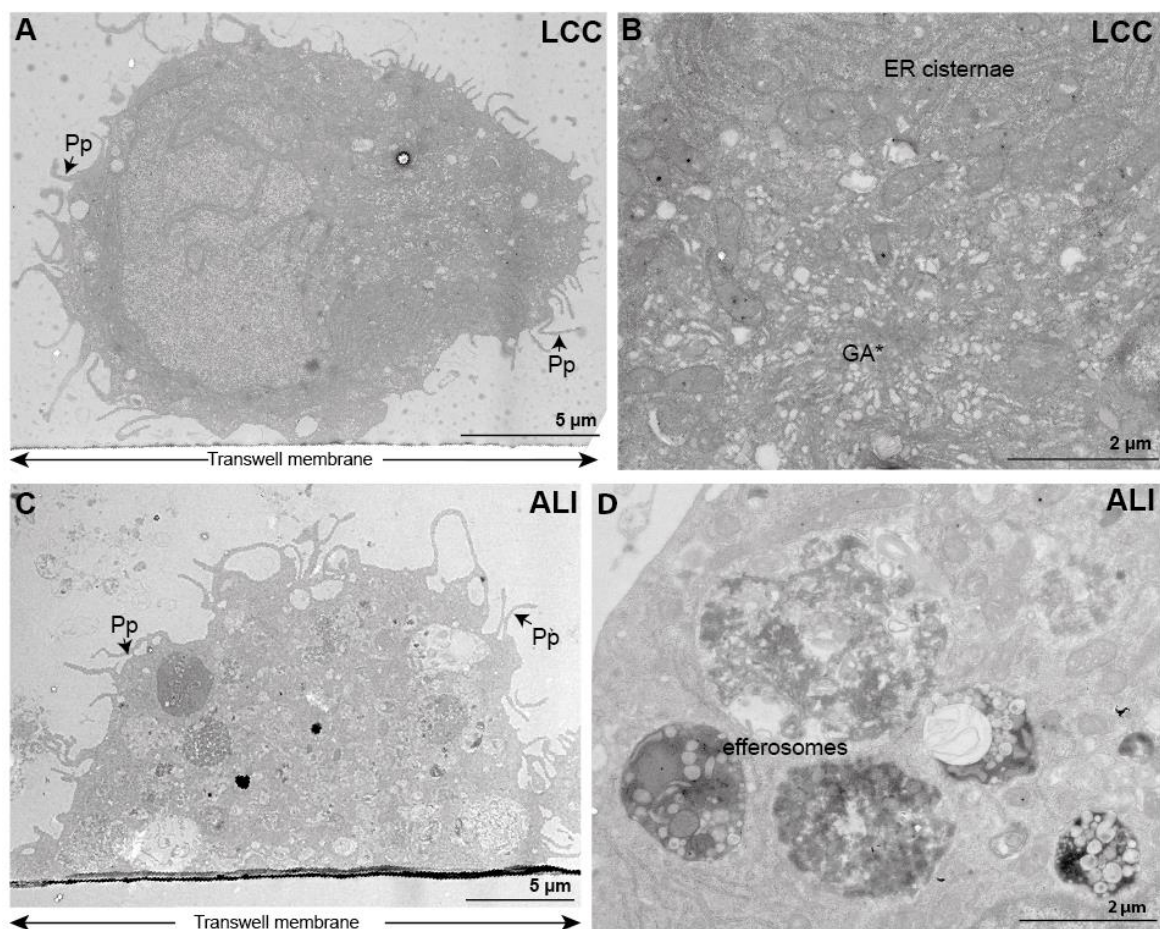


**Figure 4.12. Ultrastructural analysis of THP-1 monocultures.** Transmission electron microscopic (TEM) images of macrophage-like cells cultivated on permeable filter supports, either under LCC (A, B) or at ALI (C, D). Single THP-1 cell grown under LCC displaying pseudopodia on its surface (A) and prominent Golgi apparatus (B). THP-1 cell cultivated at ALI (C), exhibiting pseudopodia and showing prominent efferosomes (D), whereas Golgi apparatus is not notable.

The current findings indicate that THP-1 cells under LCC conditions are biosynthetically active. In contrast, THP-1 cells exposed to the air contain so-called efferosomes that are phagosomes containing cell debris (Figure 4.12 C). In addition, a Golgi apparatus is not notable, indicating that at ALI, the macrophage-like cells are less biosynthetically active. Taken together, these results suggest that cell death at ALI is more common than in samples grown under LCC.

Also the presence of prominent ER in THP-1 cells that are cocultured with hAELVi cells, comparable to THP-1 monocultures grown under LCC, indicate some communication or even a secretion of factors resulting in better viability conditions for macrophage-like cells. For detailed information about the influence of hAELVi cells on THP-1, further experiments in this respect should be involved in future studies.

#### 4.3.5 Transport studies

The prospective use of this coculture model for drug transport and absorption was assessed by evaluating the transport of NaFlu, a hydrophilic molecule. In order to modulate TJs, NaFlu was used in combination with EDTA; that is known to be able to open TJs by chelation of  $\text{Ca}^{+2}$  in a reversibly manner. As previously mentioned in chapter 3, high TEER always goes together with a low paracellular transport. This relationship could also be observed within the coculture model, and was even more prominent when compared to hAELVi monolayers. After adding EDTA, a drop in TEER and subsequent higher transport of NaFlu to the basolateral compartment could be observed in samples grown under LCC as well as in those exposed to ALI (Figure 4.13). As hAELVi cells display higher TEER values when cocultivated with THP-1 cells under LCC, this effect was much more pronounced, as hAELVi cells are in contact with a higher amount of RPMI medium during their cultivation and therefore exhibit higher TEER values.

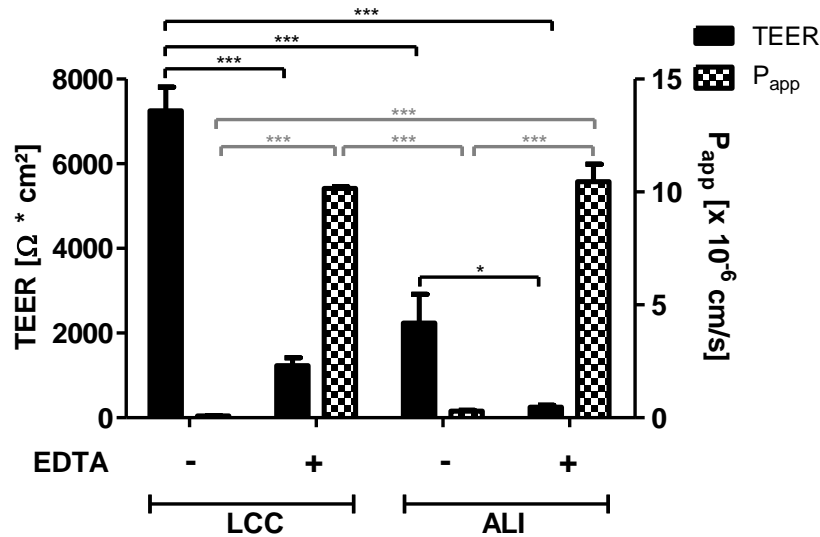


**Figure 4.13. Permeability assay on cocultures, grown under LCC and at ALI.** Transport of NaFlu across hAELVi-/THP-1 cocultures. The graph combines TEER and  $P_{app}$  values. Data shown are mean  $\pm$  SEM\* ( $n=3-9$ ) from 1-3 independent experiments; \*\*\* $P<0.001$ .

The obtained results indicated that this coculture system serves as an even more promising model to evaluate drug absorption compared to hAELVi monocultures (shown in chapter 3). Nevertheless, to get a broad insight into its applicability, studies with more model drugs (e.g. propranolol) should be included in future experiments.

Finally, as this model comprises the main cell type responsible for clearance in the alveolar region (*i.e.* macrophages), this coculture system could entirely applicable to study the clearance of new drug formulations and/or NPs.

#### 4.3.6 Long-term cocultivation

In order to have a coculture system that could be further used not only for drug delivery testing but also to study chronic diseases, hAELVi cells and THP-1 were cocultured for up to 7 days at ALI. To monitor the condition of the cells during that period of time, TEER was measured after 3 and 7 days in coculture and morphology was documented by CLSM images. TEER measurements showed that hAELVi cells maintained their tight barrier, although a decrease to

~2800  $\Omega \cdot \text{cm}^2$  could be observed after 7 days in coculture compared to a value of ~4300  $\Omega \cdot \text{cm}^2$  after 3 days. This behavior could also be observed in hAELVi monocultures which displayed a TEER value of ~2500  $\Omega \cdot \text{cm}^2$  after 3 weeks in monoculture compared to 1 week in coculture (Figure 4.14). This stability of TEER could also be observed in hAELVi monocultures grown under LCC for 28 days, showing constant values of ~2000  $\Omega \cdot \text{cm}^2$  [162].

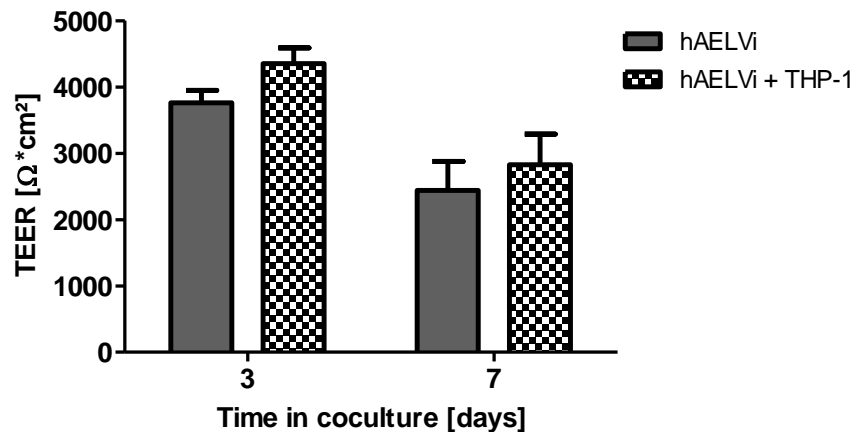


**Figure 4.14.** Long-term cocultivation of hAELVi cells and THP-1, grown at ALI. TEER measurements of hAELVi monocultures and cocultivated with THP-1 after 3 and 7 days in coculture. Data shown are mean  $\pm$  SEM\* ( $n=6$ ) from two independent experiments.

To document the cell viability during 1 week of cocultivation, THP-1 cells were pre-labeled with DDAO-SE (red) as previously described before added on hAELVi monolayers and further analyzed by CLSM. During incubation, the reagent passively diffuse into the cytoplasm of cells, where their acetate groups are cleaved by intracellular esterases; this results in the formation of carboxyfluorescein succinimidyl esters, which covalently bind to intracellular amines and form fluorescent conjugates [237]. All images showed that both cell types remain viable (Figure 4.15), however a decrease in the amount of macrophages could be observed after 7 days in coculture. To prolong the coculture (e.g. for studying longer exposure times or repeated exposure), one possibility could be to further add more macrophages after 3 days of cocultivation.

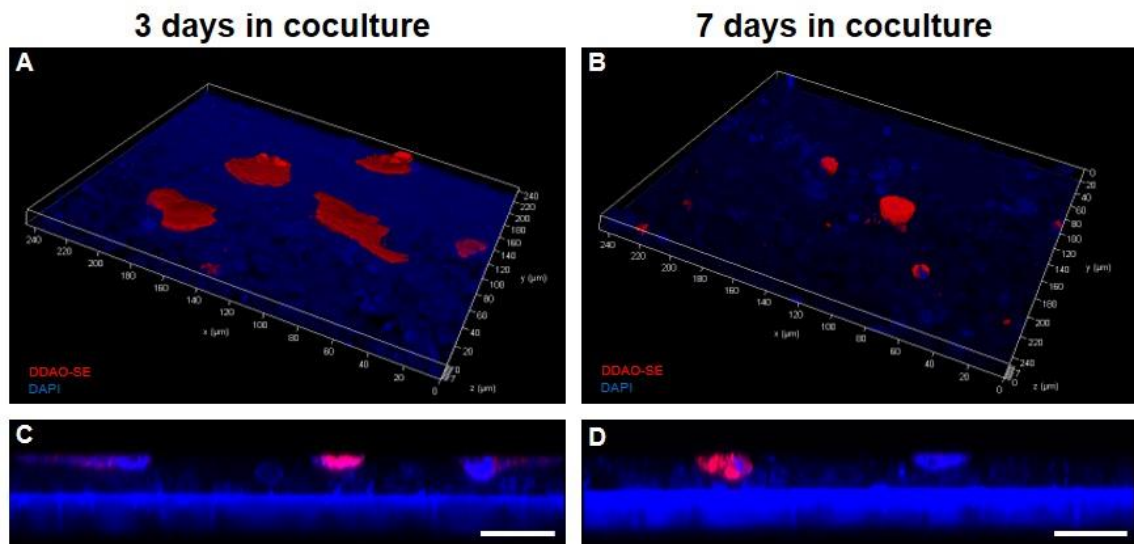


**Figure 4.15. Morphology of long-term cocultures of hAELVi cells and THP-1.** 3D images (A, B) and cross-sections (C, D) of hAELVi/THP-1 cocultures grown for 3 days (A, C) and 7 days (B, D) at ALI. THP-1 cells (DDAO-SE; red). Nuclei are counterstained with DAPI (blue). Scale bar: 20  $\mu\text{m}$ .

Taken together, the obtained results suggest that the established alveolar coculture is a promising model that can serve as a tool to assess the lung in a diseased state, for example in chronic diseases such as chronic bronchitis, asthma, COPD or CF [65].

#### **4.4 Conclusion**

This chapter describes the establishment of a new 3D coculture model mimicking the human air-blood barrier in a healthy state. The system is based on cell lines and involves the recently established hAELVi cell line. When grown on permeable filters (Transwells®), these cells form monolayers with high functional and morphological resemblance to ATI cells and tight intercellular junctions. To model the alveolar macrophages, the human cell line THP-1 was seeded on pre-formed hAELVi monolayers. As already mentioned the use of cell lines allows consistent seeding and better reproducibility, as well as better suitability for high-throughput screening of new drug candidates.

The system either grown at ALI or under LCC was further characterized with respect to its barrier properties and morphology. In general, hAELVi cells and THP-1 cells are cultivated in different media. Whereas hAELVi cells are grown in a complex medium, THP-1 cells are cultivated in basic RPMI. Even if hAELVi cells do not form any barrier when cultured in RPMI, TEER measurements showed that they display high TEER values when cultured in mixed SAGM/RPMI. Also, the presence of THP-1 cells does not interfere in the expression of a tight barrier.

Though hAELVi cells in monoculture cultivated under LCC and at ALI can be used to evaluate cytotoxicity effects, this does not hold true for cocultures. While results obtained from SEM showed a homogenous distribution of THP-1 on top of hAELVi cells under LCC, CLSM and TEM images indicated a significant reduction of macrophages on top of hAELVi cells due to low interaction of THP-1 with the epithelial layer. Therefore, use of cocultures at ALI is recommended as cultures grown under LCC are not satisfactory for studying particle-cell interactions.

Further, TEM images revealed that hAELVi cells were covered with glycocalyx-like structures. Whereas a layer of extracellular matrix at the surfaces exposed to the air could be observed on THP-1 cells when cocultured at ALI, this could not be observed in the monocultures. These findings suggest that hAELVi

cells secrete factors that modify the surface of macrophage cells or sediment on top of these cells.

Conducted permeability assays using NaFlu alone or in combination with the TJ modulator EDTA indicated that this model is a promising alternative for assessing drug transport. Additionally, as this model comprises an extra barrier structure in the form of macrophages, clearance mechanisms of applied drug formulations and/or NPs can be evaluated in parallel.

Long-term cocultivation including TEER measurements and analysis *via* CLSM showed that the system can be kept in coculture up to 7 days, during which hAELVi cells maintained their tight barrier and THP-1 and hAELVi cells remained viable. But however, a decrease in the amount of macrophages could be observed after 7 days in coculture. To prolong the coculture (*e.g.* for studying longer exposure times or repeated exposure), more macrophages could be added after 3 days in coculture. But nevertheless, besides drug delivery testing, this makes this model a promising tool to answer questions regarding cancer pathogenesis as well as chronic diseases in the future.

In summary, the newly established 3D coculture model expresses two essential components of the deep lung important for the assessment of new drug candidates and DDS: functional epithelial TJs, and macrophages.



---

## **5. Application of the established alveolar 3D coculture model for nanoparticle deposition**

The author of this thesis made the following contributions to this chapter:

Performed all cell culture experiments including application of nanoparticles, measured TEER, fixed and stained the samples for further confocal laser scanning microscopic analysis, and wrote the manuscript. PLGA-CS nanoparticles for proof-of-concept-studies were prepared and characterized by Nicole Kunschke. Sarah Barthold prepared and characterized the blank as well as loaded starch nanoparticles. Nebulization of starch nanoparticles was performed in collaboration with Sarah Barthold.

## 5.1 Introduction

Besides natural NPs generated by combustion processes, dusts or volcanic activity [73, 77], an increasing number of engineered NPs are released into the air, water and soil [73, 238, 239]. Nowadays, engineered NPs are involved in many applications and industries such as cosmetics, leisure wear, electronics, food packaging and drug delivery [71, 78, 79, 82]. This has resulted in a considerable increase in human exposure to NPs *via* the gastrointestinal tract, the skin and the respiratory system [73, 77, 240, 241].

During inhalation, airborne NPs come in contact with several cellular and non-cellular barriers that protect the respiratory tract against foreign particulate matter [73]. Once inhaled NPs reach the lung, they first come in contact with the lining fluid (Figure 5.1 (1)) before they are either entrapped in the mucus blanket of the upper airways and carried *via* the mucociliary escalator upwards to the esophagus, before being finally eliminated by excretion; further transferred to the digestive tract [16, 29, 30]; or taken up by alveolar macrophages that are responsible for clearance in the deep lung (Figure 5.1 (2)).

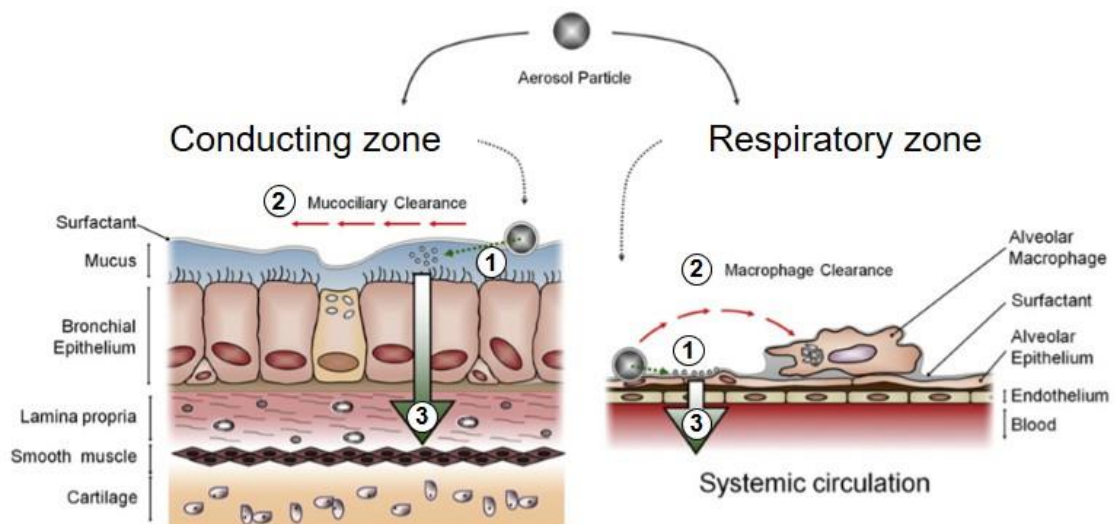


**Figure 5.1. Fate of inhaled nanoparticles.** Once reaching the lung, airborne NPs come first in contact with the lining fluid (1) before they are either eliminated by the mucociliary escalator in the conducting zone and by alveolar macrophages in the deep lung (2) or reach the underlying tissue or systemic circulation by crossing the epithelium (3). Adapted and modified with permission from [14], modified from [242].

Together with the engulfed foreign particles, the macrophages are then cleared from the alveoli to the bronchioles by the lining fluid and finally eliminated *via* the mucociliary pathway [16, 54].

But despite the existence of these barriers, several studies have revealed that small-sized NPs of various materials have the capacity to enter different cell types, and in doing so may cause adverse health effects including enhanced expression of pro-inflammatory cytokines [73, 243-245] and the generation of ROS [245-250]. Such molecules may further induce inflammation, mitochondrial damage [251, 252] or DNA strand breaks [247] that can finally result in cell death. Further, it was found that for example combustion-derived NPs are able to exacerbate preexisting respiratory diseases and an increased cardiovascular morbidity has been associated with the inhalation of NPs [73, 249, 253-260].

In general, it is known that NPs' toxicity can be affected by their size, the bulk material, shape or surface charge [84, 261-266]. Due to their size, the deposition and final fate of smaller NPs differs from that of larger particles [73], and their high surface-to-mass ratio gives them greater toxic and fibrogenic potential [249]. Airborne NPs smaller than 100 nm seem to be able to escape pulmonary clearance mechanisms [63] and are further capable of being taken up into cells and/or translocated across epithelial and endothelial cells into the underlying tissue or systemic circulation (Figure 5.1 (3)) [14].

Such an occurrence was shown in *in vivo* studies aiming to examine the pulmonary and systemic distribution of inhaled Ag NPs. A fast translocation into the systemic circulation as well as into other organs including liver, kidney and brain could be observed [267]. Further studies showed that Ag NPs induced blood-brain barrier destruction and neuronal degeneration, and within the lungs decreased tidal and minute volume on inhalation, and decrease inflammatory responses within the lungs after subcutaneous injection [268, 269].

Once inside the body, it is likely that NPs will come into contact with immune cells. As already mentioned, depending on the physicochemical properties of NPs, these interactions may have an immunomodulatory effect, resulting in the induction of inflammation and increased susceptibility to infectious diseases or

even to autoimmune diseases and cancer, by activating or suppressing the function of the immune system [270, 271].

Positively-charged NPs usually hold a greater inflammatory potential than negatively-charged or neutral NPs [272]. As macrophages display negatively-charged sialic acid on their surfaces [273], it is more likely that cationic substances interact with them by binding to TLRs that further induce an inflammatory response [274, 275].

However, to study the effects of new drug candidates or DDS such as NPs under well-controlled conditions, one cell type alone cannot mimic the behavior of a whole tissue. With respect to clinical relevance, advanced cell- and tissue-based *in vitro* models should contain immune cells, as they are involved in the activation of the signal transduction pathway and inflammatory responses.

Therefore, the successfully established alveolar 3D coculture model was utilized for the application and first evaluation of NPs. First, well-known PLGA-CS particles that have already been used for pulmonary drug delivery were applied on hAELVi-/THP-1 mono- and cocultures which were then tested for cell viability. Further, well-characterized Ag NPs were applied to show the suitability of the coculture for evaluating toxicity, by determining cell viability following exposure as well as NP impact on the epithelial barrier. Finally, newly developed starch NPs intended for pulmonary drug delivery of proteins were nebulized onto the coculture followed by the determination of their impact on cell viability and barrier properties, as well as their cellular interaction.

## **5.2 Materials and Methods**

### **5.2.1 Nanoparticle preparation and characterization**

#### ***5.2.1.1 Poly (D, L)-lactide-co-glycolide nanoparticles-/chitosan nanoparticles (PLGA NPs)***

PLGA- (Resomer® RG 752 H; Evonik Industries AG, Germany) based NPs coated with CS (chitosan chloride; Protasan® UP CL113; Novamatrix, Norway) were prepared *via* the emulsion-diffusion-evaporation technique [276, 277]. Therefore, 15 mg of the cationic CS polymer was dissolved in 5 mL of an aqueous 2.5% (w/v) polyvinyl alcohol solution (PVA; Moviol® 4-88 from Kuraray, Japan). The organic phase consisting of 100 mg PLGA in 5 mL ethyl acetate (reagent grade; Sigma Aldrich, USA) was added dropwise (160 µL/min) to a stirring aqueous solution to create a primary emulsion. After homogenizing with an aggregation unit at 15 000-17 000 rpm for 10 min, purified water was added to a final volume of 50 mL to permit the ethyl acetate to evaporate overnight. More details with regard to preparation and further characterization can be found in the thesis “*Development of a Nanotechnology enabled Drug Delivery System for Pulmonary siRNA delivery*” by Nicole Kunschke [278]. For cell viability studies, PLGA-CS NPs were diluted in cell culture medium (0-1000 µg/mL) and incubated for 24 h followed by the conduction of an MTT assay as described below in section 5.2.4.

#### ***5.2.1.2 Silver nanoparticles (Ag NPs)***

Well-characterized Ag NPs were purchased from Sigma Aldrich (730793; Sigma Aldrich, Germany). The NPs were stated by the manufacturer to be 20 ± 4 nm in size determined *via* TEM, and were dispersed in aqueous solution. Before nebulization, the NPs were re-dispersed using a pipette.

### 5.2.1.3 Starch nanoparticles (starch NPs)

Starch NPs were prepared by charge-mediated coacervation between negatively charged carboxylate groups (NegSt) and positively-charged amine groups (PosSt) of  $\alpha$ -starch derivatives in aqueous solution [279]. Briefly, materials were dissolved in purified water to obtain solutions of 0.25 mg/mL, with subsequent filtration. NegSt solutions were added to PosSt solutions in a ratio of 1:1 using a syringe pump (Harvard Apparatus PHD ULTRA, Harvard Apparatus Inc., Holliston, USA) under gentle stirring at RT. NPs formed spontaneously and were analyzed after 10 min of stirring for equilibration. The final pH value was 7.4 for all tested formulations. IgG1 - an antibody, responsible for the elimination of invading pathogens - was chosen as model cargo. For loading, 150  $\mu$ L IgG1 solution (5 mg/mL; kindly donated by Boehringer Ingelheim, Germany) was added to 40 mL of starch NP suspension.

For cellular interaction studies with hAELVi/THP-1 monocultures as well as the coculture, starch NPs were nebulized with an Aeroneb<sup>®</sup>Lab nebulizer (Aerogen Ltd., Ireland). To visualize the particles by CLSM, PosSt was labeled with a green fluorescent dye (Bodipy<sup>®</sup> FL C5 NHS Ester; LifeTechnologies, USA) before starch NP formation, and IgG1 was labeled with Alexa Fluor 647 carboxylic acid (succinimidyl ester) (LifeTechnologies, USA) according in each case to the manufacturer's protocol. Further information can be found in the thesis "*Nanotechnology enabled drug delivery of proteins and peptides to the lung*" by Sarah Barthold [280].

Physicochemical properties including particle size, size distribution (polydispersity index, Pdl) and surface charge ( $\zeta$ -potential) of NPs in preparation medium were determined using the ZetaSizer<sup>®</sup> Nano ZSP (Malvern Instruments, UK). Particle sizes were intensity based z-average values and standard deviation was of at least 3 measurements.

### 5.2.2 Cell culture

Mono- and cocultures were seeded as previously described in sections 3.2.1.1 and 3.2.1.2.

### 5.2.3 Transepithelial electrical resistance

The effects of NPs on hAELVi mono- and cocultures at ALI were determined by TEER measurements, conducted 24 h after the deposition of NPs, as previously described in 3.2.2.

### 5.2.4 Cell viability determination via MTT assay

The influence of different particles including PLGA-CS NPs, Ag NPs, blank starch NPs and loaded starch NPs on cell viability was evaluated after nebulization onto monocultures and cocultures, respectively, using the Aeroneb<sup>®</sup>Lab nebulizer. After 24 h of incubation, cell viability was evaluated by conducting the so-called MTT assay [102]. This colorimetric assay is based on the reduction of the salt MTT to its insoluble formazan by mitochondrial enzymes. The arising formazan crystals can be dissolved in DMSO, resulting in a purple color, the intensity of which correlates with the mitochondrial activity of the cells.

Briefly, mono- and cocultures were washed once with 300  $\mu$ L Hanks' balanced salt solution buffer (HBSS; composed of 1.12 mM  $\text{CaCl}_2$ , 0.49 mM  $\text{MgCl}_2 \cdot 6\text{H}_2\text{O}$ , 0.41 mM  $\text{MgSO}_4 \cdot 7\text{H}_2\text{O}$ , 5.33 mM KCl, 0.44 mM  $\text{KH}_2\text{PO}_4$ , 4.17 mM  $\text{NaCO}_3$ , 137.93 mM NaCl, 0.34 mM  $\text{Na}_2\text{HPO}_4$ , 5.55 mM D-Glucose, pH 7.4). In case of the coculture, the supernatants were centrifuged to avoid losing macrophages. The pellets were further resuspended in 300  $\mu$ L HBSS buffer, containing 10% (v/v) MTT reagent (5 mg/mL; Sigma Aldrich, USA), added back to the wells and incubated for 4 h. After aspirating the reagent, 300  $\mu$ L DMSO was added and again incubated for 20 min. Absorbance was measured with a Tecan Infinite<sup>®</sup> 200 microplate reader (Tecan Deutschland GmbH, Germany) at 550 nm. During

the experiment the plates were placed on a MTS orbital shaker (150 rpm; IKA, Germany) at 37 °C. Cell viabilities were calculated in comparison to a positive control (untreated cells: 100% cell viability) and a negative control (1% TritonX-100:0% of cell viability).

#### 5.2.5 Cellular interaction studies

Mono- and cocultures were grown at ALI as previously described. After 24 h in coculture, 250 µL of blank and IgG1-loaded starch NPs were deposited onto mono-and cocultures with the Aeroneb®Lab nebulizer and further incubated for 24 h.

The supernatant was then carefully aspirated and the cells were fixed with 3% methanol free PFA (added to the basolateral compartment) at 4 °C overnight. After fixation, the cells were permeabilized with 150 µL BSA/Saponin/PBS solution applied apically, followed by 150 µL anti-phalloidin staining (1:100) for 30 min at RT. After aspirating the staining solution, the samples were counterstained with 150 µL DAPI (1:50000 in PBS) and subsequently mounted. The samples were analyzed using CLSM. Lasers at 405 nm (DAPI), 488 nm (starch NPs), 565 nm (actin) and 633 nm (IgG1) were used for detection. Microscopic images were acquired at 1024x1024 resolution, using 63x water immersion objective. Confocal images were analyzed using ZEN 2012 software (Carl Zeiss Microscopy GmbH) and Fiji software (Fiji is a distribution of ImageJ available at <http://fiji.sc>).

#### 5.2.6 Statistical analysis

Data presented depict 1-3 independent experiments and are shown as mean ± standard error of mean (SEM\*). Two-way ANOVA with Bonferroni's post hoc test was performed using GraphPad Prism 5 software (GraphPad).



## **5.3 Results and Discussion**

### **5.3.1 Nanoparticle characterization**

Before applying the NPs onto hAELVi-/THP-1 mono- and cocultures, particle suspensions were evaluated regarding their size, Pdl and  $\zeta$ -potential. To evaluate their aerosolization stability, Ag NPs, starch NPs and starch NPs loaded with IgG1 were collected before and after nebulization (Table 5.1).

PLGA-CS particles were applied to cells grown under LCC by pipette. Measurements showed a size of  $142.1 \pm 1.9$  nm with a narrow size distribution of  $<0.2$  and a positive  $\zeta$ -potential of  $+ 30.3 \pm 0.7$  mV. Compared to the other NPs used in the following experiments, these particles were the only ones with a positive surface charge.

Measurements performed with the ZetaSizer<sup>®</sup> Nano ZSP showed an average size of 26.1 nm for Ag NPs, similar to the manufacturers information with a size distribution (Pdl) of 0.21. Despite an increase in  $\zeta$ -potential, these particles were stable during nebulization.

**Table 5.1. Particle characterization, conducted with the ZetaSizer<sup>®</sup> (Malvern, UK). Nanoparticle suspension of PLGA-CS, Ag NPs, blank starch NPs as well as loaded starch NPs were evaluated regarding size, Pdl and  $\zeta$ -potential.**

Particle	Size [nm]		Pdl		$\zeta$ -Potential [mV]		Type of application
	before	after	before	after	before	after	
PLGA-CS NPs	142.1 ± 1.9		0.118 ± 0.006		+ 30.3 ± 0.7		Pipetting (LCC)
Silver NPs	26.08	29.85	0.21	0.31	-23.10 ± 11.8	-31.4 ± 29.4	Nebulization (ALI)
Starch NPs*	150.6 ± 2.4		0.08 ± 0.004		- 25.8 ± 0.2		Pipetting (LCC)
Starch NPs	115.10 ± 1.2	107.80 ± 0.9	0.114 ± 0.016	0.110 ± 0.017	-26.50 ± 1.6	-29.9 ± 1.2	Nebulization (ALI)
Starch NPs + IgG1	130.20 ± 5.7	212.30 ± 1.8	0.283 ± 0.010	0.254 ± 0.017	-23.4 ± 1.0	-19.3 ± 2.4	Nebulization (ALI)

\* Particle suspension used for pre-screening of different concentrations on THP-1 cells; performed under LCC.

Blank starch NPs used to pre-screen the cytotoxicity of different concentrations on THP-1 monocultures grown under LCC displayed an average size of  $150.6 \pm 2.4$  nm with a Pdl below 0.1. In contrast, the same kind of particles used for cytotoxicity and cellular interaction studies in samples grown at ALI, showed a

size of  $115.10 \pm 1.2$  nm with a narrow size distribution and a negative  $\zeta$ -potential. This difference might be attributed to the storage of the particles or may be an influence of the label. Nevertheless, they were stable during nebulization.

When loaded with a model cargo (IgG1), starch NPs displayed an average size of  $130.2 \pm 5.7$  nm with a Pdl  $>0.2$ . But whereas the Pdl was stable during nebulization, an increase in size ( $212.3 \pm 1.8$  nm) and slight changes in the  $\zeta$ -potential could be observed, which can be a result of agglomeration during the nebulization process.

### 5.3.2 Proof-of-concept I: PLGA-CS nanoparticles

PLGA-CS NPs have been introduced as a flexible and efficient DDS that can be used for gene therapy [277, 281]. For initial proof-of-concept studies, they were applied on hAELVi-/THP-1 mono- and cocultures that were grown under LCC.

Due to its biocompatible and biodegradable qualities, PLGA, a co-polymer approved by the Food and Drug Administration (FDA) and the European Medicine Agency (EMA), has been used to fabricate devices for drug delivery and tissue engineering applications [282]. In general, PLGA is a copolymer of poly lactic acid (PLA) and poly glycolic acid (PGA), linked by ester bonds. Whereas PGA displays a crystalline structure, PLA can be found in highly crystalline form or can be completely amorphous [282]. When co-polymerized with PLA, PGA reduces the grade of crystallinity of PLGA, resulting in increased hydration and hydrolysis rate. It was found that the higher the content of PGA, the faster the biodegradation rate of the polymer [283]. However, PLGA shows the fastest degradation in a ratio of 50:50 of PLA and PGA [282]. In contact with water it biodegrades by hydrolysis of its ester linkages into lactic and glycolic acids. While PGA can be excreted unchanged by the kidneys, both monomers can be metabolized by entering the tricarboxylic acid cycle and eliminated from the body as carbon dioxide and water [282, 284, 285].

CS, a polysaccharide, is also known to be biocompatible and biodegradable, with low toxicity and mucoadhesive properties that supports macromolecule

permeation through well-organized epithelia [286-293]. When coated with CS, the negative surface charge of PLGA NPs increases from negative to positive without affecting the Pdl, resulting in promoted cellular adhesion and a prolonged retention time at the target site (which is beneficial for example in cancer cell targeting). Besides this, the modification of PLGA NP surfaces with CS can also decrease the burst effect in the release of an encapsulated drug, and can increase the stability of macromolecules [281, 288, 291].

Due to the well-characterized properties of PLGA-CS NPs and their capacity to deliver drugs into lung cells [277], hAELVi-/THP-1 mono- and cocultures were incubated with PLGA-CS NPs in different concentrations ranging from 0 to 1000  $\mu\text{g}/\text{mL}$  for 24 h. Results obtained from the MTT assay showed no decrease in cell viability in hAELVi monocultures. As an exception, after applying a NP concentration of 25  $\mu\text{g}/\text{mL}$ , an increase in cell viability of ~25% up to 125% could be observed (Figure 5.2), indicating stress in the epithelial cells. It was already shown that CS NPs are well-tolerated by epithelial cells even at concentration >1000  $\mu\text{g}/\text{mL}$  [289].

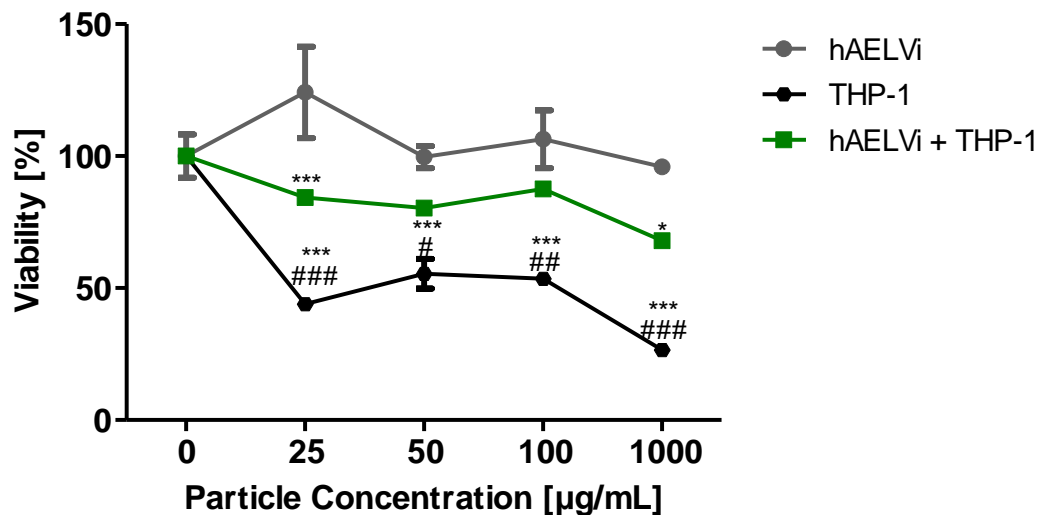


**Figure 5.2. Impact of PLGA-CS NPs on mono- and cocultures, grown under LCC.** Cell viabilities of hAELVi-/THP-1 mono- and cocultures after 24 h of NPs incubation with different concentrations. Data shown are mean  $\pm$  SEM\* (n=3) from one experiment; \* $P < 0.05$ ; \*\*\* $P < 0.001$  vs. hAELVi; # $P < 0.05$ ; ## $P < 0.01$ ; ### $P < 0.001$  vs. hAELVi + THP-1.

In contrast, THP-1 cells in monoculture showed viabilities less than 50% when incubated with PLGA-CS NPs at a concentration of 25 µg/mL, whereas higher viability levels could be observed when treated with concentrations of 50 µg/mL or 100 µg/mL. The application of 1000 µg/mL led to a decrease in cell viability of ~73% (Figure 5.2). Even if CS is considered as non-toxic and biocompatible, it has been reported that when formulated as NPs a reduction in safety can be observed, resulting in cell membrane damage followed by enzyme leakage and necrotic or autophagic cell death [294]. Furthermore, it has been proven that PLGA NPs can induce inflammation [295] after intravenous administration, that was reversible after halting the treatment [296].

In hAELVi-/THP-1 cocultures cell viabilities between 80 and 88% could be found, whereas the highest NP concentration of 1000 µg/mL led to a decrease of ~42%, resulting in ~68% of viable cells in hAELVi monocultures. These results show again that hAELVi cells are more robust compared to THP-1 cells. When cocultured, the toxic effect that could be observed in the macrophage-like cells was attenuated. This can be indicative of interplay of epithelial and macrophage-like cells, which is realistic when considering the situation *in vivo*. As PLGA-CS NPs are known to be a potent DDS for gene therapy, further analysis should be performed within this coculture system, as these studies have shown it to be a promising tool for evaluating toxicity and could be further utilized for the evaluation of other parameters, including inflammatory response or knock-down experiments.

### 5.3.3 Proof-of-concept II: Silver nanoparticles (Ag NPs)

Due to their antimicrobial properties, Ag NPs are commonly used in many consumer and medical products such as cosmetics, sanitary products, food technology, textiles, dental fixtures, catheters and wound dressings [81, 297-300]. Despite its widespread use, only limited information on silver toxicity is available. Current studies suggest that some forms of silver are more toxic than others, resulting in the induction of toxicity in different species [301-305]. Moreover, these particles can cause argyria, an irreversible skin

discoloration [306] and/or neuronal damage in humans [81]. Besides absorption *via* the skin, inhalation is one of the main exposure routes for Ag NPs; however, their interaction with mammalian cells is currently still not fully understood. Therefore, it is of primary importance to evaluate possibly adverse effects of aerosolized Ag NPs [307].

With respect to the effect of Ag NPs on the lung, commercially available Ag NPs were nebulized onto the newly established alveolar coculture model. Cell viabilities and epithelial barrier integrity were determined in hAELVi-/THP-1 mono- and cocultures after 24 h of NPs incubation.

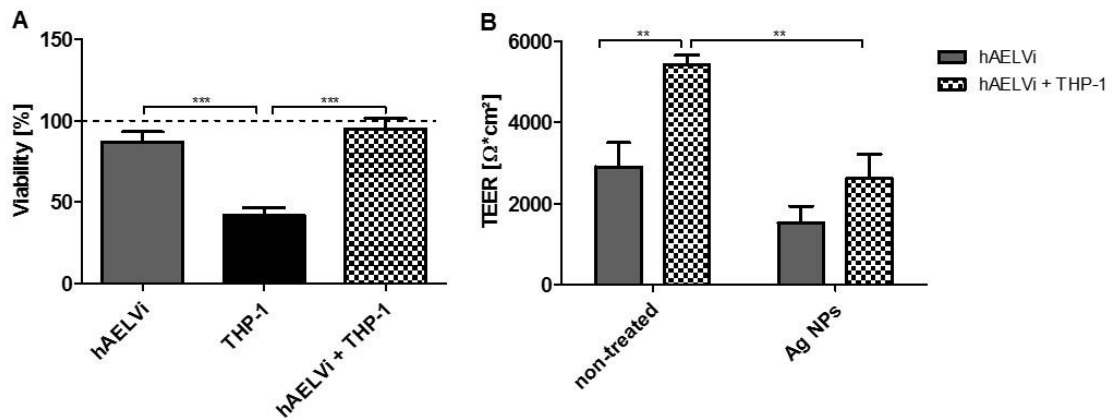


**Figure 5.3. Impact of nebulized Ag NPs on mono- and cocultures.** A: Cytotoxicity of applied Ag NPs on hAELVi-/THP-1 mono- and cocultures. B: TEER-measurements of hAELVi monocultures and cocultivated with THP-1. Data shown are mean  $\pm$  SEM\* (n=6) from two independent experiments; \*\*P<0.01, \*\*\*P<0.001.

The nebulization of Ag NPs led to a decrease in cell viability (Figure 5.3 A). In hAELVi monocultures a decrease to ~87% viability could be observed, whereas THP-1 showed levels of around 42%. In cocultivated samples only a slight effect could be observed, resulting in cell viabilities of ~95%. As previously shown in chapter 4, TEM images indicated some interaction between hAELVi and THP-1 cells, which may attenuate the toxic effects of Ag NPs. An abundant glycocalyx that has been previously been shown to shield the human airway epithelial cells from virus-mediated gene transfer [230] covers the epithelial cells, and seems somehow to extend its protective role to macrophages. Due to the fact that the extracellular matrix layer that covered THP-1 cells in coculture at ALI could not be observed in THP-1 monocultures, it can be speculated that hAELVi cells

secrete factors that modify the surface of macrophage cells or sediment on top of these cells. This finding raises the hypothesis that the hAELVi cells protect the THP-1 cells, which in monoculture are much more sensitive against applied NPs. These findings are also supported by the data of Kasper *et al.* who established a coculture model aiming to mimic the alveolar-capillary barrier for evaluating the impact of silica NPs in the deep lung. They have shown that their coculture was less sensitive to toxic effects compared to conventional monocultures [133].

Several studies have shown that the toxicity of Ag NPs can be induced *via* various mechanisms such as the induction of the expression of genes involved in cell cycle progression and apoptosis, interruption of ATP synthesis, and ROS and oxidative stress resulting in DNA damage [298, 300, 308, 309]. Besides this effect being noted in A549 cells, reduced cell viability as a result of Ag NP incubation was also observed in alveolar macrophages [310, 311]. Surprisingly, it was reported that also non-cytotoxic doses  $<0.5 \mu\text{g/mL}$  could induce the expression of genes associated with cell cycle progression and apoptosis [312, 313].

To further evaluate the impact of Ag NPs on the barrier integrity of epithelial cells, TEER measurements were conducted after 24 h of particle incubation. Non-treated samples displayed TEER values of  $\sim 2900 \Omega \cdot \text{cm}^2$  (hAELVi monoculture) and  $\sim 5400 \Omega \cdot \text{cm}^2$  (hAELVi + THP-1). Incubation with Ag NPs resulted in a decreased TEER: hAELVi cells showed values of around  $1500 \Omega \cdot \text{cm}^2$ , in contrast values of  $\sim 2600 \Omega \cdot \text{cm}^2$  which could be observed in the coculture (Figure 5.3 B). Comparing mono- and cocultures no difference could be observed, as both groups showed the same behavior after Ag NP incubation. Due to the fact that the coculture itself displays a higher TEER compared to the monoculture, the effect seems to be more pronounced.

However, the effect of a decrease in TEER should not always be directly associated with cytotoxicity. TEER values should be considered rather as an indicator for cytotoxicity [85] as it could be shown that CS for example, as a biocompatible polysaccharide, that is commonly used as an excipient in drug delivery systems, is able to open TJs [314]. Several studies showed a reversible

change in permeability after incubation with CS, indicating that opening of the TJs is not necessarily a result of cytotoxicity of a given substance [315-317].

It is also known, that paracellular permeability which is increased in a variety of diseases such as inflammatory bowel disease, and airway inflammation as occurring in asthma [135] and CF [318] can be modulated by cytokines, leading to actin remodeling and changes in the TJ structure resulting in the leakage of the epithelial barrier [319]. With this in mind, the possible induction of inflammation is also an important issue that should always be considered in the context of exposure to NPs. Therefore, experiments for evaluating inflammatory responses after NPs incubation should be included in future studies.

#### 5.3.4 Application and evaluation of newly developed starch nanoparticles

As previously mentioned in chapter 1, the work within the COMPACT project comprises the preparation and characterization of formulations either for non-invasive delivery of nucleic acid-based drugs or proteins and peptides. A DDS for the latter for pulmonary drug delivery was developed by Sarah Barthold by charge-mediated coacervation of positively- and negatively-charged starch derivatives, synthesized from potato starch. These NPs have already been tested on A549 and 16HBE14o- cells [279]. As the newly established coculture model represents two characteristic barrier structures for the deep lung - tight epithelial junctions and macrophages - and is therefore quite important for drug delivery, this new DDS was applied to determine its impact on cell viability and cellular interactions. But before these NPs were nebulized onto the alveolar coculture, they were first tested on THP-1 monocultures, as it is known from the previous experiments that these cells represent the sensitive component within this system.

Therefore,  $1 \times 10^5$  cells were grown under LCC in a 96-well plate and further incubated with different concentrations of blank starch NPs ranging from 0-133  $\mu\text{g/mL}$ , diluted in RPMI medium. After 24 h of particle incubation, an MTT assay was applied to determine DDS impact on cell viability of THP-1 cells.

Already a particle concentration of 8  $\mu\text{g}/\text{mL}$  lead to a decrease in viability to 76%, whereas at concentrations between 17 and 133  $\mu\text{g}/\text{mL}$  viability levels of 68% - 55% could be observed (Figure 5.4).

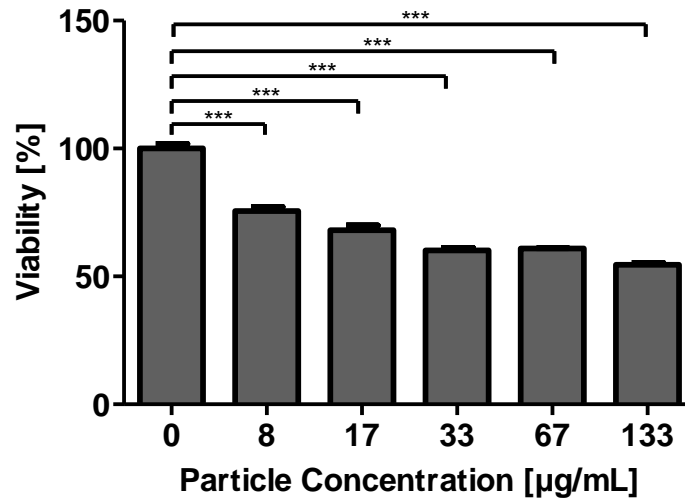


**Figure 5.4. Impact of blank starch NPs on THP-1 monocultures.** Cell viabilities of THP-1 cells grown under LCC were cultivated with different concentrations of blank starch NPs for 24 h. Data shown are mean  $\pm$  SEM\* ( $n=3$ ) from one experiment; \*\*\* $P<0.001$ .

Comparing these results with those obtained from PLGA-CS NPs, it could be observed that while PLGA-CS concentrations of 50  $\mu\text{g}/\text{mL}$  led to cell viabilities of  $\sim 55\%$ , starch NPs with a concentration of 67  $\mu\text{g}/\text{mL}$  showed values of  $\sim 61\%$ . Higher concentrations of both formulations, however, showed similar cell viability levels. It is generally accepted that positively-charged NPs are more toxic to mammalian cells [265]. In the case of starch NPs, it can be speculated that contamination with pyrogens can cause this toxicity. Immunogenicity assays combining the human TLR reporter assay and the dendritic cell maturation assay revealed that starch NPs activated TLR receptors and further increased the dendritic cell maturation. Subsequently applied endoLISA<sup>®</sup> assays showed high concentrations of endotoxins in samples of cationic starch derivatives, whereas none could be detected in negatively-charged starch. Detailed examination indicated that the synthesis time point as well as the storage time at RT could have led to contamination with bacteria, resulting in the release of pyrogens that further induced toxicity in macrophage-like cells [280]. Shorter storage periods or



lower temperatures such as 4 °C or -20 °C, as well as storage in a desiccator under low relative humidity could therefore be beneficial for newly synthesized starch derivatives.

Until now, 2D or 3D cell cultures grown under LCC have been used for assays evaluating toxicity [103], particle interactions [126, 191] and cell infection [320], giving an important and valid contribution to knowledge in these areas. However, this approach does not realistically reflect particle inhalation *in vivo* [321]. In this regard, research is now more focused on the direct delivery of aerosols to the cells which are cultivated at ALI; the following experiments also had a focus on ALI, since this condition represents better the *in vivo* situation in the deep lung, *i.e.* cells exposed to the air.

Related to the previous results (Figure 5.4), either 50 µL ( $\cong$  7.25 µg) or 250 µL ( $\cong$  41.25 µg) of starch NPs were deposited onto hAELVi cells, THP-1 cells and the coculture. After 24 h of particle incubation, cell viability studies as well as TEER measurements were conducted.

Whereas the nebulization of 7.25 µg of blank starch NPs led to a slight increase in cell viability in hAELVi monocultures up to ~110%, which can be associated with stress of the cells induced by applied NPs, slight decreases down to 91% could be found in THP-1 monocultures and the coculture (Figure 5.5 A). In contrast, the application of 41.25 µg of blank starch NPs had no effect on cell viabilities of hAELVi monocultures, while a decrease in cell viability in THP-1 (~54%) and the coculture (~84%) could be observed (Figure 5.5 B). This can possibly be explained by the fact that the cells are in contact with a higher amount of starch NPs which were speculated to be contaminated with pyrogens, as previously discussed in Figure 5.4. Nevertheless, as already discussed in 5.3.3, the interaction between hAELVi and THP-1 and also the fact that both are covered with either an extracellular matrix layer or glycocalyx-like structure when cocultured may attenuate the toxic effect of higher concentrations of blank starch NPs.

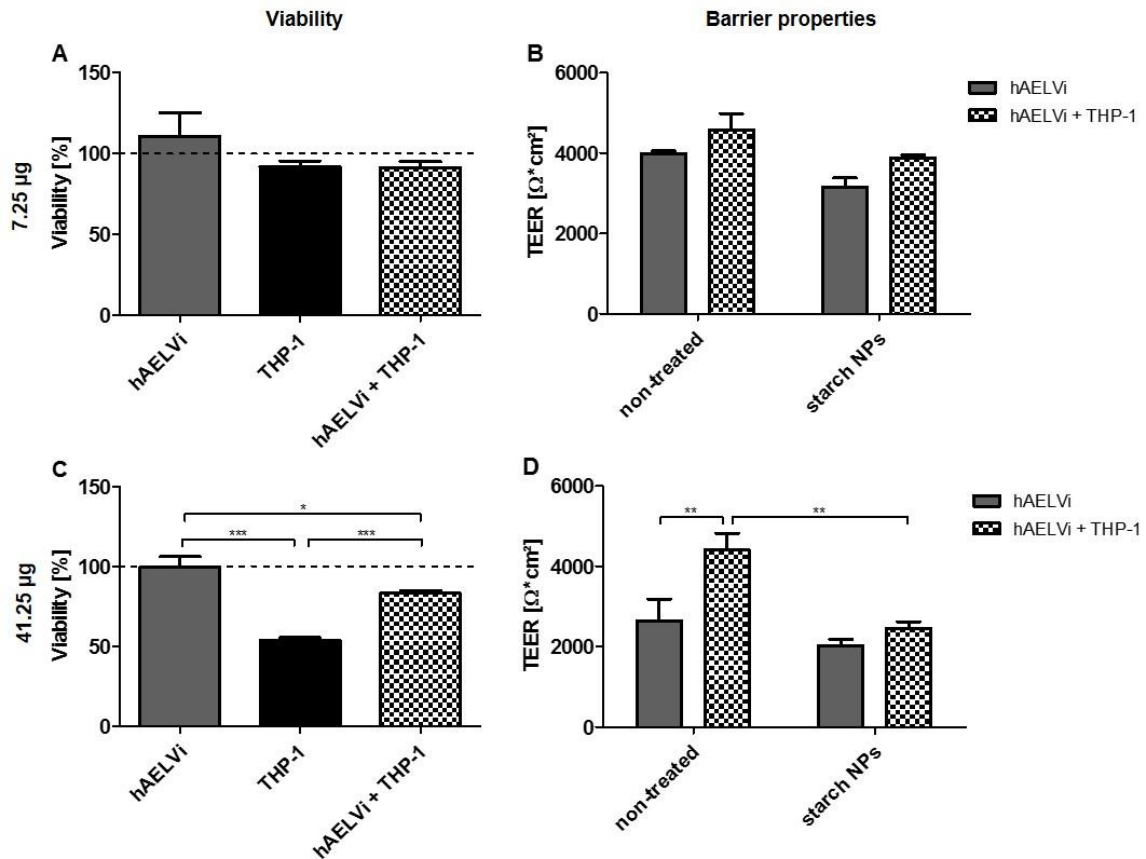


**Figure 5.5. Influence of blank starch NPs with different concentrations on mono- and cocultures, cultivated at ALI.** A, C: Cell viabilities of mono- and cocultures after incubation with blank starch NPs. B, D: TEER-measurements of hAELVi mono- and cocultures with THP-1 after incubation with blank starch NPs. Data shown are mean  $\pm$  SEM\* (n=6) from two independent experiments; \* $P < 0.05$ , \*\* $P < 0.01$ , \*\*\* $P < 0.001$ .

TEER measurements conducted to determine the effect of blank starch NPs on the epithelial barrier revealed that non-treated cells in monoculture displayed TEER values of around  $4000 \Omega^*\text{cm}^2$  and  $\sim 2600 \Omega^*\text{cm}^2$  after nebulization of  $7.25 \mu\text{g}$  and  $41.25 \mu\text{g}$ , respectively. The application of  $7.25 \mu\text{g}$  of blank starch NPs showed values of  $\sim 3100 \Omega^*\text{cm}^2$ , and  $\sim 2000 \Omega^*\text{cm}^2$  after the treatment with  $41.25 \mu\text{g}$  of starch NPs. A similar effect could be observed in the coculture, exhibiting TEER values of  $\sim 3880 \Omega^*\text{cm}^2$  and  $\sim 2500 \Omega^*\text{cm}^2$  after incubation of  $7.25 \mu\text{g}$  and  $41.25 \mu\text{g}$ , respectively. Due to the higher TEER in non-treated samples, this effect seemed to be more pronounced in the coculture (Figure 5.5 B, D).

Even if the obtained results showed that epithelial cells are more robust and resistant to the effects of starch NPs, and that no differences could be observed

in terms of evaluating the impact of applied NPs onto the epithelial barrier, both cell types are needed to mimic the situation *in vivo* where cells can interact with each other as well as with the applied particle.

Additionally, as these NPs were prepared for pulmonary drug delivery of proteins and peptides, they were loaded with a model cargo, IgG1 and subsequently applied to the mono- and cocultures with the Aeroneb®Lab nebulizer. IgG1 is a subclass of the family of IgG antibodies that are responsible for the elimination of invading pathogens and their products. A deficiency in IgG1 is reported to be associated with respiratory diseases / inflammatory states including asthma [322-324].

The nebulization of loaded starch NPs led to a decrease in viability in hAELVi (~80%) and THP-1 (~36%) monocultures (Figure 5.6 A). This observation can be a result of the agglomeration of loaded starch NPs, as previous results have shown that the physicochemical properties of NPs changed upon nebulization - observed as an increase in size from 130 nm up to 212 nm, and a slight change in an increase in the  $\zeta$ -potential from -23 mV to -19 mV. This effect could not be observed in the cocultures, which supports the assumption that communication between epithelial cells and THP-1 cells leads to higher resistance to NPs.

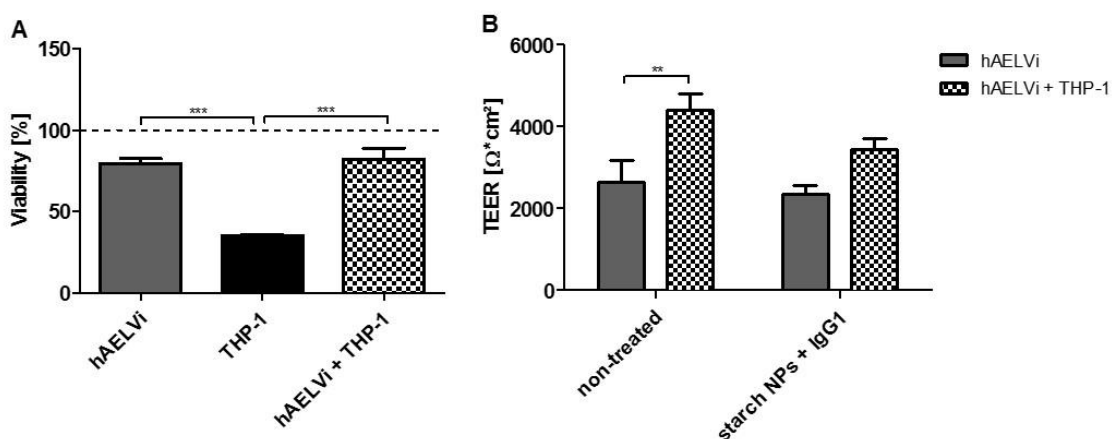


**Figure 5.6. Influence of loaded starch NPs on mono- and cocultures, cultivated at ALI.** A: Cell viabilities of mono- and cocultures after incubation with loaded starch NPs. B: TEER measurements of hAELVi mono- and cocultures with THP-1 after incubation with loaded starch NPs. Data shown are mean  $\pm$  SEM\* (n=6) from two independent experiments; \*\*P<0.01, \*\*\*P<0.001.

To evaluate the impact of starch NPs + IgG1 on the barrier integrity, TEER was measured after 24 h of particle incubation. hAELVi monocultures were only slightly affected by the incubation with starch NPs + IgG1 ( $\sim 2400 \Omega \cdot \text{cm}^2$ ), whereas the coculture showed a drop in TEER to  $\sim 3500 \Omega \cdot \text{cm}^2$  (starch NPs + IgG1; Figure 5.6 B). In contrast to the results obtained from MTT assays, no cytotoxic effect could be observed *via* TEER measurements. Even if mono- and cocultures showed lower TEER values upon NP exposure compared to the untreated cells, hAELVi cells do still maintain their tight barrier.

As the newly developed starch NPs are intended for intracellular delivery, cellular interactions were evaluated by nebulizing either blank starch NPs or NPs loaded with IgG1 onto hAELVi-/THP-1 mono- and cocultures. Starch was labeled with a green fluorescent dye (Bodipy<sup>®</sup> FL C5 NHS Ester) and IgG1 was labeled with Alexa Fluor 647 carboxylic acid to visualize the NPs by CLSM. The nebulization was followed by 24 h of incubation at 37 °C. After fixation, the samples were further stained with anti-phalloidin (actin, red) and DAPI (nucleus, blue).

Z-stacks of CLSM indicated an internalization of blank starch NPs into hAELVi cells when grown in monocultures (Figure 5.7 A). An uptake into epithelial cells could already be observed in previous studies conducted with A549 and 16HBE14o- exposed to these starch NPs [279].

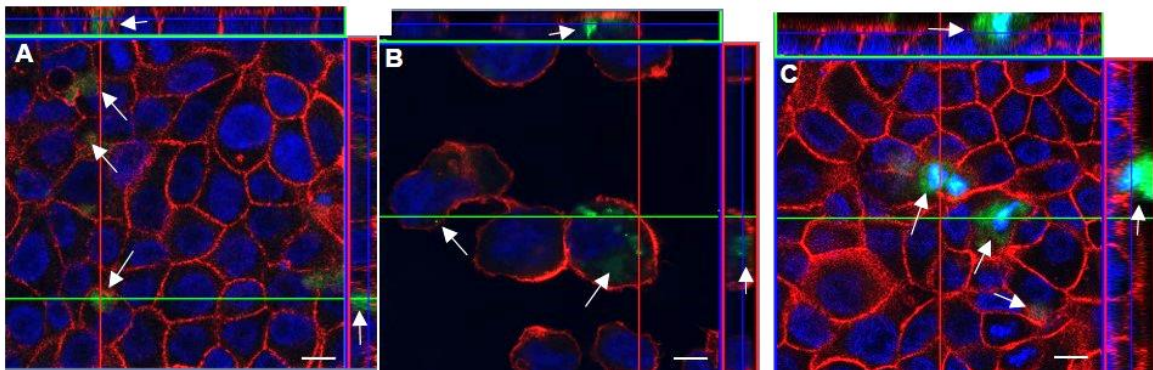


**Figure 5.7. Cellular interaction studies of nebulized starch NPs.** Confocal laser scanning microscopic images of monocultures of hAELVi (A), THP-1 (B) and the coculture (C) cultivated at ALI after 24 h of incubation with nebulized blank starch NPs. hAELVi cells / THP-1: anti-phalloidin (actin; red); NPs: Bodipy<sup>®</sup> C5 NHS Ester; green. Nuclei were counterstained with DAPI (blue). Images are representative of two independent experiments. Arrows indicate starch NPs. Scale bar: 10  $\mu\text{m}$ .

An internalization could also be observed in THP-1 monocultures after 24 h of incubation (Figure 5.7 B). As they mimic alveolar macrophages, which are responsible for the clearance of foreign matter in the deep lung *in vivo*, this was not unexpected. As already mentioned earlier, the interaction behavior of NPs is governed by their shape and surface charge as well as their size. Depending on the cell type, the optimum particle size for efficient endocytic uptake varies [325]. For macrophages it is known that they are able to ingest large particles with a diameter between 1 and 10  $\mu\text{m}$  [325-327]. For drug delivery *via* liposomes it was found that negatively-charged liposomes with a diameter of 0.05-0.1  $\mu\text{m}$  were internalized more efficiently than larger ones [328, 329]. For microspheres maximum phagocytosis was observed for those displaying sizes in a range of 1-3  $\mu\text{m}$  [329-331] which corresponds to the general size of bacteria that are commonly targets of phagocytes [332]. For alveolar macrophages in particular, optimal sizes between 3 and 6  $\mu\text{m}$  were found [333]. In contrast, the starch NPs display a size of  $\sim 115$  nm; and yet, they were taken up into the macrophage-like cells. NPs are known to aggregate when in contact with biological solutions, resulting in increased overall size [332]. Another explanation can again be the previously described contamination with pyrogens that may affect the uptake behavior of macrophages. Pyrogens like lipopolysaccharides (LPS) are known to activate TLR receptors resulting in an increased phagocytic activity of macrophages [334].

Within the coculture, however, no uptake into epithelial cells but only into macrophage-like cells could be observed (Figure 5.7 C). Considering the situation *in vivo*, where macrophages are patrolling the alveolar epithelium, this behavior was expected. Nevertheless, it was surprising that negligible numbers of particles were taken up into the epithelium, as it is known that particles smaller than 200 nm are able to evade lung clearance mechanisms and therefore are suitable for intracellular delivery into epithelial cells [335, 336].

The analysis of cellular interaction of starch NPs + IgG1 showed no difference compared to blank starch NPs, as the labeled IgG1 could not be detected (data not shown). This can be ascribed to the rather low concentration of IgG1 that was used for the loading of starch NPs.

Nevertheless, these results indicate that the newly developed starch NPs are able to be taken up into epithelial cells and macrophages, even if the uptake into the epithelium is not observable when cocultured with macrophages. Previously conducted experiments revealed a contamination of the cationic starch derivatives with pyrogens due to long storage periods. As this can also possibly affect cell viabilities, it is of utmost importance to control and to ensure that NPs are pyrogen-free before their application.

In addition, the increasing knowledge of the uptake behavior of NPs into macrophages with respect to their alteration within the body (e.g. by opsonization) can help in the modification of these NPs in a way that enables them to easily reach their target cells.

## **5.4 Conclusion**

As humans are increasingly exposed to naturally-derived or engineered NPs, the evaluation of their impact on cellular systems is of utmost importance. For this, several *in vitro* models either comprising single cell layers or complex cocultures have been used to analyze cytotoxicity or cellular interactions. With regard to the complexity that can be found *in vivo*, there is still a need for *in vitro* models containing more than one cell type, that allow cell-cell as well as cell-particle interactions.

Within this chapter, the newly established alveolar coculture model was successfully utilized for the application of several kinds of NPs. In first proof-of-concept studies, the use of the coculture showed benefits with respect to evaluation of the toxicity of well-characterized PLGA-CS NPs.

Further, Ag NPs were nebulized onto hAELVi and THP-1 monocultures as well as the combined system. An amount as low as 7.25 µg showed high cytotoxicity in macrophage-like cells, whereas in the coculture almost no toxicity could be observed. As already shown in chapter 4, TEM images indicated some interaction between hAELVi and THP-1 cells that may attenuate the toxic effects of Ag NPs. An abundant glycocalyx-like layer that covers the epithelial cells seems somehow to extend its protective role to macrophages, due to the fact that the extracellular matrix layer could be observed on THP-1 cells in coculture at ALI but could not be seen in THP-1 monocultures. Therefore, it can be speculated that hAELVi cells protect the THP-1s by secreting factors that may modify the surface of macrophages or sediment on top of these cells. The possible induction of inflammation is also an important issue that should always be considered in the context of exposure to NPs. With this in mind, experiments for evaluating inflammatory responses after NPs incubation should be included in future studies.

Further, a newly developed DDS intended for the pulmonary delivery of proteins and peptides based on starch NPs was nebulized onto the coculture and was evaluated regarding its toxicity and cellular interaction. Besides low toxicity, CLSM images indicated the suitability of starch NPs for intracellular delivery,

even if no uptake could be observed into epithelial cells when cocultured with THP-1.

In summary, the obtained results indicate the promising use of the newly established coculture model to pre-screen new formulations for toxicity and cellular interactions. The established involvement of the main cell types contributing to the air-blood barrier and the increasing knowledge of their uptake behavior (macrophages in particular) makes this model a promising tool to contribute to the optimization of new DDS to allow them to reach their target cells.



---

## 6. Summary and outlook

Besides naturally-derived NPs, the rising number of engineered NPs that are incorporated into many consumer products or used as DDS has resulted in an increased exposure of humans to NPs. As the lung is a major route for entering the human body, NP impact on pulmonary cellular systems has to be carefully evaluated. For this purpose, *in vitro* models able to evaluate new drug candidates or DDS with respect to their safety and efficacy represent an important alternative for animal testing. Isolated cells in primary culture are the gold standard in terms of reflecting physiological phenotypes and functions, however, their use is restricted due to limited access to primary material, short cell life-spans and large inter-individual cellular differences, leading to low reproducibility and limited usability for high-throughput screening applications. In this regard, the aim of this thesis was to establish a human cell line-based coculture model mimicking the human air-blood barrier that is suitable for studying the interaction with aerosolized drug carriers.

Within the current work a coculture of the recently described human lentivirus immortalized alveolar epithelial cell line hAELVi with overlying differentiated macrophage-like cells (THP-1) was successfully set up; this was followed by its subsequent characterization and application to NPs testing. TEER measurements and microscopic analysis revealed that hAELVi cells maintain their TJs and the resulting diffusional barrier is not affected by macrophages that are added on top. But, whereas hAELVi monocultures cultivated under both LCC and at ALI can be used to evaluate cytotoxicity, the coculture system requires ALI conditions. While SEM imaging showed a homogenous distribution of THP-1s on top of hAELVi cells under both conditions, CLSM and TEM images indicated a significant reduction of macrophages under LCC, most likely occurring during the change of cell culture medium in the apical compartment. TEM also revealed a rather weak interaction between macrophages and epithelial cells when cultivated under LCC as compared to samples grown at ALI.

Besides this technical limitation, ALI is preferred anyway because it better represents the physiological situation in the lung *in vivo*, and allows the deposition of aerosolized particles. Transport studies using NaFlu alone or in combination with the TJ modulator EDTA indicated that this model is a promising alternative for assessing drug transport. Additionally, as this model comprises an extra barrier in form of macrophages, clearance mechanisms of applied drug formulations and/or NPs can be evaluated in parallel.

Additional, long-term cocultivation for up to 7 days revealed that both cell types remained viable, however a decrease in the amount of macrophages could be observed after 7 days in coculture. One possibility to prolong the coculture *e.g.* for studying longer exposure times or repeated exposure could be to further add more macrophages after 3 days of cocultivation. But nevertheless, besides drug delivery testing, this makes this model a promising tool to answer questions regarding cancer pathogenesis as well as chronic diseases in the future.

First experiments involving the nebulization of small concentrations of Ag NPs showed high cytotoxicity in macrophage-like cells, whereas in the coculture a reduced toxicity could be observed. This implies some interaction between both cell types that results in the attenuation of toxic effects. In addition, TEM images revealed that THP-1 cells are covered with a layer of extracellular matrix when cocultured with hAELVi cells. In contrast, this protective layer could not be observed in THP-1 monocultures, suggesting a synergistic crosstalk between macrophage-like cells and the epithelium by *e.g.* secreted factors. Further, a newly developed DDS intended for the pulmonary delivery of proteins and peptides based on starch NPs was nebulized onto the coculture and subsequently evaluated regarding toxicity and cellular interaction. Besides low toxicity, CLSM images indicated the suitability of starch NPs for intracellular delivery, even if no uptake could be observed into epithelial cells when cocultured with THP-1s. The increasing knowledge of *e.g.* macrophage uptake behavior can contribute to the optimization of new DDS allowing them to better reach their specific target cells.

Nevertheless, there are still open questions and suggestions that can provide the basis for future work. Among these, the following should be mentioned: The

possible genesis of inflammation should always be considered in terms of NP exposure / application. The established coculture model includes immune cells in the form of macrophages - these represent a main source of cytokine production and play a crucial role in host responses to infection, immune responses and inflammation. To further determine the capacity of this model for evaluating inflammatory responses, inflammatory stimuli like LPS should be applied and cytokine release should be analyzed. Moreover, to study the treatment of respiratory diseases, the model could perhaps be extended towards an infection with relevant pathogens such as *Pseudomonas aeruginosa* or *Streptococcus pneumoniae*.

Besides that, the endothelial barrier has not been sufficiently investigated with regard to drug delivery so far. Also, as it can be assumed that these structures at least partly contribute to the tight barrier *in vivo*, endothelial cells can be further included in the system. Moreover, the model as it was set up and described here implicates rather static conditions.

To mimic more closely the *in vivo*-like conditions, in which blood perfusion and breathing applies some shear stress to the cells, the system could be connected to a flow system. Another point that should be considered when evaluating drug-cell interactions is the opsonization of the NPs by plasma or lining fluid proteins. Although the small volume of medium in cultures set up at ALI may mimic the amount of lung lining fluid in the alveoli. The latter, however, has a very peculiar composition, containing lung surfactant proteins and phospholipids. Therefore, it could be interesting to evaluate to what extent hAELVi cells produce these molecules as well, and to investigate the composition of the resulting alveolar lining fluid on top of these cocultures.

Apart from these still open questions, the newly established coculture of two human cell lines, representing alveolar epithelial cells and macrophages, appears as a useful tool for studying the interaction with aerosol particles in the context of testing the safety of air-born nanomaterials as well as novel inhalation (nano) pharmaceuticals.

---

## List of abbreviations

Ag NPs	Silver nanoparticles
ALI	Air liquid interface
ANOVA	Analysis of variance
API	Active pharmaceutical ingredient
ATI	Alveolar type I cells
ATII	Alveolar type II cells
BCRP	Breast cancer resistance protein
BSA	Bovine serum albumin
Ca	Calcium
CF	Cystic fibrosis
CFDA-SE	Carboxyfluorescein diacetate succinimidyl ester
CLSM	Confocal laser scanning microscopy
COL	Collagen
COMPACT	Collaboration on the optimization of macromolecular pharmaceutical access to cellular targets
COPD	Chronic obstructive pulmonary disease
CS	Chitosan
DAPI	4',6-diamidino-2-phenylindole
DDS	Drug delivery system
DDAO-SE	N, N-Dimethyldodecylamine N-oxide succinimidyl ester
DMSO	Dimethyl sulfoxide
DSMZ	Deutsche Sammlung von Mikroorganismen und Zellkulturen
EDTA	Ethylenediaminetetraacetic acid

Efpia	European Federation of Pharmaceutical Industries and Associations
EMA	European Medicine Agency
ER	Endoplasmic reticulum
EVOM	Epithelial volttohmmeter
FBS	Fetal bovine serum
FDA	Food and Drug Administration
FN	Fibronectin
GA	Glutaraldehyde
GA*	Golgi apparatus
hAELVi	human alveolar epithelial lentivirus immortalized cells
hAEpC	human alveolar epithelial primary cells
HBSS	Hank's balanced salt solution
HEPES	4-(2-hydroxyethyl)-1-piperazineethanesulfonic acid
HMDS	Hexamethyldisilazane
hPMECs	human pulmonary microvascular endothelial cells
HUVEC	Human umbilical vein endothelial cells
ICAM-I	Intracellular adhesion molecule-I
IgG1	Immunoglobulin G1
IMI	Innovative Medicines Initiative
JAMs	Junctional adhesion molecules
KRB	Krebs-Ringer Buffer
LCC	Liquid covered conditions
LPS	Lipopolysaccharide
LRP	Lung resistance-related protein

MHC	Major histocompatibility complex
MRPs	Multidrug resistance-related proteins
MTT	3-(4,5-dimethylthiazol-2-yl)-2,5-diphenyltetrazolium bromide
Mv	Microvilli
NaFlu	Sodium fluorescein
NHBE	Normal human bronchial epithelial
NPs	Nanoparticles
OCLN	Occludin
OCTs	Organic cation transporters
PADDOCC	Pharmaceutical Aerosol Deposition Device on Cell Cultures
$P_{app}$	Apparent permeability coefficient
PBS	Phosphate buffered saline
PCR	Polymerase chain reaction
PdI	Poly dispersity index
PFA	Paraformaldehyde
PGA	Poly glycolic acid
P-gp	P-glycoprotein
PLA	Poly lactic acid
PLGA	Poly(D,L)-lactide-co-glycolide
PMA	Phorbol-12-myristate-13-acetate
Pp	Pseudopodia
P/S	Penicillin/Streptomycin
PVA	Polyvinyl alcohol
ROS	Reactive oxygen species
RPMI	Roswell Park Memorial Institute

RT	Room temperature
SAGM	Small airway growth medium
SD	Standard deviation
SEM	Scanning electron microscopy
SEM*	Standard error of the mean
SN <sub>A</sub>	Supernatant A
SN <sub>B</sub>	Supernatant B
SPs	Surfactant-associated proteins
TEER	Transepithelial electrical resistance
TEM	Transmission electron microscopy
TJs	Tight junctions
TLR	Toll-like receptor
TT1	Transduced type I cell line
ZO-1	Zonula Occludens-1

---

## References

1. Sporty, J.L., L. Horalkova, and C. Ehrhardt, *In vitro cell culture models for the assessment of pulmonary drug disposition*. Expert Opin Drug Metab Toxicol, 2008. **4**(4): p. 333-45.
2. Bosquillon, C., *Drug transporters in the lung--do they play a role in the biopharmaceutics of inhaled drugs?* J Pharm Sci, 2010. **99**(5): p. 2240-55.
3. Salomon, J.J. and C. Ehrhardt, *Organic cation transporters in the blood-air barrier: expression and implications for pulmonary drug delivery*. Ther Deliv, 2012. **3**(6): p. 735-47.
4. Groneberg, D.A., et al., *Distribution and function of the peptide transporter PEPT2 in normal and cystic fibrosis human lung*. Thorax, 2002. **57**(1): p. 55-60.
5. van der Deen, M., et al., *ATP-binding cassette (ABC) transporters in normal and pathological lung*. Respir Res, 2005. **6**: p. 59.
6. Endter, S., et al., *P-glycoprotein (MDR1) functional activity in human alveolar epithelial cell monolayers*. Cell Tissue Res, 2007. **328**(1): p. 77-84.
7. Ehrhardt, C., et al., *Salbutamol is actively absorbed across human bronchial epithelial cell layers*. Pulm Pharmacol Ther, 2005. **18**(3): p. 165-70.
8. Horvath, G., et al., *Epithelial organic cation transporters ensure pH-dependent drug absorption in the airway*. Am J Respir Cell Mol Biol, 2007. **36**(1): p. 53-60.
9. Salomon, J.J., et al., *Organic cation transporter function in different in vitro models of human lung epithelium*. Eur J Pharm Sci, 2015. **80**: p. 82-8.
10. Nickel, S., et al., *Transport mechanisms at the pulmonary mucosa: implications for drug delivery*. Expert Opin Drug Deliv, 2016. **13**(5): p. 667-90.
11. Klein, S.G., et al., *Potential of coculture in vitro models to study inflammatory and sensitizing effects of particles on the lung*. Toxicol In Vitro, 2011. **25**.
12. Ochs, M. and E. Weibel, *Functional design of the human lung for gas exchange*. Fishman's pulmonary diseases and disorders, 2008. **4**.
13. Steimer, A., E. Haltner, and C.M. Lehr, *Cell culture models of the respiratory tract relevant to pulmonary drug delivery*. J Aerosol Med, 2005. **18**(2): p. 137-82.
14. de Souza Carvalho, C., N. Daum, and C.M. Lehr, *Carrier interactions with the biological barriers of the lung: advanced in vitro models and challenges for pulmonary drug delivery*. Adv Drug Deliv Rev, 2014. **75**: p. 129-40.
15. Nakajima, M., et al., *Immunohistochemical and ultrastructural studies of basal cells, Clara cells and bronchiolar cuboidal cells in normal human airways*. Pathol Int, 1998. **48**(12): p. 944-53.
16. Bur, M. and C.M. Lehr, *Pulmonary cell culture models to study the safety and efficacy of innovative aerosol medicines*. Expert Opin Drug Deliv, 2008. **5**(6): p. 641-52.
17. McDowell, E.M., et al., *The respiratory epithelium. I. Human bronchus*. J Natl Cancer Inst, 1978. **61**(2): p. 539-49.



18. Tsukita, S. and M. Furuse, *The structure and function of claudins, cell adhesion molecules at tight junctions*. Ann N Y Acad Sci, 2000. **915**: p. 129-35.
19. Tsukita, S. and M. Furuse, *Pores in the wall: claudins constitute tight junction strands containing aqueous pores*. J Cell Biol, 2000. **149**(1): p. 13-6.
20. Tsukita, S., M. Furuse, and M. Itoh, *Multifunctional strands in tight junctions*. Nat Rev Mol Cell Biol, 2001. **2**(4): p. 285-93.
21. Rennard, S.I., J.D. Beckmann, and R.A. Robbins, *Biology of airway epithelial cells.*, in *The Lung: Scientific Foundations*, R.G. Crystal and J.B. Wes, Editors. 1991, Raven Press: New York. p. 157–168.
22. Plopper, C.G., et al., *Comparison of nonciliated tracheal epithelial cells in six mammalian species: ultrastructure and population densities*. Exp Lung Res, 1983. **5**(4): p. 281-94.
23. Salomon, J.J., et al., *The cell line NCI-H441 is a useful in vitro model for transport studies of human distal lung epithelial barrier*. Mol Pharm, 2014. **11**(3): p. 995-1006.
24. Forbes, I.I., *Human airway epithelial cell lines for in vitro drug transport and metabolism studies*. Pharm Sci Technolo Today, 2000. **3**(1): p. 18-27.
25. Rawlins, E.L. and B.L. Hogan, *Epithelial stem cells of the lung: privileged few or opportunities for many?* Development, 2006. **133**(13): p. 2455-65.
26. Rock, J.R. and B.L. Hogan, *Epithelial progenitor cells in lung development, maintenance, repair, and disease*. Annu Rev Cell Dev Biol, 2011. **27**: p. 493-512.
27. Zheng, D., et al., *A cellular pathway involved in Clara cell to alveolar type II cell differentiation after severe lung injury*. PLoS One, 2013. **8**(8): p. e71028.
28. Sanders, N., et al., *Extracellular barriers in respiratory gene therapy*. Adv Drug Deliv Rev, 2009. **61**(2): p. 115-27.
29. Knowles, M.R. and R.C. Boucher, *Mucus clearance as a primary innate defense mechanism for mammalian airways*. J Clin Invest, 2002. **109**(5): p. 571-7.
30. Adler, K.B., M.J. Tuvim, and B.F. Dickey, *Regulated mucin secretion from airway epithelial cells*. Front Endocrinol (Lausanne), 2013. **4**: p. 129.
31. Yoneda, K., *Mucous blanket of rat bronchus: an ultrastructural study*. Am Rev Respir Dis, 1976. **114**(5): p. 837-42.
32. Samet, J.M. and P.W. Cheng, *The role of airway mucus in pulmonary toxicology*. Environ Health Perspect, 1994. **102 Suppl 2**: p. 89-103.
33. Patton, J.S., *Mechanisms of macromolecular absorption by the lungs*. Adv Drug Deliv Rev, 1996. **19**: p. 3-36.
34. Lopez-Vidriero, M.T. and L. Reid, *Bronchial mucus in health and disease*. Br Med Bull, 1978. **34**(1): p. 63-74.
35. Fehrenbach, H., *Alveolar epithelial type II cell: defender of the alveolus revisited*. Respir Res, 2001. **2**(1): p. 33-46.
36. Cumming, G., et al., *Gaseous diffusion in the airways of the human lung*. Respir Physiol, 1966. **1**(1): p. 58-74.
37. Crandall, E.D. and M.A. Matthay, *Alveolar epithelial transport. Basic science to clinical medicine*. Am J Respir Crit Care Med, 2001. **163**(4): p. 1021-9.

38. Adamson, I.Y. and D.H. Bowden, *The type 2 cell as progenitor of alveolar epithelial regeneration. A cytodynamic study in mice after exposure to oxygen.* Lab Invest, 1974. **30**(1): p. 35-42.
39. Cunningham, A.C. and J.A. Kirby, *Regulation and function of adhesion molecule expression by human alveolar epithelial cells.* Immunology, 1995. **86**(2): p. 279-86.
40. Cunningham, A.C., et al., *Constitutive expression of MHC and adhesion molecules by alveolar epithelial cells (type II pneumocytes) isolated from human lung and comparison with immunocytochemical findings.* J Cell Sci, 1994. **107 ( Pt 2)**: p. 443-9.
41. Cunningham, A.C., et al., *A comparison of the antigen-presenting capabilities of class II MHC-expressing human lung epithelial and endothelial cells.* Immunology, 1997. **91**(3): p. 458-63.
42. Batenburg, J.J., *Surfactant phospholipids: synthesis and storage.* Am J Physiol, 1992. **262**(4 Pt 1): p. L367-85.
43. Batenburg, J.J. and H.P. Haagsman, *The lipids of pulmonary surfactant: dynamics and interactions with proteins.* Prog Lipid Res, 1998. **37**(4): p. 235-76.
44. Haller, T., et al., *Dynamics of surfactant release in alveolar type II cells.* Proc Natl Acad Sci U S A, 1998. **95**(4): p. 1579-84.
45. Penney, D.P., *The ultrastructure of epithelial cells of the distal lung.* . Int. Rev. Cytol., 1988. **111**: p. 231–269.
46. Goerke, J., *Pulmonary surfactant: functions and molecular composition.* Biochim Biophys Acta, 1998. **1408**(2-3): p. 79-89.
47. Wattiez, R. and P. Falmagne, *Proteomics of bronchoalveolar lavage fluid.* J Chromatogr B Analyt Technol Biomed Life Sci, 2005. **815**(1-2): p. 169-78.
48. Hamm, H., H. Fabel, and W. Bartsch, *The surfactant system of the adult lung: physiology and clinical perspectives.* Clin Investig, 1992. **70**(8): p. 637-57.
49. Elbert, K.J., *Alveolare epithelzellkultursysteme als in vitro—modell für die pulmonale absorpition von arzneistoffen.* . 1998, Saarland University, Saarbrücken.: Saarland, Germany.
50. Bastacky, J., et al., *Alveolar lining layer is thin and continuous: low-temperature scanning electron microscopy of rat lung.* J Appl Physiol (1985), 1995. **79**(5): p. 1615-28.
51. Weaver, T.E. and J.A. Whitsett, *Function and regulation of expression of pulmonary surfactant-associated proteins.* Biochem J, 1991. **273**(Pt 2): p. 249-64.
52. Veldhuizen, R., et al., *The role of lipids in pulmonary surfactant.* Biochim Biophys Acta, 1998. **1408**(2-3): p. 90-108.
53. Weibel, E.R., *Morphometry of the Human Lung.* 1963, Berlin, New York: Springer Verlag and Academic Press.
54. Bowden, D.H., *The alveolar macrophage.* Environ Health Perspect, 1984. **55**: p. 327-41.
55. Gabor, F., et al., *Improving oral delivery.* Handb Exp Pharmacol, 2010(197): p. 345-98.
56. Ensign, L.M., R. Cone, and J. Hanes, *Oral drug delivery with polymeric nanoparticles: the gastrointestinal mucus barriers.* Adv Drug Deliv Rev, 2012. **64**(6): p. 557-70.

57. Singh, B.N., *Effects of food on clinical pharmacokinetics*. Clin Pharmacokinet, 1999. **37**(3): p. 213-55.
58. Lentz, K.A., *Current methods for predicting human food effect*. Aaps j, 2008. **10**(2): p. 282-8.
59. Prow, T.W., et al., *Nanoparticles and microparticles for skin drug delivery*. Adv Drug Deliv Rev, 2011. **63**(6): p. 470-91.
60. Gehr, P., M. Bachofen, and E.R. Weibel, *The normal human lung: ultrastructure and morphometric estimation of diffusion capacity*. Respiration Physiology, 1978. **32**(2): p. 121-140.
61. Macé, K., et al., *Characterisation of xenobiotic-metabolising enzyme expression in human bronchial mucosa and peripheral lung tissues*. European Journal of Cancer, 1998. **34**(6): p. 914-920.
62. Tronde, A., et al., *Pulmonary absorption rate and bioavailability of drugs in vivo in rats: structure-absorption relationships and physicochemical profiling of inhaled drugs*. J Pharm Sci, 2003. **92**(6): p. 1216-33.
63. Bur, M., et al., *Inhalative nanomedicine--opportunities and challenges*. Inhal Toxicol, 2009. **21 Suppl 1**: p. 137-43.
64. Jaafar-Maalej, C., et al., *Assessment methods of inhaled aerosols: technical aspects and applications*. Expert Opin Drug Deliv, 2009. **6**(9): p. 941-59.
65. Adamson, J., et al., *In Vitro Models of Chronic Obstructive Pulmonary Disease (COPD)*, in *Bronchitis*, I. Martan-Loeches, Editor. 2011, InTech. p. 41-66.
66. d'Angelo, I., et al., *Improving the efficacy of inhaled drugs in cystic fibrosis: challenges and emerging drug delivery strategies*. Adv Drug Deliv Rev, 2014. **75**: p. 92-111.
67. Mastrandrea, L.D., *Inhaled insulin: overview of a novel route of insulin administration*. Vasc Health Risk Manag, 2010. **6**: p. 47-58.
68. Scheuch, G., et al., *Clinical perspectives on pulmonary systemic and macromolecular delivery*. Adv Drug Deliv Rev, 2006. **58**(9-10): p. 996-1008.
69. Bai, S. and F. Ahsan, *Inhalable liposomes of low molecular weight heparin for the treatment of venous thromboembolism*. J Pharm Sci, 2010. **99**(11): p. 4554-64.
70. Patton, J.S. and R.M. Platz, *Routes of Drug Delivery: Case studies(D) Routes of delivery: Case studies*. Advanced Drug Delivery Reviews, 1992. **8**(2): p. 179-196.
71. Moghimi, S.M., A.C. Hunter, and J.C. Murray, *Nanomedicine: current status and future prospects*. Faseb j, 2005. **19**(3): p. 311-30.
72. Bawa, R., *Nanopharmaceuticals for Drug Delivery – A Review*. Touch Briefings 2009. **6**: p. 135-155.
73. Rothen-Rutishauser, B., et al., *Translocation of particles and inflammatory responses after exposure to fine particles and nanoparticles in an epithelial airway model*. Part Fibre Toxicol, 2007. **4**: p. 9.
74. Almeida, A.J. and E. Souto, *Solid lipid nanoparticles as a drug delivery system for peptides and proteins*. Adv Drug Deliv Rev, 2007. **59**(6): p. 478-90.
75. Auffan, M., et al., *Towards a definition of inorganic nanoparticles from an environmental, health and safety perspective*. Nat Nanotechnol, 2009. **4**(10): p. 634-41.

76. Moore, M.N., *Do nanoparticles present ecotoxicological risks for the health of the aquatic environment?* Environ Int, 2006. **32**(8): p. 967-76.
77. Byrne, J.D. and J.A. Baugh, *The significance of nanoparticles in particle-induced pulmonary fibrosis.* McGill J Med, 2008. **11**(1): p. 43-50.
78. Nowack, B. and T.D. Bucheli, *Occurrence, behavior and effects of nanoparticles in the environment.* Environ Pollut, 2007. **150**(1): p. 5-22.
79. Ju-Nam, Y. and J.R. Lead, *Manufactured nanoparticles: an overview of their chemistry, interactions and potential environmental implications.* Sci Total Environ, 2008. **400**(1-3): p. 396-414.
80. Lee, J., S. Mahendra, and P.J. Alvarez, *Nanomaterials in the construction industry: a review of their applications and environmental health and safety considerations.* ACS Nano, 2010. **4**(7): p. 3580-90.
81. Greßler, S., René Fries, R. *Nanosilber in Kosmetika, Hygieneartikeln und Lebensmittelkontaktmaterialien* 2010 Februar 2010; 1-87]. Available from: <http://www.bmg.gv.at>
82. Magnuson, B.A., T.S. Jonaitis, and J.W. Card, *A brief review of the occurrence, use, and safety of food-related nanomaterials.* J Food Sci, 2011. **76**(6): p. R126-33.
83. Geiser, M., et al., *Ultrafine particles cross cellular membranes by nonphagocytic mechanisms in lungs and in cultured cells.* Environ Health Perspect, 2005. **113**(11): p. 1555-60.
84. Oberdorster, G., E. Oberdorster, and J. Oberdorster, *Nanotoxicology: an emerging discipline evolving from studies of ultrafine particles.* Environ Health Perspect, 2005. **113**.
85. Hittinger, M., et al., *Preclinical safety and efficacy models for pulmonary drug delivery of antimicrobials with focus on in vitro models.* Adv Drug Deliv Rev, 2015. **85**: p. 44-56.
86. Projan, S.J. and D.M. Shlaes, *Antibacterial drug discovery: is it all downhill from here?* Clin Microbiol Infect, 2004. **10 Suppl 4**: p. 18-22.
87. Andes, D. and W.A. Craig, *Animal model pharmacokinetics and pharmacodynamics: a critical review.* Int J Antimicrob Agents, 2002. **19**(4): p. 261-8.
88. White, R.L., *What in vitro models of infection can and cannot do.* Pharmacotherapy, 2001. **21**(11 Pt 2): p. 292s-301s.
89. Yang, J., et al., *An integrated microfluidic platform for evaluating in vivo antimicrobial activity of natural compounds using a whole-animal infection model.* Lab Chip, 2013. **13**(17): p. 3373-82.
90. Troemel, E.R., et al., *p38 MAPK regulates expression of immune response genes and contributes to longevity in C. elegans.* PLoS Genet, 2006. **2**(11): p. e183.
91. Bogaerts, A., et al., *Proteome changes of Caenorhabditis elegans upon a Staphylococcus aureus infection.* Biol Direct, 2010. **5**: p. 11.
92. Sem, X. and M. Rhen, *Pathogenicity of Salmonella enterica in Caenorhabditis elegans relies on disseminated oxidative stress in the infected host.* PLoS One, 2012. **7**(9): p. e45417.
93. Jia, K., et al., *Autophagy genes protect against Salmonella typhimurium infection and mediate insulin signaling-regulated pathogen resistance.* Proc Natl Acad Sci U S A, 2009. **106**(34): p. 14564-9.
94. Shukla, V., et al., *Iridoid compound 10-O-trans-p-coumaroylcatalpol extends longevity and reduces alpha synuclein aggregation in*

- Caenorhabditis elegans*. CNS Neurol Disord Drug Targets, 2012. **11**(8): p. 984-92.
95. van Heeckeren, A.M. and M.D. Schluchter, *Murine models of chronic Pseudomonas aeruginosa lung infection*. Lab Anim, 2002. **36**(3): p. 291-312.
96. Barrios, R., *Animal Models of Lung Disease*, in *Molecular Pathology of Lung Diseases*, D.S. Zander, et al., Editors. 2008, Springer New York: New York, NY. p. 144-149.
97. McGonigle, P. and B. Ruggeri, *Animal models of human disease: challenges in enabling translation*. Biochem Pharmacol, 2014. **87**(1): p. 162-71.
98. Arora, T., et al., *Substitute of Animals in Drug Research: An Approach Towards Fulfillment of 4R's*. Indian Journal of Pharmaceutical Sciences, 2011. **73**(1): p. 1-6.
99. Coleman, R.A., *Human Tissue in the Evaluation of Safety and Efficacy of New Medicines: A Viable Alternative to Animal Models?* ISRN Pharmaceutics, 2011. **2011**: p. 806789.
100. Elbert, K.J., et al., *Monolayers of human alveolar epithelial cells in primary culture for pulmonary absorption and transport studies*. Pharm Res, 1999. **16**(5): p. 601-8.
101. Grainger, C.I., et al., *Culture of Calu-3 cells at the air interface provides a representative model of the airway epithelial barrier*. Pharm Res, 2006. **23**(7): p. 1482-90.
102. Mosmann, T., *Rapid colorimetric assay for cellular growth and survival: application to proliferation and cytotoxicity assays*. J Immunol Methods, 1983. **65**(1-2): p. 55-63.
103. Roggen, E.L., N.K. Soni, and G.R. Verheyen, *Respiratory immunotoxicity: an in vitro assessment*. Toxicol In Vitro, 2006. **20**(8): p. 1249-64.
104. Fogh, J., J.M. Fogh, and T. Orfeo, *One Hundred and Twenty-Seven Cultured Human Tumor Cell Lines Producing Tumors in Nude Mice*. Journal of the National Cancer Institute, 1977. **59**(1): p. 221-226.
105. Florea, B.I., et al., *Drug transport and metabolism characteristics of the human airway epithelial cell line Calu-3*. Journal of Controlled Release, 2003. **87**(1-3): p. 131-138.
106. Foster, K.A., et al., *Characterization of the Calu-3 cell line as a tool to screen pulmonary drug delivery*. Int J Pharm, 2000. **208**(1-2): p. 1-11.
107. Haghi, M., et al., *Deposition, diffusion and transport mechanism of dry powder microparticulate salbutamol, at the respiratory epithelia*. Mol Pharm, 2012. **9**(6): p. 1717-26.
108. Haghi, M., et al., *Time- and passage-dependent characteristics of a Calu-3 respiratory epithelial cell model*. Drug Dev Ind Pharm, 2010. **36**(10): p. 1207-14.
109. Ehrhardt, C., et al., *Drug absorption by the respiratory mucosa: cell culture models and particulate drug carriers*. J Aerosol Med, 2002. **15**(2): p. 131-9.
110. Manford, F., et al., *Drug permeability in 16HBE14o- airway cell layers correlates with absorption from the isolated perfused rat lung*. Eur J Pharm Sci, 2005. **26**(5): p. 414-20.
111. Forbes, B. and C. Ehrhardt, *Human respiratory epithelial cell culture for drug delivery applications*. Eur J Pharm Biopharm, 2005. **60**(2): p. 193-205.

112. Forbes, B., et al., *The human bronchial epithelial cell line 16HBE14o- as a model system of the airways for studying drug transport*. International Journal of Pharmaceutics, 2003. **257**(1-2): p. 161-167.
113. Lehmann, A.D., et al., *An in vitro triple cell co-culture model with primary cells mimicking the human alveolar epithelial barrier*. Eur J Pharm Biopharm, 2011. **77**(3): p. 398-406.
114. Ehrhardt, C., et al., *16HBE14o- human bronchial epithelial cell layers express P-glycoprotein, lung resistance-related protein, and caveolin-1*. Pharm Res, 2003. **20**(4): p. 545-51.
115. Woollhead, A.M. and D.L. Baines, *Forskolin-induced cell shrinkage and apical translocation of functional enhanced green fluorescent protein-human alphaENaC in H441 lung epithelial cell monolayers*. J Biol Chem, 2006. **281**(8): p. 5158-68.
116. Lin, H., et al., *Air-liquid interface (ALI) culture of human bronchial epithelial cell monolayers as an in vitro model for airway drug transport studies*. J Pharm Sci, 2007. **96**(2): p. 341-50.
117. Becker, S., et al., *TLR-2 is involved in airway epithelial cell response to air pollution particles*. Toxicol Appl Pharmacol, 2005. **203**(1): p. 45-52.
118. Giard, D.J., et al., *In vitro cultivation of human tumors: establishment of cell lines derived from a series of solid tumors*. J Natl Cancer Inst, 1973. **51**(5): p. 1417-23.
119. Foster, K.A., et al., *Characterization of the A549 cell line as a type II pulmonary epithelial cell model for drug metabolism*. Exp Cell Res, 1998. **243**(2): p. 359-66.
120. Kobayashi, S., S. Kondo, and K. Juni, *Permeability of peptides and proteins in human cultured alveolar A549 cell monolayer*. Pharm Res, 1995. **12**(8): p. 1115-9.
121. Kim, K.-J., Z. Borok, and E.D. Crandall, *A Useful In Vitro Model for Transport Studies of Alveolar Epithelial Barrier*. Pharmaceutical Research, 2001. **18**(3): p. 253-255.
122. Wang, Z. and Q. Zhang, *Transport of proteins and peptides across human cultured alveolar A549 cell monolayer*. Int J Pharm, 2004. **269**(2): p. 451-6.
123. Moschini, E., et al., *The modality of cell-particle interactions drives the toxicity of nanosized CuO and TiO<sub>2</sub> in human alveolar epithelial cells*. Toxicol Lett, 2013. **222**(2): p. 102-16.
124. Saigal, A., et al., *Development of controlled release inhalable polymeric microspheres for treatment of pulmonary hypertension*. Int J Pharm, 2013. **450**(1-2): p. 114-22.
125. Kendall, M., et al., *Surfactant protein D (SP-D) alters cellular uptake of particles and nanoparticles*. Nanotoxicology, 2013. **7**(5): p. 963-73.
126. Rothen-Rutishauser, B.M., S.G. Kiama, and P. Gehr, *A three-dimensional cellular model of the human respiratory tract to study the interaction with particles*. Am J Respir Cell Mol Biol, 2005. **32**.
127. Daum, N., et al., *Isolation, cultivation, and application of human alveolar epithelial cells*. Methods Mol Biol, 2012. **806**: p. 31-42.
128. Fuchs, S., et al., *Differentiation of human alveolar epithelial cells in primary culture: morphological characterization and synthesis of caveolin-1 and surfactant protein-C*. Cell Tissue Res, 2003. **311**(1): p. 31-45.

129. Kemp, S.J., et al., *Immortalization of human alveolar epithelial cells to investigate nanoparticle uptake*. Am J Respir Cell Mol Biol, 2008. **39**(5): p. 591-7.
130. van den Bogaard, E.H., et al., *Inflammatory response and barrier properties of a new alveolar type 1-like cell line (TT1)*. Pharm Res, 2009. **26**(5): p. 1172-80.
131. Kuhn, D.A., et al., *Cellular uptake and cell-to-cell transfer of polyelectrolyte microcapsules within a triple co-culture system representing parts of the respiratory tract*. Science and Technology of Advanced Materials, 2015. **16**(3): p. 034608.
132. Klein, S.G., et al., *An improved 3D tetraculture system mimicking the cellular organisation at the alveolar barrier to study the potential toxic effects of particles on the lung*. Part Fibre Toxicol, 2013. **10**: p. 31.
133. Kasper, J., et al., *Inflammatory and cytotoxic responses of an alveolar-capillary coculture model to silica nanoparticles: comparison with conventional monocultures*. Part Fibre Toxicol, 2011. **8**(1): p. 6.
134. Hermanns, M.I., et al., *An impaired alveolar-capillary barrier in vitro: effect of proinflammatory cytokines and consequences on nanocarrier interaction*. J R Soc Interface, 2010. **7** **Suppl 1**: p. S41-54.
135. Holgate, S.T., *Epithelium dysfunction in asthma*. Journal of Allergy and Clinical Immunology, 2007. **120**(6): p. 1233-1244.
136. Godfrey, R.W., *Human airway epithelial tight junctions*. Microsc Res Tech, 1997. **38**(5): p. 488-99.
137. Hittinger, M., et al., *Autologous coculture of primary human alveolar macrophages and epithelial cells for investigating aerosol medicines – part I – characterization of the model*. ATLA, 2016. **submitted**.
138. Huh, D., et al., *Reconstituting organ-level lung functions on a chip*. Science, 2010. **328**(5986): p. 1662-8.
139. Huh, D., G.A. Hamilton, and D.E. Ingber, *From 3D cell culture to organs-on-chips*. Trends Cell Biol, 2011. **21**(12): p. 745-54.
140. Russell, W.M.S., Burch, R.L., *The Principles of Humane Experimental Technique*. 1959, London: Methuen.
141. Swain, R.J., et al., *Assessment of cell line models of primary human cells by Raman spectral phenotyping*. Biophys J, 2010. **98**(8): p. 1703-11.
142. Eglén, R. and T. Reisine, *Primary cells and stem cells in drug discovery: emerging tools for high-throughput screening*. Assay Drug Dev Technol, 2011. **9**(2): p. 108-24.
143. Kuehn, A., *Immortalization of primary human alveolar epithelial cell: A new in vitro model of the air-blood barrier forming functional tight junctions.*, in *Biopharmacy and Pharmaceutical Technology*. 2016, Saarland University: Saarbruecken.
144. Leonard, F., E.M. Collnot, and C.M. Lehr, *A three-dimensional coculture of enterocytes, monocytes and dendritic cells to model inflamed intestinal mucosa in vitro*. Mol Pharm, 2010. **7**(6): p. 2103-19.
145. Srinivasan, B., et al., *TEER measurement techniques for in vitro barrier model systems*. J Lab Autom, 2015. **20**(2): p. 107-26.
146. de Souza Carvalho, C., et al., *Internalization, phagolysosomal biogenesis and killing of mycobacteria in enucleated epithelial cells*. Cell Microbiol, 2011. **13**(8): p. 1234-49.

147. Marchiando, A.M., W.V. Graham, and J.R. Turner, *Epithelial barriers in homeostasis and disease*. Annu Rev Pathol, 2010. **5**: p. 119-44.
148. Feldman, G.J., J.M. Mullin, and M.P. Ryan, *Occludin: structure, function and regulation*. Adv Drug Deliv Rev, 2005. **57**(6): p. 883-917.
149. Farquhar, M.G. and G.E. Palade, *Junctional complexes in various epithelia*. J Cell Biol, 1963. **17**: p. 375-412.
150. Salama, N.N., N.D. Eddington, and A. Fasano, *Tight junction modulation and its relationship to drug delivery*. Adv Drug Deliv Rev, 2006. **58**(1): p. 15-28.
151. Paris, L., et al., *Structural organization of the tight junctions*. Biochim Biophys Acta, 2008. **1778**(3): p. 646-59.
152. Chiba, H., et al., *Transmembrane proteins of tight junctions*. Biochim Biophys Acta, 2008. **1778**(3): p. 588-600.
153. Deli, M.A., *Potential use of tight junction modulators to reversibly open membranous barriers and improve drug delivery*. Biochim Biophys Acta, 2009. **1788**(4): p. 892-910.
154. Martin, T.A. and W.G. Jiang, *Loss of tight junction barrier function and its role in cancer metastasis*. Biochim Biophys Acta, 2009. **1788**(4): p. 872-91.
155. Chen, Y., et al., *COOH terminus of occludin is required for tight junction barrier function in early Xenopus embryos*. J Cell Biol, 1997. **138**(4): p. 891-9.
156. Furuse, M., et al., *Claudin-1 and -2: novel integral membrane proteins localizing at tight junctions with no sequence similarity to occludin*. J Cell Biol, 1998. **141**(7): p. 1539-50.
157. Gonzalez-Mariscal, L., R. Tapia, and D. Chamorro, *Crosstalk of tight junction components with signaling pathways*. Biochim Biophys Acta, 2008. **1778**(3): p. 729-56.
158. Farkas, A.E., C.T. Capaldo, and A. Nusrat, *Regulation of epithelial proliferation by tight junction proteins*. Ann N Y Acad Sci, 2012. **1258**: p. 115-24.
159. Anderson, J.M., C.M. Van Itallie, and A.S. Fanning, *Setting up a selective barrier at the apical junction complex*. Curr Opin Cell Biol, 2004. **16**(2): p. 140-5.
160. Niessen, C.M., *Tight junctions/adherens junctions: basic structure and function*. J Invest Dermatol, 2007. **127**(11): p. 2525-32.
161. Susewind, J., et al., *A 3D co-culture of three human cell lines to model the inflamed intestinal mucosa for safety testing of nanomaterials*. Nanotoxicology, 2015: p. 1-10.
162. Kuehn, A., et al., *Human alveolar epithelial cells expressing tight junctions to model the air-blood barrier*. Altex, 2016.
163. Furuse, M., et al., *Occludin: a novel integral membrane protein localizing at tight junctions*. J Cell Biol, 1993. **123**(6 Pt 2): p. 1777-88.
164. Wong, V., *Phosphorylation of occludin correlates with occludin localization and function at the tight junction*. Am J Physiol, 1997. **273**(6 Pt 1): p. C1859-67.
165. Van Itallie, C.M. and J.M. Anderson, *Occludin confers adhesiveness when expressed in fibroblasts*. J Cell Sci, 1997. **110 ( Pt 9)**: p. 1113-21.
166. Fanning, A.S., et al., *The tight junction protein ZO-1 establishes a link between the transmembrane protein occludin and the actin cytoskeleton*. J Biol Chem, 1998. **273**(45): p. 29745-53.



167. Hollander, D., *Crohn's disease--a permeability disorder of the tight junction?* Gut, 1988. **29**(12): p. 1621-4.
168. Gassler, N., et al., *Inflammatory bowel disease is associated with changes of enterocytic junctions.* Am J Physiol Gastrointest Liver Physiol, 2001. **281**(1): p. G216-28.
169. Kwon, E.E. and J.W. Prineas, *Blood-brain barrier abnormalities in longstanding multiple sclerosis lesions. An immunohistochemical study.* J Neuropathol Exp Neurol, 1994. **53**(6): p. 625-36.
170. Moolenaar, W.H., *Lysophosphatidic acid, a multifunctional phospholipid messenger.* J Biol Chem, 1995. **270**(22): p. 12949-52.
171. Vermeer, P.D., et al., *MMP9 modulates tight junction integrity and cell viability in human airway epithelia.* Am J Physiol Lung Cell Mol Physiol, 2009. **296**(5): p. L751-62.
172. Brown, D.M., et al., *Calcium and ROS-mediated activation of transcription factors and TNF- $\alpha$  cytokine gene expression in macrophages exposed to ultrafine particles.* American Journal of Physiology - Lung Cellular and Molecular Physiology, 2004. **286**(2): p. L344-L353.
173. Bhat, M., et al., *Regulation of tight junction permeability by calcium mediators and cell cytoskeleton in rabbit tracheal epithelium.* Pharm Res, 1993. **10**(7): p. 991-7.
174. McCarthy, K.M., et al., *Occludin is a functional component of the tight junction.* J Cell Sci, 1996. **109** ( Pt 9): p. 2287-98.
175. Klingler, C., et al., *Disruption of epithelial tight junctions is prevented by cyclic nucleotide-dependent protein kinase inhibitors.* Histochem Cell Biol, 2000. **113**(5): p. 349-61.
176. Tria, S., et al., *Sensing of EGTA Mediated Barrier Tissue Disruption with an Organic Transistor.* Biosensors (Basel), 2013. **3**(1): p. 44-57.
177. Lieber, M., et al., *A continuous tumor-cell line from a human lung carcinoma with properties of type II alveolar epithelial cells.* Int J Cancer, 1976. **17**(1): p. 62-70.
178. Shapiro, D.L., et al., *Phospholipid biosynthesis and secretion by a cell line (A549) which resembles type II alveolar epithelial cells.* Biochimica et Biophysica Acta (BBA) - Lipids and Lipid Metabolism, 1978. **530**(2): p. 197-207.
179. Hermanns, M.I., et al., *Lung epithelial cell lines in coculture with human pulmonary microvascular endothelial cells: development of an alveolo-capillary barrier in vitro.* Lab Invest, 2004. **84**(6): p. 736-52.
180. Cordon-Cardo, C., et al., *Expression of the multidrug resistance gene product (P-glycoprotein) in human normal and tumor tissues.* J Histochem Cytochem, 1990. **38**(9): p. 1277-87.
181. Ejendal, K.F. and C.A. Hrycyna, *Multidrug resistance and cancer: the role of the human ABC transporter ABCG2.* Curr Protein Pept Sci, 2002. **3**(5): p. 503-11.
182. Hein, S., et al., *The Pharmaceutical Aerosol Deposition Device on Cell Cultures (PADDOCC) in vitro system: design and experimental protocol.* Altern Lab Anim, 2010. **38**(4): p. 285-95.
183. Clowes, H.M., R.C. Scott, and J.R. Heylings, *Skin absorption: Flow-through or static diffusion cells.* Toxicol In Vitro, 1994. **8**(4): p. 827-30.
184. Ng, S.F., et al., *Validation of a static Franz diffusion cell system for in vitro permeation studies.* AAPS PharmSciTech, 2010. **11**(3): p. 1432-41.

185. Raber, A.S., et al., *Quantification of nanoparticle uptake into hair follicles in pig ear and human forearm*. J Control Release, 2014. **179**: p. 25-32.
186. Sambuy, Y., et al., *The Caco-2 cell line as a model of the intestinal barrier: influence of cell and culture-related factors on Caco-2 cell functional characteristics*. Cell Biol Toxicol, 2005. **21**(1): p. 1-26.
187. Bur, M., et al., *Assessment of transport rates of proteins and peptides across primary human alveolar epithelial cell monolayers*. Eur J Pharm Sci, 2006. **28**(3): p. 196-203.
188. Hermanns, M.I., et al., *Primary human coculture model of alveolo-capillary unit to study mechanisms of injury to peripheral lung*. Cell Tissue Res, 2009. **336**(1): p. 91-105.
189. Wottrich, R., S. Diabate, and H.F. Krug, *Biological effects of ultrafine model particles in human macrophages and epithelial cells in mono- and co-culture*. Int J Hyg Environ Health, 2004. **207**(4): p. 353-61.
190. Salomon, J.J. and C. Ehrhardt, *Nanoparticles attenuate P-glycoprotein/MDR1 function in A549 human alveolar epithelial cells*. Eur J Pharm Biopharm, 2011. **77**(3): p. 392-7.
191. Alfaro-Moreno, E., et al., *Co-cultures of multiple cell types mimic pulmonary cell communication in response to urban PM10*. Eur Respir J, 2008. **32**(5): p. 1184-94.
192. Sueki, A., et al., *Epithelial-mesenchymal transition of A549 cells is enhanced by co-cultured with THP-1 macrophages under hypoxic conditions*. Biochem Biophys Res Commun, 2014. **453**(4): p. 804-9.
193. Kasper, J.Y., et al., *Pulmonary surfactant augments cytotoxicity of silica nanoparticles: Studies on an in vitro air-blood barrier model*. Beilstein J Nanotechnol, 2015. **6**: p. 517-28.
194. Kasper, J.Y., et al., *A responsive human triple-culture model of the air-blood barrier: incorporation of different macrophage phenotypes*. J Tissue Eng Regen Med, 2015.
195. Blank, F., B. Rothen-Rutishauser, and P. Gehr, *Dendritic cells and macrophages form a transepithelial network against foreign particulate antigens*. Am J Respir Cell Mol Biol, 2007. **36**(6): p. 669-77.
196. Tsuchiya, S., et al., *Establishment and characterization of a human acute monocytic leukemia cell line (THP-1)*. Int J Cancer, 1980. **26**(2): p. 171-6.
197. Auwerx, J., *The human leukemia cell line, THP-1: a multifaceted model for the study of monocyte-macrophage differentiation*. Experientia, 1991. **47**(1): p. 22-31.
198. Schwende, H., et al., *Differences in the state of differentiation of THP-1 cells induced by phorbol ester and 1,25-dihydroxyvitamin D3*. J Leukoc Biol, 1996. **59**(4): p. 555-61.
199. Traore, K., et al., *Signal transduction of phorbol 12-myristate 13-acetate (PMA)-induced growth inhibition of human monocytic leukemia THP-1 cells is reactive oxygen dependent*. Leuk Res, 2005. **29**(8): p. 863-79.
200. Daigneault, M., et al., *The identification of markers of macrophage differentiation in PMA-stimulated THP-1 cells and monocyte-derived macrophages*. PLoS One, 2010. **5**(1): p. e8668.
201. Dreskin, S.C., et al., *Isoforms of Jun kinase are differentially expressed and activated in human monocyte/macrophage (THP-1) cells*. J Immunol, 2001. **166**(9): p. 5646-53.

202. Qin, Z., *The use of THP-1 cells as a model for mimicking the function and regulation of monocytes and macrophages in the vasculature*. *Atherosclerosis*, 2012. **221**(1): p. 2-11.
203. Tsuchiya, S., et al., *Induction of maturation in cultured human monocytic leukemia cells by a phorbol diester*. *Cancer Res*, 1982. **42**(4): p. 1530-6.
204. Bodet, C., F. Chandad, and D. Grenier, *Inflammatory responses of a macrophage/epithelial cell co-culture model to mono and mixed infections with Porphyromonas gingivalis, Treponema denticola, and Tannerella forsythia*. *Microbes Infect*, 2006. **8**(1): p. 27-35.
205. Chanput, W., J.J. Mes, and H.J. Wichers, *THP-1 cell line: An in vitro cell model for immune modulation approach*. *International Immunopharmacology*, 2014. **23**(1): p. 37-45.
206. Chanput, W., V. Peters, and H. Wichers, *THP-1 and U937 Cells*, in *The Impact of Food Bioactives on Health: in vitro and ex vivo models*, K. Verhoeckx, et al., Editors. 2015, Springer International Publishing: Cham. p. 147-159.
207. Rogers, P.D., et al., *Pneumolysin-dependent and -independent gene expression identified by cDNA microarray analysis of THP-1 human mononuclear cells stimulated by Streptococcus pneumoniae*. *Infect Immun*, 2003. **71**(4): p. 2087-94.
208. Cousins, R.J., et al., *A global view of the selectivity of zinc deprivation and excess on genes expressed in human THP-1 mononuclear cells*. *Proc Natl Acad Sci U S A*, 2003. **100**(12): p. 6952-7.
209. Mills, C.D., *M1 and M2 Macrophages: Oracles of Health and Disease*. *Crit Rev Immunol*, 2012. **32**(6): p. 463-88.
210. Schildberger, A., et al., *Monocytes, peripheral blood mononuclear cells, and THP-1 cells exhibit different cytokine expression patterns following stimulation with lipopolysaccharide*. *Mediators Inflamm*, 2013. **2013**: p. 697972.
211. Needham, L.A., et al., *Drug targeting to monocytes and macrophages using esterase-sensitive chemical motifs*. *J Pharmacol Exp Ther*, 2011. **339**(1): p. 132-42.
212. Kelly, C., C. Jefferies, and S.-A. Cryan, *Targeted Liposomal Drug Delivery to Monocytes and Macrophages*. *Journal of Drug Delivery*, 2011. **2011**: p. 11.
213. Lawlor, C., et al., *The application of high-content analysis in the study of targeted particulate delivery systems for intracellular drug delivery to alveolar macrophages*. *Mol Pharm*, 2011. **8**(4): p. 1100-12.
214. Ferrer, M.C.C., et al., *Cellular Uptake and Intracellular Cargo Release From Dextran Based Nanogel Drug Carriers*. *Journal of Nanotechnology in Engineering and Medicine*, 2013. **4**(1): p. 0110021-0110028.
215. Lukasiewicz, S., et al., *Biocompatible Polymeric Nanoparticles as Promising Candidates for Drug Delivery*. *Langmuir*, 2015. **31**(23): p. 6415-25.
216. Chanput, W., et al., *Transcription profiles of LPS-stimulated THP-1 monocytes and macrophages: a tool to study inflammation modulating effects of food-derived compounds*. *Food Funct*, 2010. **1**(3): p. 254-61.
217. Palacio, J.R., U.R. Markert, and P. Martinez, *Anti-inflammatory properties of N-acetylcysteine on lipopolysaccharide-activated macrophages*. *Inflamm Res*, 2011. **60**(7): p. 695-704.

218. Schiliro, T., et al., *Inflammation response and cytotoxic effects in human THP-1 cells of size-fractionated PM10 extracts in a polluted urban site*. Chemosphere, 2016. **145**: p. 89-97.
219. Riendeau, C.J. and H. Kornfeld, *THP-1 cell apoptosis in response to Mycobacterial infection*. Infect Immun, 2003. **71**(1): p. 254-9.
220. Voth, D.E., D. Howe, and R.A. Heinzen, *Coxiella burnetii inhibits apoptosis in human THP-1 cells and monkey primary alveolar macrophages*. Infect Immun, 2007. **75**(9): p. 4263-71.
221. Estrella, J.L., et al., *A Novel in vitro Human Macrophage Model to Study the Persistence of Mycobacterium tuberculosis Using Vitamin D(3) and Retinoic Acid Activated THP-1 Macrophages*. Front Microbiol, 2011. **2**: p. 67.
222. Iona, E., et al., *Infection of human THP-1 cells with dormant Mycobacterium tuberculosis*. Microbes Infect, 2012. **14**(11): p. 959-67.
223. Gupta, A., et al., *Inhalable particles containing rapamycin for induction of autophagy in macrophages infected with Mycobacterium tuberculosis*. Mol Pharm, 2014. **11**(4): p. 1201-7.
224. Stone, K.C., et al., *Allometric relationships of cell numbers and size in the mammalian lung*. Am J Respir Cell Mol Biol, 1992. **6**(2): p. 235-43.
225. Chowdhury, F., et al., *Interactions between endothelial cells and epithelial cells in a combined cell model of airway mucosa: effects on tight junction permeability*. Exp Lung Res, 2010. **36**(1): p. 1-11.
226. Kreft, M.E., et al., *The characterization of the human cell line Calu-3 under different culture conditions and its use as an optimized in vitro model to investigate bronchial epithelial function*. Eur J Pharm Sci, 2015. **69**: p. 1-9.
227. Coffey, R.G. and J.W. Hadden, *Cyclic Nucleotide Pharmacology of Macrophage Functions*, in *Pharmacology*, J.W. Hadden and A. Szentivanyi, Editors. 1985, Springer US: Boston, MA. p. 27-48.
228. Swanson, J.A., Johnson, M.T., Beningo, K., Post, P., Mooseker, M., Araki, N., *A contractile activity that closes phagosomes in macrophages*. Journal of Cell Science 1999. **112**: p. 307-316.
229. Gordon, S., *The macrophage: Past, present and future*. European Journal of Immunology, 2007. **37**(S1): p. S9-S17.
230. Pickles, R.J., et al., *Retargeting the Coxsackievirus and Adenovirus Receptor to the Apical Surface of Polarized Epithelial Cells Reveals the Glycocalyx as a Barrier to Adenovirus-Mediated Gene Transfer*. Journal of Virology, 2000. **74**(13): p. 6050-6057.
231. Hartwig, J.H. and T.P. Stossel, *Macrophage movements*, in *Mononuclear Phagocytes: Characteristics, Physiology and Function*, R. van Furth, Editor. 1985, Springer Netherlands: Dordrecht. p. 329-336.
232. Sackmann, E. *VII Analogies to Cell Locomotion*. in *Symposium on Oscillations in Heterogeneous Chemical and Biological Systems*. 1984. University of Bremen: Springer-Verlag.
233. Jones, J.G., *Clearance of inhaled particles from the alveoli*, in *Aerosols and the Lung: Clinical and Experimental Aspects*, S.W. Clarke, Pavia, D., Editor. 1984, Butterworth Scientific Limited: Surrey, England. p. 170-196.
234. Hartwig, J.H., *Actin filament architecture and movements in macrophage cytoplasm*. Ciba Found Symp, 1986. **118**: p. 42-53.
235. Jones, G.E., *Cellular signaling in macrophage migration and chemotaxis*. Journal of Leukocyte Biology, 2000. **68**(5): p. 593-602.

236. Clark, R.K., *Anatomy and Physiology: Understanding the Human Body*. 2005: Jones and Bartlett Publishers.
237. *CellTrace Reagents for Cell Proliferation*. 02/05/2016; Available from: <https://www.thermofisher.com/de/de/home/life-science/cell-analysis/flow-cytometry/cell-health-and-viability-assays-for-flow-cytometry/cell-proliferation-assays-for-flow-cytometry/celltrace-reagents-for-cell-proliferation.html>.
238. Mazzola, L., *Commercializing nanotechnology*. Nat Biotech, 2003. **21**(10): p. 1137-1143.
239. Paull, R., et al., *Investing in nanotechnology*. Nat Biotech, 2003. **21**(10): p. 1144-1147.
240. Cupaioli, F.A., et al., *Engineered nanoparticles. How brain friendly is this new guest?* Prog Neurobiol, 2014. **119-120**: p. 20-38.
241. Kononenko, V., M. Narat, and D. Drobne, *Nanoparticle interaction with the immune system*. Arh Hig Rada Toksikol, 2015. **66**(2): p. 97-108.
242. Ruge, C.A., J. Kirch, and C.M. Lehr, *Pulmonary drug delivery: from generating aerosols to overcoming biological barriers-therapeutic possibilities and technological challenges*. Lancet Respir Med, 2013. **1**(5): p. 402-13.
243. Muller, J., et al., *Respiratory toxicity of multi-wall carbon nanotubes*. Toxicology and Applied Pharmacology, 2005. **207**(3): p. 221-231.
244. Li, J.J., et al., *Nanoparticle-induced pulmonary toxicity*. Experimental Biology and Medicine, 2010. **235**(9): p. 1025-1033.
245. Manke, A., L. Wang, and Y. Rojanasakul, *Mechanisms of nanoparticle-induced oxidative stress and toxicity*. Biomed Res Int, 2013. **2013**: p. 942916.
246. Vallyathan, V. and X. Shi, *The role of oxygen free radicals in occupational and environmental lung diseases*. Environ Health Perspect, 1997. **105 Suppl 1**: p. 165-77.
247. Vinzents, P.S., et al., *Personal exposure to ultrafine particles and oxidative DNA damage*. Environ Health Perspect, 2005. **113**(11): p. 1485-90.
248. Karakoti, A.S., L.L. Hench, and S. Seal, *The potential toxicity of nanomaterials—The role of surfaces*. JOM. **58**(7): p. 77-82.
249. Bonner, J.C., *Lung fibrotic responses to particle exposure*. Toxicol Pathol, 2007. **35**(1): p. 148-53.
250. Hussain, S., et al., *Oxidative stress and proinflammatory effects of carbon black and titanium dioxide nanoparticles: role of particle surface area and internalized amount*. Toxicology, 2009. **260**.
251. Li, N., et al., *Ultrafine particulate pollutants induce oxidative stress and mitochondrial damage*. Environ Health Perspect, 2003. **111**(4): p. 455-60.
252. Hou, L., et al., *Airborne particulate matter and mitochondrial damage: a cross-sectional study*. Environmental Health, 2010. **9**(1): p. 1-9.
253. Pope, C.A., D.W. Dockery, and J. Schwartz, *Review of Epidemiological Evidence of Health Effects of Particulate Air Pollution*. Inhalation Toxicology, 1995. **7**(1): p. 1-18.
254. Peters, A., et al., *Respiratory effects are associated with the number of ultrafine particles*. American Journal of Respiratory and Critical Care Medicine, 1997. **155**(4): p. 1376-1383.

255. Lighty, J.S., J.M. Veranth, and A.F. Sarofim, *Combustion aerosols: factors governing their size and composition and implications to human health*. J Air Waste Manag Assoc, 2000. **50**(9): p. 1565-618; discussion 1619-22.
256. Schulz, H., et al., *Cardiovascular effects of fine and ultrafine particles*. J Aerosol Med, 2005. **18**(1): p. 1-22.
257. Gehr, P., F. Blank, and B.M. Rothen-Rutishauser, *Fate of inhaled particles after interaction with the lung surface*. Paediatr Respir Rev, 2006. **7 Suppl 1**: p. S73-5.
258. Pope, C.A., *Review: Epidemiological Basis for Particulate Air Pollution Health Standards*. Aerosol Science and Technology, 2000. **32**(1): p. 4-14.
259. Du, Y., et al., *Air particulate matter and cardiovascular disease: the epidemiological, biomedical and clinical evidence*. J Thorac Dis, 2016. **8**(1): p. E8-e19.
260. Lanzinger, S., et al., *Associations between ultrafine and fine particles and mortality in five central European cities - Results from the UFIREG study*. Environ Int, 2016. **88**: p. 44-52.
261. Foged, C., et al., *Particle size and surface charge affect particle uptake by human dendritic cells in an in vitro model*. Int J Pharm, 2005. **298**(2): p. 315-22.
262. Kreyling, W.G., M. Semmler-Behnke, and W. Moller, *Ultrafine particle-lung interactions: does size matter?* J Aerosol Med, 2006. **19**(1): p. 74-83.
263. Nel, A., et al., *Toxic potential of materials at the nanolevel*. Science, 2006. **311**.
264. He, C., et al., *Effects of particle size and surface charge on cellular uptake and biodistribution of polymeric nanoparticles*. Biomaterials, 2010. **31**(13): p. 3657-66.
265. Frohlich, E., *The role of surface charge in cellular uptake and cytotoxicity of medical nanoparticles*. Int J Nanomedicine, 2012. **7**: p. 5577-91.
266. Braakhuis, H.M., et al., *Physicochemical characteristics of nanomaterials that affect pulmonary inflammation*. Particle and Fibre Toxicology, 2014. **11**(1): p. 1-25.
267. Takenaka, S., et al., *Pulmonary and systemic distribution of inhaled ultrafine silver particles in rats*. Environ Health Perspect, 2001. **109 Suppl 4**: p. 547-51.
268. Sung, J.H., et al., *Lung function changes in Sprague-Dawley rats after prolonged inhalation exposure to silver nanoparticles*. Inhal Toxicol, 2008. **20**(6): p. 567-74.
269. Tang, J., et al., *Distribution, translocation and accumulation of silver nanoparticles in rats*. J Nanosci Nanotechnol, 2009. **9**(8): p. 4924-32.
270. Zolnik, B.S., et al., *Nanoparticles and the immune system*. Endocrinology, 2010. **151**(2): p. 458-65.
271. Smith, M.J., et al., *From immunotoxicity to nanotherapy: the effects of nanomaterials on the immune system*. Toxicol Sci, 2014. **138**(2): p. 249-55.
272. Dobrovolskaia, M.A. and S.E. McNeil, *Immunological properties of engineered nanomaterials*. Nat Nanotechnol, 2007. **2**(8): p. 469-78.
273. Roseman, S., *The synthesis of complex carbohydrates by multiglycosyltransferase systems and their potential function in intercellular adhesion*. Chem Phys Lipids, 1970. **5**(1): p. 270-97.
274. Dwivedi, P.D., et al., *Are nanomaterials a threat to the immune system?* Nanotoxicology, 2009. **3**(1): p. 19-26.

275. R., K., et al., *Silver nanoparticles interactions with the immune system: implications for health and disease*, in *Silver nanoparticles*, P.P. D., Editor. 2010, In TechOpen: Rijeka. p. 309-24.
276. Kumar, M.N., et al., *Chitosan chemistry and pharmaceutical perspectives*. Chem Rev, 2004. **104**(12): p. 6017-84.
277. Nafee, N., et al., *Chitosan-coated PLGA nanoparticles for DNA/RNA delivery: effect of the formulation parameters on complexation and transfection of antisense oligonucleotides*. Nanomedicine, 2007. **3**(3): p. 173-83.
278. Kunschke, N., *Development of a Nanotechnology enabled for Pulmonary siRNA delivery*, in *Biopharmacy and Pharmaceutical Technology*. expected 2017, Saarland University: Saarbruecken.
279. Barthold, S., et al., *Preparation of nanosized coacervates of positive and negative starch derivatives intended for pulmonary delivery of proteins*. Journal of Materials Chemistry B, 2016. **4**(13): p. 2377-2386.
280. Barthold, S., *Nanotechnology enabled drug delivery of proteins and peptides to the lung*, in *Biopharmacy and Pharmaceutical Technology*. 2016, Saarland University: Saarbruecken.
281. Chronopoulou, L., et al., *Chitosan-coated PLGA nanoparticles: a sustained drug release strategy for cell cultures*. Colloids Surf B Biointerfaces, 2013. **103**: p. 310-7.
282. Makadia, H.K. and S.J. Siegel, *Poly Lactic-co-Glycolic Acid (PLGA) as Biodegradable Controlled Drug Delivery Carrier*. Polymers (Basel), 2011. **3**(3): p. 1377-1397.
283. Wang, N. and X.S. Wu, *Synthesis, characterization, biodegradation, and drug delivery application of biodegradable lactic/glycolic acid oligomers: Part II. Biodegradation and drug delivery application*. J Biomater Sci Polym Ed, 1997. **9**(1): p. 75-87.
284. Crotts, G. and T.G. Park, *Protein delivery from poly(lactic-co-glycolic acid) biodegradable microspheres: release kinetics and stability issues*. J Microencapsul, 1998. **15**(6): p. 699-713.
285. Danhier, F., et al., *PLGA-based nanoparticles: an overview of biomedical applications*. J Control Release, 2012. **161**(2): p. 505-22.
286. Lehr, C.M., Bouwstra, J.A., Schacht, E.H., Junginger, H.E., *In vitro evaluation of mucoadhesive properties of chitosan and some other natural polymers*. Int. J. Pharm., 1992. **78**: p. 43-48.
287. Illum, L., *Chitosan and its use as a pharmaceutical excipient*. Pharm Res, 1998. **15**(9): p. 1326-31.
288. Felt, O., P. Buri, and R. Gurny, *Chitosan: a unique polysaccharide for drug delivery*. Drug Dev Ind Pharm, 1998. **24**(11): p. 979-93.
289. Grenha, A., et al., *Chitosan nanoparticles are compatible with respiratory epithelial cells in vitro*. Eur J Pharm Sci, 2007. **31**(2): p. 73-84.
290. Nagpal, K., S.K. Singh, and D.N. Mishra, *Chitosan nanoparticles: a promising system in novel drug delivery*. Chem Pharm Bull (Tokyo), 2010. **58**(11): p. 1423-30.
291. Wang, J.J., et al., *Recent advances of chitosan nanoparticles as drug carriers*. Int J Nanomedicine, 2011. **6**: p. 765-74.
292. Smith, A., M. Perelman, and M. Hinchcliffe, *Chitosan: a promising safe and immune-enhancing adjuvant for intranasal vaccines*. Hum Vaccin Immunother, 2014. **10**(3): p. 797-807.

293. Ngoc, Q.N., et al., *Honokiol loaded PLGA nanoparticles with modified surface by chitosan*. Science, 2015. **5**(2): p. 724-728.
294. Loh, J.W., et al., *Uptake and cytotoxicity of chitosan nanoparticles in human liver cells*. Toxicol Appl Pharmacol, 2010. **249**(2): p. 148-57.
295. Athanasiou, K.A., G.G. Niederauer, and C.M. Agrawal, *Sterilization, toxicity, biocompatibility and clinical applications of polylactic acid/polyglycolic acid copolymers*. Biomaterials, 1996. **17**(2): p. 93-102.
296. Mura, S., et al., *Influence of surface charge on the potential toxicity of PLGA nanoparticles towards Calu-3 cells*. Int J Nanomedicine, 2011. **6**: p. 2591-605.
297. Miura, N. and Y. Shinohara, *Cytotoxic effect and apoptosis induction by silver nanoparticles in HeLa cells*. Biochem Biophys Res Commun, 2009. **390**(3): p. 733-7.
298. Park, E.J., et al., *Silver nanoparticles induce cytotoxicity by a Trojan-horse type mechanism*. Toxicol In Vitro, 2010. **24**(3): p. 872-8.
299. Kaur, J. and K. Tikoo, *Evaluating cell specific cytotoxicity of differentially charged silver nanoparticles*. Food Chem Toxicol, 2013. **51**: p. 1-14.
300. Chairuangkitti, P., et al., *Silver nanoparticles induce toxicity in A549 cells via ROS-dependent and ROS-independent pathways*. Toxicol In Vitro, 2013. **27**(1): p. 330-8.
301. Piao, M.J., et al., *Silver nanoparticles induce oxidative cell damage in human liver cells through inhibition of reduced glutathione and induction of mitochondria-involved apoptosis*. Toxicol Lett, 2011. **201**(1): p. 92-100.
302. Navarro, E., et al., *Toxicity of silver nanoparticles to Chlamydomonas reinhardtii*. Environ Sci Technol, 2008. **42**(23): p. 8959-64.
303. Chae, Y.J., et al., *Evaluation of the toxic impact of silver nanoparticles on Japanese medaka (Oryzias latipes)*. Aquatic Toxicology, 2009. **94**(4): p. 320-327.
304. Wu, Y., et al., *Effects of silver nanoparticles on the development and histopathology biomarkers of Japanese medaka (Oryzias latipes) using the partial-life test*. Aquatic Toxicology, 2010. **100**(2): p. 160-167.
305. Bilberg, K., et al., *Silver nanoparticles disrupt olfaction in Crucian carp (Carassius carassius) and Eurasian perch (Perca fluviatilis)*. Aquat Toxicol, 2011. **104**(1-2): p. 145-52.
306. Liu, J., et al., *Chemical transformations of nanosilver in biological environments*. ACS Nano, 2012. **6**(11): p. 9887-99.
307. Herzog, F., et al., *Exposure of silver-nanoparticles and silver-ions to lung cells in vitro at the air-liquid interface*. Part Fibre Toxicol, 2013. **10**: p. 11.
308. AshaRani, P.V., et al., *Cytotoxicity and genotoxicity of silver nanoparticles in human cells*. ACS Nano, 2009. **3**(2): p. 279-90.
309. Ahamed, M., M.S. Alsalhi, and M.K. Siddiqui, *Silver nanoparticle applications and human health*. Clin Chim Acta, 2010. **411**(23-24): p. 1841-8.
310. Soto, K., K.M. Garza, and L.E. Murr, *Cytotoxic effects of aggregated nanomaterials*. Acta Biomater, 2007. **3**(3): p. 351-8.
311. Carlson, C., et al., *Unique cellular interaction of silver nanoparticles: size-dependent generation of reactive oxygen species*. J Phys Chem B, 2008. **112**(43): p. 13608-19.



312. Kawata, K., M. Osawa, and S. Okabe, *In vitro toxicity of silver nanoparticles at noncytotoxic doses to HepG2 human hepatoma cells*. Environ Sci Technol, 2009. **43**(15): p. 6046-51.
313. Greulich, C., et al., *Studies on the biocompatibility and the interaction of silver nanoparticles with human mesenchymal stem cells (hMSCs)*. Langenbeck's Archives of Surgery, 2009. **394**(3): p. 495-502.
314. Smith, J.M., M. Dornish, and E.J. Wood, *Involvement of protein kinase C in chitosan glutamate-mediated tight junction disruption*. Biomaterials, 2005. **26**(16): p. 3269-3276.
315. Dodane, V., M. Amin Khan, and J.R. Merwin, *Effect of chitosan on epithelial permeability and structure*. Int J Pharm, 1999. **182**(1): p. 21-32.
316. Vllasaliu, D., et al., *Tight junction modulation by chitosan nanoparticles: comparison with chitosan solution*. Int J Pharm, 2010. **400**(1-2): p. 183-93.
317. Yeh, T.H., et al., *Mechanism and consequence of chitosan-mediated reversible epithelial tight junction opening*. Biomaterials, 2011. **32**(26): p. 6164-73.
318. Coyne, C.B., et al., *Regulation of airway tight junctions by proinflammatory cytokines*. Mol Biol Cell, 2002. **13**(9): p. 3218-34.
319. Capaldo, C.T. and A. Nusrat, *Cytokine regulation of tight junctions*. Biochim Biophys Acta, 2009. **1788**(4): p. 864-71.
320. Kusek, M.E., et al., *In vitro Coculture Assay to Assess Pathogen Induced Neutrophil Trans-epithelial Migration*. 2014(83): p. e50823.
321. Raemy, D.O., et al., *Effects of flame made zinc oxide particles in human lung cells - a comparison of aerosol and suspension exposures*. Part Fibre Toxicol, 2012. **9**: p. 33.
322. Loftus, B.G., et al., *IgG subclass deficiency in asthma*. Arch Dis Child, 1988. **63**(12): p. 1434-7.
323. Jr., J.C.A., et al., *The distribution and functions of immunoglobulin isotypes*. 5th ed. Immunobiology: The Immune System in Health and Disease. 2001, New York: Garland Science.
324. Williams, J.W., M.Y. Tjota, and A.I. Sperling, *The contribution of allergen-specific IgG to the development of th2-mediated airway inflammation*. J Allergy (Cairo), 2012. **2012**: p. 236075.
325. Hirota, K. and H. Terada, *Endocytosis of Particle Formulations by Macrophages and Its Application to Clinical Treatment*, in *Molecular Regulation of Endocytosis*, B. Ceresa, Editor. 2012, InTech.
326. Makino, K., et al., *Phagocytic uptake of polystyrene microspheres by alveolar macrophages: effects of the size and surface properties of the microspheres*. Colloids and Surfaces B: Biointerfaces, 2003. **27**(1): p. 33-39.
327. Hasegawa, T., et al., *Phagocytic activity of alveolar macrophages toward polystyrene latex microspheres and PLGA microspheres loaded with anti-tuberculosis agent*. Colloids and Surfaces B: Biointerfaces, 2007. **60**(2): p. 221-228.
328. Allen, T.M., et al., *Uptake of liposomes by cultured mouse bone marrow macrophages: influence of liposome composition and size*. Biochim Biophys Acta, 1991. **1061**(1): p. 56-64.
329. Ahsan, F., et al., *Targeting to macrophages: role of physicochemical properties of particulate carriers—liposomes and microspheres—on the*

- phagocytosis by macrophages*. Journal of Controlled Release, 2002. **79**(1–3): p. 29-40.
330. Tabata, Y. and Y. Ikada, *Effect of the size and surface charge of polymer microspheres on their phagocytosis by macrophage*. Biomaterials, 1988. **9**(4): p. 356-62.
331. Champion, J.A., A. Walker, and S. Mitragotri, *Role of particle size in phagocytosis of polymeric microspheres*. Pharm Res, 2008. **25**(8): p. 1815-21.
332. Oh, N. and J.H. Park, *Endocytosis and exocytosis of nanoparticles in mammalian cells*. Int J Nanomedicine, 2014. **9 Suppl 1**: p. 51-63.
333. Hirota, K., et al., *Optimum conditions for efficient phagocytosis of rifampicin-loaded PLGA microspheres by alveolar macrophages*. J Control Release, 2007. **119**(1): p. 69-76.
334. <http://www.medicoconsult.de/Makrophagen/>. 30-05-2016.
335. Hu, Y., et al., *Effect of PEG conformation and particle size on the cellular uptake efficiency of nanoparticles with the HepG2 cells*. J Control Release, 2007. **118**(1): p. 7-17.
336. Rytting, E., et al., *Biodegradable polymeric nanocarriers for pulmonary drug delivery*. Expert Opin Drug Deliv, 2008. **5**(6): p. 629-39.

---

## Scientific output

### List of publications

#### Research paper

S. Barthold, **S. Kletting**, R. Haberkorn, G. Kickelbick, C. de Souza Carvalho-Wodarz, E. Lepeltier, B. Loretz, C.M. Lehr: "A carrier system for enhanced nanoparticle deposition in the deep lung - nanoparticles embedded in microparticles" *Pharm. Res. (in preparation)*

**S. Kletting**, S. Barthold, U. Repnik, G. Griffith, B. Loretz, N. Schneider-Daum, C. de Souza Carvalho-Wodarz, C.M. Lehr: "Co-culture of human alveolar epithelial (hAELVi) and macrophage (THP-1) cell lines" *ALTEX (submitted)*

A. Kühn\*, **S. Kletting\***, C. de Souza Carvalho-Wodarz\*, U. Repnik, G. Griffith, U. Fischer, E. Meese, H. Huwer, D. Wirth, T. May, N. Schneider-Daum, C.M. Lehr: "Immortalization of primary human alveolar epithelial cells expressing tight junctions as needed for a model of the air-blood barrier" *ALTEX*. 2016 Mar 17. doi: 10.14573/altex.1511131

S. Barthold, **S. Kletting**, J. Taffner, C. de Souza Carvalho-Wodarz, E. Lepeltier, B. Loretz, C.M. Lehr: "Nanosized Coacervates Of Positive And Negative Starch Derivatives For Pulmonary Delivery Of Proteins" *J. Mater. Chem. B*, 2016, **4**, 2377-2386

#### Review article

M. Hittinger\*, J. Juntke\*, **S. Kletting\***, N. Schneider-Daum, C. de Souza Carvalho-Wodarz, C.M. Lehr: „Preclinical safety and efficacy models for pulmonary drug delivery of antimicrobials with focus on in vitro models“ *Advanced Drug Delivery Reviews* Vol 85, pp. 44-56, 2015

**Poster**

**S. Kletting\***, R. Hendrix\*, C. Carvalho-Wodarz, U. Repnik, G. Griffith, N. Schneider-Daum, C.M. Lehr: "3D co-culture of human alveolar macrophages and epithelial cells: new perspectives for developing pulmonary medicines" DEHEMA; 3D Cell Culture 2016: How close to '*in vivo*' can we get? Models, applications & translation, April 2016, Freiburg, Germany

R. Hendrix\*, **S. Kletting\***, C. de Souza Carvalho-Wodarz, N. Schneider-Daum, C.M. Lehr: "Modeling the air-blood barrier in healthy and disease state to evaluate safety and efficacy of inhaled(nano) medicines" 14<sup>th</sup> Lung Science Conference: "System approaches in lung disease", March 2016, Estoril, Portugal

R. Hendrix\*, **S. Kletting\***, C. de Souza Carvalho-Wodarz, N. Schneider-Daum, C.M. Lehr: "Exploring the established 3D co-culture model of the deep lung: creating a diseased state for pulmonary delivery evaluation in vulnerable conditions" Biological Barriers, March 2016, Saarbrücken, Germany

A. Costa, **S. Kletting**, C. de Souza Carvalho-Wodarz, V. Seabra, B. Sarmiento, C.M. Lehr: "Assessing the permeability of nanocarriers across the *in vitro* alveolar epithelium" Biological Barriers, March 2016, Saarbrücken, Germany

R. Hendrix\*, **S. Kletting\***, C. de Souza Carvalho-Wodarz, N. Schneider-Daum, C.M. Lehr: "Modeling the air-blood barrier in healthy and disease state to evaluate safety and efficacy of pulmonary (nano) medicines" Crossing Biological Barriers-Advances in Nanocarrier Design for Targeted Drug Delivery, November 2015, Dresden, Germany

**S. Kletting**, C. de Souza Carvalho-Wodarz, N. Schneider-Daum, C.M. Lehr: "A new 3D coculture model of the human Air-Blood Barrier to study the interaction with aerosolized drug carriers" 5<sup>th</sup> International HIPS Symposium, July 2015, Saarbrücken, Germany

**S. Kletting**, C. de Souza Carvalho-Wodarz, N. Schneider-Daum, C.M. Lehr: "3D Coculture of Immortalized Alveolar Type I cells and Macrophages: A New *In Vitro* Model of the Human Air-Blood Barrier for Pulmonary Drug Delivery" 20<sup>th</sup> ISAM Congress, June 2015, Munich, Germany

**S. Kletting**, C. de Souza Carvalho-Wodarz, N. Schneider-Daum, C.M. Lehr: "Establishment of a New *In Vitro* Model of the Human Air-Blood Barrier relevant for Pulmonary Drug Delivery" NanoBionet Size Matters 2015, April 2015, Saarbrücken, Germany

**S. Kletting**, C. de Souza Carvalho-Wodarz, N. Schneider-Daum, C.M. Lehr: "Establishment of an *in vitro* model of the human air-blood barrier by using immortalized alveolar epithelial cells and macrophages" CRS-Germany Local Chapter, February 2015, Muttenz, Switzerland

**S. Kletting**, C. de Souza Carvalho-Wodarz, N. Schneider-Daum, C.-M. Lehr: "Establishment of an *In Vitro* Model of the Human Air-Blood Barrier using Immortalized Alveolar Epithelial Cells and Macrophages" 3<sup>rd</sup> Consortium's Face-to-Face Meeting COMPACT, February 2015, Ludwigshafen, Germany

**S. Kletting**, C. de Souza Carvalho, N. Daum, C.M. Lehr: "Establishment of an *in vitro* model of the human alveolar barrier using immortalized epithelial cells and macrophages" 2. Doktorandentag der Naturwissenschaftlich-Technischen Fakultät III, November 2014, Saarbrücken, Germany

**S. Kletting\***, S. Barthold\*, N. Kunschke\*, C. de Souza Carvalho-Wodarz, B. Loretz, N. Schneider-Daum, C.M. Lehr: "COMPACT - a European Collaboration on the Optimization of Macromolecular Pharmaceutical Access to Cellular Targets" 4<sup>th</sup> International HIPS Symposium, June 2014, Saarbrücken, Germany

**S. Kletting**, C. de Souza Carvalho, N. Daum, C.-M. Lehr: "Establishment of an *in vitro* model of the human alveolar barrier using immortalized epithelial cells and macrophages" 2<sup>nd</sup> Consortium's Face-to-Face Meeting COMPACT, February 2014, Stevenage, England

### **Oral presentations**

C. Carvalho-Wodarz, **S. Kletting\***, R. Hendrix\*, U. Repnik, G. Griffith, N. Schneider-Daum, C.M. Lehr: "New pulmonary *in vitro* models of the deep lung for inhaled medicines" ACTC 2016 - Advances in Cell and Tissue Culture, May/June 2016, Barcelona, Spain

M. Hittinger, **S. Kletting**, X. Murgia, N. Mell, C. Tscheka, H. Groß, H. Huwer, C. de Souza Carvalho-Wodarz, B. Loretz, N. Schneider-Daum, C.-M. Lehr: “What happens when the particle has landed? - *In vitro* models for studying post-deposition events of aerosolized particles” EUSAAT, September 2015, Linz, Austria

**S. Kletting**, C. de Souza Carvalho-Wodarz, N. Schneider-Daum, C.-M. Lehr: “Establishment of a Coculture Model of the Human Air-Blood Barrier to Study Interactions with Inhaled Nanoparticles” 4<sup>th</sup> Face-to-Face Meeting WP6 COMPACT, September 2015, Brussels, Belgium

**S. Kletting**, C. de Souza Carvalho-Wodarz, N. Schneider-Daum, C.-M. Lehr: “3D Coculture of Immortalized Alveolar Type I cells and Macrophages: A New *In Vitro* Model of the Human Air-Blood Barrier for Pulmonary Drug Delivery” ISAM Congress, June 2015, Munich, Germany

**S. Kletting**, C. de Souza Carvalho, N. Schneider-Daum, C.-M. Lehr: “Establishment of an *in vitro* model of the human air-blood barrier using immortalized alveolar epithelial cells and macrophages” 3<sup>rd</sup> Face-to-Face Meeting WP6 COMPACT, November 2014, Brussels, Belgium

**S. Kletting**, C. de Souza Carvalho, N. Daum, C.-M. Lehr: “WP6: Pulmonary delivery: Establishment of an *in vitro* model of the human alveolar barrier using immortalized epithelial cells and macrophages” 2<sup>nd</sup> Consortium’s Face-to-Face Meeting COMPACT, February 2014, Stevenage, England

**S. Kletting**, C. de Souza Carvalho, N. Daum, C.-M. Lehr: “Establishment of an *in vitro* model of the human alveolar and bronchial barrier” 2<sup>nd</sup> Face-to-Face Meeting WP6 COMPACT, January 2014, Chilly-Mazarin, Paris, France

**S. Kletting**, N. Daum, C. de Souza Carvalho, C.-M. Lehr: “Establishment of a complex *in vitro* model of the lung” 1<sup>st</sup> Face-to-Face Meeting WP6 COMPACT, April 2013, Saarbrücken, Germany

\* The authors have equally contributed to the work.

---

## Curriculum vitae

### Personal information

Name: Stephanie Kletting  
Date of birth: 04.06.1987  
Place of birth: Ulm  
Nationality: German

### Doctoral Thesis

10/2012 - 12/2015 Helmholtz-Institute for Pharmaceutical Research Saarland (HIPS); Institute for Biopharmacy and Pharmaceutical Technology, Saarland University, Saarbrücken  
Supervised by Prof. Dr. Claus-Michael Lehr  
Title: "A new cell line-based coculture model of the human air-blood barrier to evaluate the interaction with aerosolized drug carriers"

### Diploma Thesis

05/2011 - 02/2012 Institute of Toxicology, University Hospital, Mainz  
Supervised by Prof. Dr. C. Dietrich  
Title: „Untersuchungen zum Mechanismus der JunD-Promotoraktivität und Effekte auf Ovalzellen der Mausleber nach Behandlung mit TCDD"

### Undergraduate study

10/2006 - 02/2012 Studies in biology; Johannes Gutenberg-University Mainz  
Focus areas: toxicology, microbiology, zoology  
Minor fields: anthropology

**Internships**

- 12/2010 Institute of Medical Microbiology and Hygiene,  
University Hospital, Mainz
- 06/2006 Institute of Laboratory and Transfusion Medicine,  
Westpfalz-Klinikum, Kaiserslautern
- 07/2005 - 08/2005 Institute of Pathology, Westpfalz-Klinikum, Kaiserslautern

**School**

- 1997 - 2006 Secondary high school "Hohenstaufen-Gymnasium",  
Kaiserslautern
- 1995 - 1997 Basic primary school "Geschwister-Scholl-Grundschule",  
Kaiserslautern
- 1993 - 1995 Basic primary school „Meinloh-Grundschule“, Ulm-Söflingen

**Awards**

- 02/2015 Poster Award at the 3<sup>rd</sup> COMPACT consortium's Face-to-Face meeting Ludwigshafen, Germany for work entitled: "Establishment of an *In Vitro* Model of the Human Air-Blood Barrier using Immortalized Alveolar Epithelial Cells and Macrophages"



---

## Acknowledgements / Danksagung

An dieser Stelle möchte ich die Gelegenheit nutzen, allen, die auf unterschiedlichste Weise zum Gelingen dieser Arbeit beigetragen haben, meinen Dank auszusprechen.

Meinem Doktorvater, Herrn Claus-Michael Lehr möchte ich für die Bereitstellung des interessanten Themas und die Betreuung meiner Doktorarbeit danken. Darüber hinaus danke ich Dir für Dein Vertrauen und Deiner Unterstützung mich auch außerhalb des Instituts in die internationale Forschungsgesellschaft einbringen zu können.

Des Weiteren bedanke ich mich bei Herrn Jun.-Prof. Dr. Thorsten Lehr für die Anfertigung des Zweitgutachtens sowie bei der gesamten Prüfungskommission.

Mein herzlicher Dank gebührt meinen beiden Betreuerinnen: Frau Dr. Nicole Schneider-Daum, die mich in den ersten Monaten meiner Doktorandenzeit betreut und mir den Einstieg in mein Forschungsthema erleichtert hat. Auch Frau Dr. Cristiane de Souza Carvalho-Wodarz danke ich für die Betreuung der letzten Jahre. Danke für die Diskussionsbereitschaft und hilfreichen Ratschläge, egal zu welcher Tageszeit.

Ein großes Dankeschön auch an Frau Dr. Brigitta Loretz für Ihre stets offene Tür bei noch so vielen Fragen trotz der Betreuung ihrer eigenen Doktoranden und Bergen von Arbeit.

Vielen Dank auch an das „Office“: Karin Groß, Isabelle Conrad-Kehl, Sarah Müller und Stephanie Kallenborn, für die kleinen Gespräche zwischendurch und Ihre Unterstützung in allen organisatorischen Belangen.

Sarah Gordon gebührt nicht nur Dank für das Korrekturlesen meiner Arbeit! Ich freue mich schon auf die Hot-Dogs in Kopenhagen! ☺

Für das Anfertigen der TEM-Aufnahmen der Mono- und Kokulturen danke ich Frau Dr. Urska Repnik und Herrn Prof. Dr. Gareth Griffiths der Universität in Oslo.

Ein weiterer Dank gebührt dem ganzen COMPACT-Team, auch über WP 6 hinaus, für die gute Zusammenarbeit, den Blick über den Tellerrand und die Möglichkeit, Einblicke in die Arbeitsweise in der Industrie zu erhalten.

Ein riesengroßes Dankeschön geht auch an das Techniker Team, das Herzstück des Instituts: von Peter Meiers über Marijas Jurisic, dem ich für das Anfertigen der Histoschnitte sowie für die Hilfe am Konfokalmikroskop herzliche danke bis hin zu den drei Musketieren.

Chiara, herzlichen Dank für Deine Unterstützung und Geduld am Konfokal und SEM.

Ein herzliches Dankeschön auch an Dich, Jana, neben den morgendlichen/nachmittäglichen Schwätzchen vor allem für die Zeit neben der Arbeit.

Ein besonderer Dank gebührt Petra König, nicht nur für ihre Diskussionsbereitschaft und hilfreichen Tipps auf den zahlreichen Autofahrten, die lustigen Mittagspausen oder die amüsanten Momente in der Zellkultur, sondern auch für die immer aufbauenden Worte und Unterstützung, vor allem am Ende der Laborzeit!

Vielen Dank auch an meine Mitstreiter und Freunde vor allem an René, Hiroe, Nico, Anna, Jenny, Arianna, Nici, Hanzey, Chrissi, Nathalie, Marius, Flo, Julia und Simon. Euch danke ich für die freundschaftliche Atmosphäre im Institut und die lustigen Wochenenden, egal ob Altstadtfest, grillen oder einfach darten.

Besonderer Dank gebührt Dir, Xabi, nicht nur für die hilfreichen Anmerkungen im Labor, sondern viel mehr für Deine Unterstützung und die aufmunternden Worte, wenn mal wieder alles zu viel wurde. Muchas Gracias, ein Bier steht noch aus! ☺

Thanks Remi, mijn niet- opvolger, voor de prettige samenwerking, de discussies en de tijd over uit te werken. Het was geweldig om een deel van het te zijn "rijke team". Voor uw resterende tijd, ik wens u het allerbeste. Altijd denken: komt wel goed ! ☺

Dir, Sarah, danke ich für die unvergessliche Zeit in Saarbrücken. Vom ersten Tag an ein eingeschworenes Team, das neben angenehmen Zusammenarbeiten, sei es im „Sterile Team“ oder für unsere Forschung auch neben der Arbeit vieles zusammen erlebt hat wie Mäuseplagen, zusammen kochen, thermen oder Städteurlaub. Ich danke Dir für die schöne Zeit und auch das gegenseitige Aufmuntern und Motivieren, wenn mal wieder alles schiefging. Es ist schön, Dich als Freundin zu haben!

Anna, Katja, Christian, Tina, Mareike, Willi, Elli und Sabrina: Euch danke ich für Eure langjährige Freundschaft und Unterstützung außerhalb von Saarbrücken!

Mein herzlichster Dank gebührt meiner Familie. Meinen Eltern danke ich für den jahrelangen Rückhalt und das Vertrauen, was mir sowohl das Studium als auch die Promotion ermöglicht hat. Meinem Bruder danke ich für seine immerwährende Unterstützung, ob nun bei PC-Problemen oder Ratschlägen egal welcher Natur.

Meinem Freund Thomas danke ich für seine Geduld und die Gewissheit, dass ich mich immer auf Dich verlassen kann!